

---

Electronic Thesis and Dissertation Repository

---

8-5-2015 12:00 AM

# Investigation of Pancreatic $\beta$ -Cell Insulin Receptor Regulation of $\beta$ -Cell Growth, Function, and Survival Via a Temporal Conditional Knockout

Liangyi Zhou, *The University of Western Ontario*

Supervisor: Rennian Wang, *The University of Western Ontario*

A thesis submitted in partial fulfillment of the requirements for the Master of Science degree in Pathology

© Liangyi Zhou 2015

Follow this and additional works at: <https://ir.lib.uwo.ca/etd>



Part of the [Developmental Biology Commons](#), and the [Endocrinology, Diabetes, and Metabolism Commons](#)

---

## Recommended Citation

Zhou, Liangyi, "Investigation of Pancreatic  $\beta$ -Cell Insulin Receptor Regulation of  $\beta$ -Cell Growth, Function, and Survival Via a Temporal Conditional Knockout" (2015). *Electronic Thesis and Dissertation Repository*. 2989.

<https://ir.lib.uwo.ca/etd/2989>

This Dissertation/Thesis is brought to you for free and open access by Scholarship@Western. It has been accepted for inclusion in Electronic Thesis and Dissertation Repository by an authorized administrator of Scholarship@Western. For more information, please contact [wlsadmin@uwo.ca](mailto:wlsadmin@uwo.ca).

INVESTIGATION OF PANCREATIC  $\beta$ -CELL INSULIN RECEPTOR REGULATION  
OF  $\beta$ -CELL GROWTH, FUNCTION, AND SURVIVAL VIA A TEMPORAL  
CONDITIONAL KNOCKOUT

(Thesis format: Monograph)

by

Liangyi Zhou

Graduate Program in Pathology and Laboratory Medicine

A thesis submitted in partial fulfillment  
of the requirements for the degree of  
Master of Science

The School of Graduate and Postdoctoral Studies  
The University of Western Ontario  
London, Ontario, Canada

© Liangyi Zhou 2015

## Abstract

The expression of insulin receptor (IR) in  $\beta$ -cells suggests an autocrine role for insulin signalling in  $\beta$ -cell function and regulation. Studies have demonstrated that  $\beta$ -cell *Ir* knockout ( $\beta$ IrKO) mice develop age-dependent glucose intolerance. We investigated the temporal role of  $\beta$ -cell IR signaling in pre- and postnatal islet development and function, and under high-fat diet stress, using a tamoxifen-inducible Cre-recombinase *Ir* knockout mouse model.

Prenatal  $\beta$ IrKO mice exhibited increased mean islet area,  $\beta$ -cell area, and islet area percentage. Additionally, there was upregulation of insulin-like growth factor-2 levels, increased Akt activity, and increased proliferation in islets. Postnatally-induced  $\beta$ IrKO mice did not exhibit impaired glucose tolerance at 4, 8, and 20 weeks post-tamoxifen. Similarly, no differences were observed between groups on high-fat diet. Results suggest that while loss of fetal  $\beta$ -cell IR causes an islet growth response through alternate pathways, postnatal  $\beta$ -cell IR may not play a pivotal role for adult  $\beta$ -cell function.

## Keywords

Diabetes mellitus, insulin receptor,  $\beta$ -cell, tamoxifen-inducible, IGF2, high-fat diet

## Co-Authorship Statement

The methods described in Chapter 2 of this thesis were conducted by Liangyi Zhou with contributions from several other lab members. Mark Trinder performed some of the tamoxifen injections into pregnant female mice, fetal pancreas collection, fetal mouse genotyping, immunofluorescence staining followed by islet morphology analysis, western blotting, and assisted with manuscript writing for the fetal study. Dr. Matthew Riopel assisted with western blotting for the fetal study. Dr. Zhi-Chao Feng contributed to adult mice genotyping, *in vivo* metabolic studies, and ELISA. Jason Peart and Amanda Oakie provided assistance with mouse genotyping, immunofluorescence staining, *in vivo* metabolic studies, and thesis manuscript editing. Jinming Li provided technical help with mouse genotyping, immunofluorescence staining, and western blots. Dr. Rennian Wang and Jinming Li conducted adult mouse islet isolations. Dr. Rennian Wang designed the studies, provided guidance with data interpretation and analyses, and revised the manuscript.

## Acknowledgments

I would like to thank my graduate research supervisor, Dr. Rennian Wang, for the opportunity to pursue a master's degree in her lab. I am grateful for all of her guidance with experimental designs and data interpretation. I have matured as a researcher through Dr. Rennain Wang's encouragement in self-directed learning and critical thinking. I would also like to thank Jinming Li for his expertise in laboratory techniques and trouble shooting. Furthermore, I thank past and present Wang lab members, my friends, Dr. Matthew Riopel, Dr. Zhi-Chao Feng, Dr. Bijun Chen, Alex Popell, Mark Trinder, Jason Peart, Amanda Oakie, and Tara White for their experimental assistance and for creating an enjoyable research environment.

I would like to thank my advisory committee, Dr. Savita Dhanvantari and Dr. Chandan Chakraborty for their questions, suggestions, and advices to improve my thesis project.

Finally, I would like to acknowledge the Canadian Institute of Health Research, the Children's Health Research Institute, and the Department of Pathology and Laboratory Medicine at the University of Western Ontario for their financial support throughout my research project.

# Table of Contents

Abstract.....	ii
Co-Authorship Statement.....	iii
Acknowledgments.....	iv
Table of Contents.....	v
List of Tables.....	viii
List of Figures.....	ix
List of Appendices.....	xi
List of Abbreviations.....	xii
Chapter 1 - Introduction.....	1
1.1    Significance of study.....	1
1.2    The pancreas and islet of Langerhans.....	1
1.3    Pancreas development & $\beta$ -cell formation.....	2
1.4    Islet vascularization.....	3
1.5    Overview of diabetes mellitus.....	4
1.6    Insulin receptors.....	5
1.7    Insulin receptor ligands.....	6
1.8    Insulin production and secretion.....	8
1.9    Insulin receptor signalling pathways.....	9
1.10   Insulin receptor in different tissues.....	10
1.11   Insulin receptor and $\beta$ -cells.....	11
1.12   High-fat diet, $\beta$ -cell insulin resistance and dysfunction.....	11
1.13   Rationale, objectives, and hypothesis.....	13

Chapter 2 - Materials and Methods.....	16
2.1    Generation of $\beta$ -cell-specific <i>Ir</i> knockout mice .....	16
2.2    Mouse genotyping.....	18
2.3    Tamoxifen preparation and administration .....	18
2.4    Postnatal glucose metabolic studies.....	19
2.5    Pancreatic islet isolation.....	20
2.6    Insulin enzyme-linked immunosorbent assay (ELISA).....	20
2.7    Tissue processing, immunohistology, and TUNEL.....	21
2.8    Morphometric analysis.....	25
2.9    Protein extraction and western blot analyses .....	26
2.10   Statistical analysis .....	27
Chapter 3 - Results.....	28
3.1    Verification of $\beta$ -cell-specific <i>Ir</i> knockout in fetal $\beta$ IrKO mice.....	28
3.2    Fetal $\beta$ IrKO mice exhibit a hyperplastic islet growth response .....	31
3.3    Increased $\beta$ -cell proliferation in $\beta$ IrKO mice.....	34
3.4    Fetal $\beta$ IrKO islet cells present enhanced replication and pro-survival signalling pathway activity .....	43
3.5    Increased vascularization in fetal $\beta$ IrKO pancreatic islets.....	46
3.6 $\beta$ -cell-specific <i>Ir</i> knockout at the second transition of pancreatic development does not affect $\beta$ -cell identity.....	51
3.7    Postnatal $\beta$ IrKO confirmation.....	54
3.8    Phenotypical analysis of postnatally induced $\beta$ -cell specific <i>Ir</i> knockout mice .....	57
3.9    Metabolic studies of postnatally induced $\beta$ IrKO mice.....	60
3.10   Pancreas morphology at 20 weeks post-tamoxifen injection.....	65
3.11   Under high-fat diet, postnatally induced $\beta$ IrKO mice display comparable glucose metabolism to control mice.....	68

Chapter 4 - Discussion .....	73
4.1 Does $\beta$ -cell-specific <i>Ir</i> knockout affect islet formation during secondary transition?.....	73
4.2 Could the $\beta$ -cell-specific <i>Ir</i> knockout promote activity of homologous signalling pathways? .....	75
4.3 Is the level of islet vascularization associated with islet growth during prenatal life?.....	78
4.4 Do postnatally induced $\beta$ -cell-specific knockout mice exhibit age-dependent glucose intolerance?.....	79
4.4.1 Recombination efficiency of inducible postnatal $\beta$ -cell-specific <i>Ir</i> knockout? .....	79
4.4.2 Does postnatal $\beta$ -cell-specific <i>Ir</i> knockout affect glucose metabolism? ..	79
4.5 Do postnatally induced $\beta$ -cell-specific knockout mice exhibit glucose intolerance after high-fat diet stress? .....	82
4.6 Limitations .....	83
4.7 Future directions .....	84
Chapter 5 - References.....	86
Appendices.....	98
Curriculum Vitae .....	103

## **List of Tables**

Table 1: List of Antibodies used for Immunostaining and Western-Blot Analyses .....36

## List of Figures

<i>Figure 1.1.</i> Ligand signalling through the Insulin/IGF1 receptor family .....	7
<i>Figure 1.2.</i> A schematic of experimental $\beta$ -cell <i>Ir</i> knockout time points with reference to important islet development events in rodents.....	15
<i>Figure 2.1.</i> Generation of experimental mouse groups .....	30
<i>Figure 3.1.</i> Confirmation of $\beta$ -cell specific <i>Ir</i> knockout .....	30
<i>Figure 3.2.</i> Islet growth in fetal $\beta$ IrKO pancreata .....	33
<i>Figure 3.3.</i> Enhanced $\beta$ -cell proliferation in fetal $\beta$ IrKO pancreata.....	36
<i>Figure 3.4.</i> Similar levels of islet neogenesis from epithelial ducts in fetal $\beta$ IrKO and control pancreata.....	38
<i>Figure 3.5.</i> No change in cell apoptosis in fetal $\beta$ IrKO pancreata .....	40
<i>Figure 3.6.</i> Downstream IR signalling pathway analysis .....	42
<i>Figure 3.7.</i> Strong localization and increased levels of IGF2 in fetal $\beta$ IrKO pancreata .....	45
<i>Figure 3.8.</i> Fetal $\beta$ IrKO display increased vascularization .....	48
<i>Figure 3.9.</i> Increased Vegf-a levels in fetal $\beta$ IrKO pancreata.....	50
<i>Figure 3.10.</i> Fetal $\beta$ IrKO islets expressed TFs necessary for $\beta$ -cell identity and function ...	53
<i>Figure 3.11.</i> Western blot analysis of $\beta$ -cell <i>Ir</i> knockout efficiency .....	56
<i>Figure 3.12.</i> Phenotypic analysis of postnatal tamoxifen-induced $\beta$ IrKO mice .....	59

*Figure 3.13.* Adult  $\beta$ IrKO mice demonstrate normal glucose metabolism at 4 and 8 weeks after *Ir* knockout .....62

*Figure 3.14.* Aged experimental groups appear to exhibit similar levels of glucose intolerance.....64

*Figure 3.15.* No differences in pancreatic morphology were observed between  $\beta$ IrKO and control mice .....67

*Figure 3.16.* Phenotypes of experimental male mice after 6 weeks of high-fat diet .....70

*Figure 3.17.* Metabolic studies at 8 weeks post-tamoxifen in male mice after 6 weeks on high-fat diet.....72

*Figure 4.1.* Proposed adaptive signalling mechanisms in fetal  $\beta$ IrKO mice .....77

## **List of Appendices**

Appendix A: Classification II Laboratory Approval Form.....	99
Appendix B: Biosafety Approval Form.....	101
Appendix C: Animal Use Protocol .....	102

## List of Abbreviations

ANOVA	Analysis of variance
AUC	Area under the curve
BSA	Bovine serum albumin
CreERT	Tamoxifen-inducible cre recombinase
Ctrl	Control
DAPI	4',6-diamidino-2-phenylindole
ELISA	Enzyme-linked immunosorbent assay
Gcg	Glucagon
GSIS	Glucose-stimulated insulin secretion
GTT	Glucose tolerance test
i.p.	Intraperitoneal
Ins	Insulin
INS-1	Rat insulinoma cell line
IR	Insulin receptor
ISL1	Islet-1
ITT	Insulin tolerance test
MafA	v-maf avian musculoaponeurotic fibrosarcoma oncogene homolog A
MIP	Mouse insulin promoter
Ngn3	Neurogenin 3
Nkx6.1	NK6 homeobox 1
Pan-CK	Pan-Cytokeratin
PBS	Phosphate-buffered saline

PCR	Polymerase chain reaction
Pdx-1	Pancreatic duodenal homeobox-1
PECAM-1	Platelet endothelial cell adhesion molecule-1
PFA	Paraformaldehyde
Ptf1a	Pancreas transcription factor 1a
RIP	Rat insulin promoter
SEM	Standard error of mean
TF	Transcription factor
IGF1	Insulin-like growth factor-1
IGF2	Insulin-like growth factor-2
IGF1R	Insulin-like growth factor-1 receptor
Glut-2	Glucose transporter 2
TUNEL	Terminal deoxynucleotidyl transferase mediated nick end-labelling
Vegf-a	Vascular endothelial growth factor-a
$\beta$ IrKO	$\beta$ -cell-specific insulin receptor knockout

# Chapter 1 - Introduction

## 1.1 Significance of study

Pancreatic development is a complex process that requires temporal regulation of both transcription factor expression and intricate signalling pathways to generate physiologically functional mature adult islets. The  $\beta$ -cell insulin receptor (IR) has been previously shown to influence islet survival and function through autocrine insulin signalling in postnatal life. However, the temporal importance of  $\beta$ -cell insulin receptor signalling on the islet morphology, expression of transcription factors, and metabolic proteins necessary for  $\beta$ -cell maturation, proliferation, and survival has yet to be sufficiently investigated. In addition, the knowledge of the physiological function of insulin signalling during fetal  $\beta$ -cell embryogenesis is crucial for understanding abnormal islet development and maturation *in utero*. This thesis demonstrates that the intracellular mechanisms of insulin receptor-mediated signalling that regulate  $\beta$ -cell development, survival, and function vary during different stages of life and during diabetes progression. These results will contribute to improving long-term success of current cell-based therapies for diabetes.

## 1.2 The pancreas and islet of Langerhans

The pancreas is an organ that contributes to digestion and glucose regulation, and consists of both exocrine and endocrine compartments. In the exocrine tissue (~98% of the pancreas), acinar cells secrete digestive enzymes through specialized duct cells into the duodenum. The endocrine compartment (~2% of the pancreas) is composed of functional clusters of cells known as the islets of Langerhans, which contain multiple cell types that secrete distinct hormones. Murine islets are comprised of predominantly insulin-secreting  $\beta$ -cells (~80%) that form the central core and are surrounded by glucagon-secreting  $\alpha$ -cells (~10%), while the remaining endocrine cell types are pancreatic polypeptide secreting  $\gamma$ -cells, somatostatin-secreting  $\delta$ -cells, and ghrelin-secreting  $\epsilon$ -cells. Out of these endocrine cells,  $\alpha$ - and  $\beta$ -cells have important opposing

physiological effects on blood glucose homeostasis. In response to sensing hypoglycemia,  $\alpha$ -cells secrete glucagon that then promotes the liver to facilitate glycogenolysis and gluconeogenesis, leading to an increase in blood glucose concentrations. In contrast, high blood glucose levels stimulate  $\beta$ -cells to produce and release insulin, which stimulates glucose uptake from the bloodstream into skeletal muscle, liver, and adipose tissues for energy storage. Therefore, proper development of the pancreas, specifically the  $\beta$ -cells, is critical in meeting the dynamic metabolic demand under both physiological and pathological conditions (Montanya et al. 2000).

### 1.3 Pancreas development & $\beta$ -cell formation

The murine pancreas undergoes three different transition stages of pancreatic development, where the pancreas starts to form from the endoderm at embryonic day 8.5 (e8.5, where e0.5 is defined as the day of observing vaginal plug in the pregnant female). During the primary transition (e9.5-e12.5), regions of endodermal gut tube express the required transcription factors needed for pancreatic development, pancreatic duodenal homeobox 1 (Pdx-1) and pancreas transcription factor 1a (Ptf1a), and form the ventral and dorsal buds of the pancreas (Offield et al. 1996, Kawaguchi et al. 2002, Gittes 2008). During this time, the first wave of endocrine differentiation begins and is critically dependent on the expression of the transcription factor neurogenin 3 (Ngn3), which is activated after Notch activity is downregulated, and the subsequent activation of NK homeobox 6.1 (Nkx6.1). However, the insulin-positive  $\beta$ -cells that emerge early in the development within endocrine clusters do not contribute to the postnatal mature islets (Pan et al. 2011, Gunasekaran et al. 2012). Throughout the secondary transition (e12.5-e18), the primitive ventral and dorsal pancreatic buds rotate and fuse to form a single organ, and the cellular architecture changes dramatically in the pancreas. The pancreatic progenitor cells adopt either 'tip' or 'trunk' identity. The cells in the 'tip' region are fated to become acinar cells while the 'trunk' region can differentiate into either ducts or endocrine cells. There is rapid differentiation and branching of acinar and duct cells to form a complex network. Similarly, there is extensive neogenesis and expansion of endocrine cells, especially the  $\beta$ -cells, accompanied by the expressions of their essential

transcription factors. These expanding islet cells form from or adjacent to pancreatic ducts, suggesting that precursor cells migrate out of the ductal region to form islet clusters (Nielsen et al. 1999, Al-Hasani et al. 2013). Unlike primitive endocrine cells from primary transition,  $\beta$ -cells from secondary transition form mature, functional islets and serve as the primary source for  $\beta$ -cell replication during late gestation and in adult mice (Gunasekaran et al. 2012). Lastly, the third transition spans from e18 to 3 weeks after birth, where the endocrine cells undergo high levels of neogenesis, replication, and apoptosis, indicating islet expansion, remodelling, and organization in the developing endocrine pancreas (Kaung 1994, Scaglia et al. 1997). By the end of the third transition,  $\beta$ -cell neogenesis is rapidly diminished and replaced by  $\beta$ -cell replication, the primary mechanism responsible for postnatal  $\beta$ -cell formation (Dor et al. 2004). In order to maintain glucose homeostasis in adult mice, the  $\beta$ -cell mass dynamically changes through a balance of  $\beta$ -cell replication and apoptosis (Montanya et al. 2000). However, impaired prenatal development and maturation of islets may lead to the formation of  $\beta$ -cells that are inadequate for managing metabolic stress in adult life.

## 1.4 Islet vascularization

Although the endocrine compartment only comprises ~2% of the mature pancreas volume, it receives ~10% of the total pancreatic blood flow from the celiac and superior mesenteric arteries. The islets are highly vascularized, with a dense network of capillaries that are more fenestrated than the exocrine tissue (Jansson et al. 1983, Henderson et al. 1985, Jansson et al. 2002). This allows for the rapid and efficient exchange of nutrients and hormones between endocrine cells and the bloodstream. Pancreatic  $\beta$ -cells express high levels of vascular endothelial growth factor-a (Vegf-a), which stimulates the recruitment of endothelial cells, promotes the formation of blood vessels during embryonic pancreas development, and maintains islet vasculature and integrity in postnatal life (Christofori et al. 1995, Brissova et al. 2006, Reinert et al. 2013). Furthermore, vascular growth is closely associated with  $\beta$ -cell proliferation (Johansson et al. 2006) as seen in mice with short-term (~2 weeks)  $\beta$ -cell-specific *Vegf-a* overexpression that resulted in islet hypervascularization simultaneous with increased  $\beta$ -

cell proliferation (De Leu et al. 2014). In contrast, long-term (~2 month) overexpression of *Vegf-a* in  $\beta$ -cells resulted in disorganized islets with hypervascularization, increased inflammation, impaired insulin secretion, and decreased  $\beta$ -cell mass with age (Agudo et al. 2012). These studies suggest that Vegf-a signalling plays an important role in islet vasculature,  $\beta$ -cell survival, and function in a time-dependent manner.

## 1.5 Overview of diabetes mellitus

Glucose homeostasis relies on the fine balance between production by the liver and utilization by insulin-dependent tissues such as fat and muscle, as well as insulin-independent tissues. Diabetes mellitus is a chronic metabolic disease characterized by a disruption in glucose homeostasis that can arise due to multiple dysfunctions in the insulin production and secretion pathway. The resulting hyperglycemia leads to a high insulin secretory demand, which further exacerbates  $\beta$ -cell function and accelerates  $\beta$ -cell death. While type 1 diabetes mellitus is characterized by a near absolute deficiency of  $\beta$ -cells, the onset of type 2 diabetes mellitus is due to insufficient insulin production, islet hypervascularization, and progressive  $\beta$ -cell mass reduction. In both cases,  $\beta$ -cell dysfunction and failure are perceived as the main cause.

Type 1 diabetics (~10% of the total diabetic population) suffer from persistent autoimmune destruction of the  $\beta$ -cells, and the pathological indicators typically begin to develop in children and young adults. Due to a loss of up to ~90% of  $\beta$ -cells, patients rely on perpetual exogenous injections of insulin to regulate their blood glucose levels. Alternatively, the Edmonton protocol is a standard cell-based therapy that involves isolation of islets from several cadaveric donors and transplantation into the hepatic portal vein of immunosuppressed patients, restoring endogenous insulin secretion and allowing these patients to become independent from exogenous insulin for as long as 5 years (Shapiro 2012). However, islet transplantation is heavily limited by the availability of cadaveric donors and the therapeutic effectiveness of the current transplantation protocol.

Type 2 diabetes (~90% of the total diabetic population) is characterized by several pathological defects and typically manifests itself later in adult life. Genetic composition and environmental factors, especially obesity, have been closely linked to type 2 diabetes progression. Typically, insulin resistance in insulin-responsive peripheral tissue occurs, reducing the clearance of glucose from circulation and leading to multiple health problems that develop from hyperglycemia. The  $\beta$ -cell mass initially expands to compensate for this insulin resistance but the compensatory mechanism eventually fails, resulting in decreased  $\beta$ -cell mass and relative deterioration of insulin production and secretion (Kahn 1994). Furthermore, the chronic islet hypervascularization seen in type 2 diabetics can result in islet fibrosis, inflammation, and ultimately contributes to  $\beta$ -cell death (Agudo et al. 2012). Type 2 diabetes can be managed by lifestyle improvements, insulin sensitizers, and if necessary, exogenous insulin. Although symptoms are well-characterized, the causes for type 2 diabetes is multifactorial and complex, and some form of insulin resistance may involve the alteration in the insulin receptor itself, including decreased receptor levels and activation in the periphery tissues as well as in  $\beta$ -cells (Taylor et al. 1990, Pessin et al. 2000, Folli et al. 2011).

## 1.6 Insulin receptors

The insulin receptor is a receptor tyrosine kinase that contains two extracellular regulatory  $\alpha$ -subunits and two transmembrane catalytic  $\beta$ -subunits that are linked by disulfide bonds (Kahn 1993, Lee et al. 1994). IR exists as two isoforms, IR-A and IR-B, by alternative splicing of the exon 11 in the  $\alpha$ -subunit. These isoforms show tissue-specific expression - IR-A (exon 11-) is primarily expressed in fetal cells, with lower expression in metabolically active adult tissues, such as muscle, liver, and adipose (Frasca et al. 1999), whereas IR-B (exon 11+) is mainly expressed in liver and muscle tissues (Frasca et al. 1999, Nakae et al. 2001). Ligand binding to one of the IR  $\alpha$ -subunits induces a conformational change that promotes  $\beta$ -subunits to bind ATP and autophosphorylate multiple tyrosine residues, leading to the phosphorylation of the insulin receptor substrate (IRS) proteins and activation of downstream signalling pathways. Consequently, any loss of tyrosine kinase activity is accompanied by a loss in

the ability of the receptor to signal (Kahn 1993). Interestingly, IR and insulin-like growth factor 1 receptor (IGF1R) have a high degree of structural homology and share similar downstream substrates, and compensatory upregulation of IGF1R in the absence of IR has been previously reported (Van Schravendijk et al. 1987, Assmann et al. 2009).

## 1.7 Insulin receptor ligands

In low concentrations, insulin binds to IR while insulin-like growth factor-1 (IGF1) activates IGF1R; however, due to the homology between IR and IGF1R structures, insulin and IGF1 are able to bind to both receptors under higher ligand concentrations. In addition, insulin-like growth factor-2 (IGF2), which activates its corresponding receptor (IGF2R), has the ability to bind to both receptors with relatively high affinities (**Figure 1.1**)(Louvi et al. 1997, Nakae et al. 2001, Assmann et al. 2009). In rodents, IGF2 levels rapidly diminishes after birth, indicating its importance in prenatal development but not in postnatal life (Murphy et al. 1987).

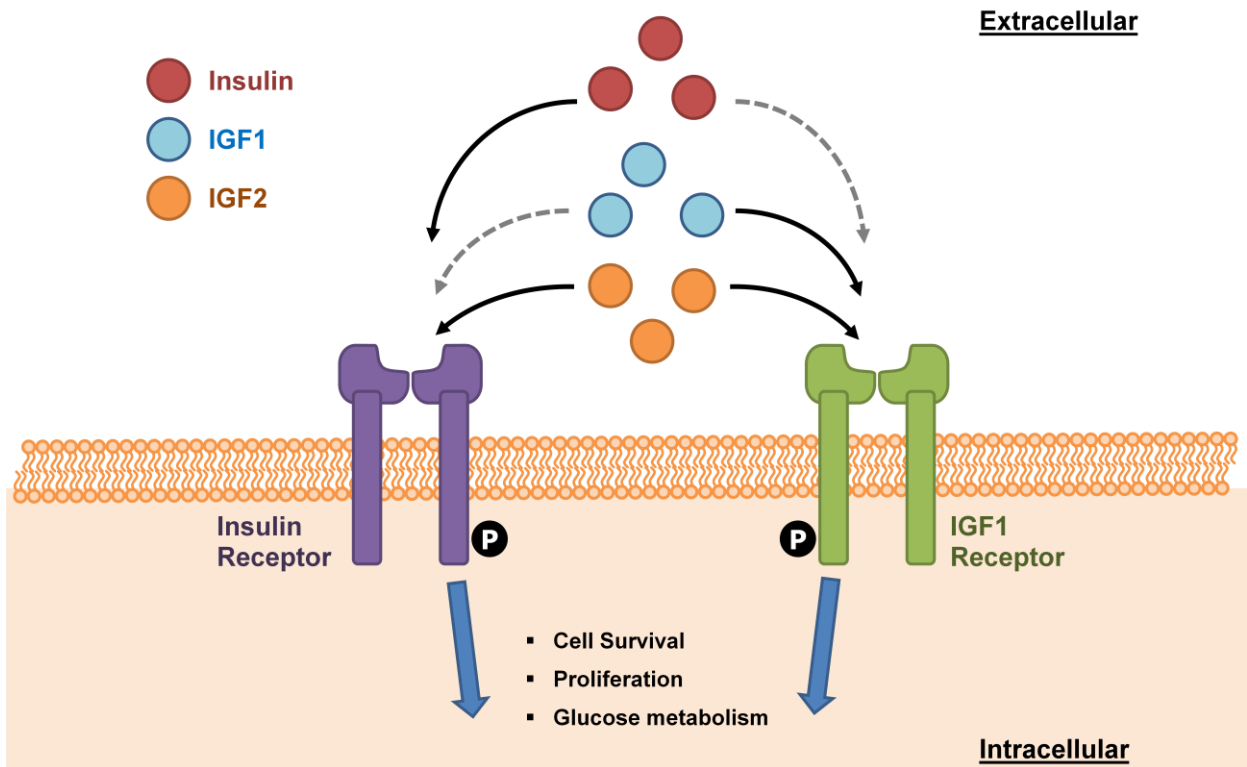


*Figure 1.1. Ligand signalling through the Insulin/IGF1 receptor family*

While insulin and IGF1 ligand bind to their own receptors with high affinity (solid arrows), they are able to signal through the cognate receptor with lower affinity (dashed arrows) under high concentrations. Alternatively, IGF2 has the ability to bind to both receptors with relatively high affinities. Insulin and IGF1 receptor share similar downstream signalling pathways that contribute to cell proliferation, survival, and glucose metabolism.

## 1.8 Insulin production and secretion

The production of functional insulin involves multiple post-translational cleaving steps from preproinsulin (the precursor form) to mature insulin and its storage in secretory granules. The precise control of  $\beta$ -cell insulin secretion is essential to ensure regulated glucose homeostasis. Normally, an increase in blood glucose concentration stimulates insulin secretion by allowing the transport of free calcium into  $\beta$ -cells. This results in a biphasic insulin secretion response. The first phase (~10 min) corresponds to the exocytosis of prepared insulin-containing granules triggered by the initial  $\text{Ca}^{2+}$  influx. The second phase involves the prolonged slow release of insulin from granules mobilized from the reserve pool until euglycemia is achieved, as well as replenishment of insulin-containing granules (Rosman et al. 2000).

It is well established that insulin has a positive autocrine feedback on insulin production through IR activity (Leibiger et al. 1998, Leibiger et al. 2001). Interestingly, IR-A and IR-B isoforms show functionally different selective insulin signalling in pancreatic  $\beta$ -cells. Insulin binding and activation of IR-A promotes insulin gene transcription, while the activation of IR-B leads to upregulation of the glucokinase expression in an autocrine feedback loop (Leibiger et al. 2001, Leibiger et al. 2008). However, the autocrine regulation of exogenous insulin on insulin secretion in  $\beta$ -cells is controversial. Using 5-hydroxytryptamine (5-HT) secretion as a marker of exocytosis in  $\beta$ -cells, amperometric measurements of exocytosis from single, isolated human and mouse islets demonstrated increased insulin secretion in response to exogenous insulin treatment (Aspinwall et al. 1999). In contrast, when C-peptide release rates were measured as an indicator of insulin secretion, exogenous insulin application had no stimulatory effect on endogenous insulin secretion in isolated perfused rat islets (Zawalich et al. 2002). Transcription factor levels in  $\beta$ -cells are also responsible for regulating insulin secretion. A reduction in Pdx-1 and Islet-1 has been linked to impaired glucose-stimulated insulin secretion in  $\beta$ -cells (Brissova et al. 2002, Gauthier et al. 2009, Ediger et al. 2014), while overexpression of *MafA* in neonatal rat islets enhanced insulin synthesis and secretion in response to glucose stimulation (Aguayo-Mazzucato et al. 2011).

## 1.9 Insulin receptor signalling pathways

Upon insulin binding to IR, the two major signalling pathways that are activated are the phosphoinositide 3-kinase (PI3K)/Akt pathway and the Ras/Raf-1/mitogen-activated protein kinase (MAPK) cascade. Insulin receptor signalling plays a mitotic and metabolic role in a wide variety of tissues. In most metabolically active tissues (muscle, liver, adipose), the primary function of insulin signalling is to activate PI3K, Akt, and P70S6K to stimulate protein synthesis, glycogen synthesis, and GLUT-4 translocation to the cell membrane for facilitating glucose clearance. However, IR signalling in these tissues contributes to mitogenesis to a lesser degree (Shymko et al. 1997). On the other hand, in addition to increasing metabolic activities such as insulin synthesis, IR signalling also plays an essential role in  $\beta$ -cell proliferation and survival (Johnson et al. 2006, Johnson et al. 2008, Alejandro et al. 2010). Mice lacking IR in  $\beta$ -cells, but not IGF1R, have increased apoptosis, decreased proliferation, and reduced  $\beta$ -cell mass, demonstrating the necessity of IR in  $\beta$ -cell survival (Johnson et al. 2008, Wang et al. 2013). In fact, overexpression of *IR* in *in vitro*  $\beta$ -cell cell lines led to enhanced  $\beta$ -cell proliferation and increased metabolic activities such as insulin production (Xu et al. 1998, Kim et al. 2013).

When examining downstream substrates, studies of *in vitro* insulinoma cells and transgenic mouse models overexpressing *Akt* have suggested that IR signalling promotes  $\beta$ -cell survival through the Akt pathway (Bernal-Mizrachi et al. 2001). However, adult mice lacking  $\beta$ -cell Akt activity did not exhibit increased  $\beta$ -cell apoptosis and retained normal  $\beta$ -cell mass despite the presence of glucose intolerance due to defective insulin secretion (Bernal-Mizrachi et al. 2004). This result indicates the involvement of Akt-independent signalling pathways on  $\beta$ -cell survival. Alternatively, the anti-apoptotic and pro-mitogenic effects of Raf-1/MAPK activities have been strongly implicated in  $\beta$ -cells. For instance, subjecting mouse islets to exogenous insulin rapidly activated Raf-1 pathway and enhanced  $\beta$ -cell survival, while treatments with Raf-1 inhibitor resulted in increased  $\beta$ -cell death (Alejandro et al. 2010, Johnson et al. 2008). These studies emphasize on the essential roles of Akt and Raf-1 signalling pathways on  $\beta$ -cell

regulation, but a full understanding of how these pathways control  $\beta$ -cell function is not yet clear.

## 1.10 Insulin receptor in different tissues

IR is expressed in a wide range of tissues and its activation by insulin typically promotes the uptake of glucose from the blood into skeletal muscle, liver, and adipose tissues. Global heterozygous deletion of *Ir* in mice displayed normal phenotype and physiological glucose homeostasis at 2 months of age, demonstrating that expression of one *Ir* allele is sufficient for maintaining euglycemia. Ubiquitous *Ir* knockout mice, however, displayed increasing postnatal growth retardation, hyperglycemia, hyperinsulinemia, and died within one week after birth due to diabetic ketoacidosis (Joshi et al. 1996, Folli et al. 2011). Similarly, insulin knockout mice also died shortly after birth due to severe diabetic ketoacidosis and exhibited slight growth retardation (Duvillie 1997). Surprisingly, null *Ir* mice were indistinguishable at birth from littermates, suggesting that IR is not required for normal embryonic development (Joshi et al. 1996, Wicksteed et al. 2010). *Igf1*, *Igf2*, and *Igf1r* were also investigated in a global knockout manner and were determined to be necessary for proper embryonic development in mice (DeChiara et al. 1990, Liu et al. 1993).

Since the disruption of insulin signalling in different tissues contributes to type 2 diabetes pathogenesis, several site-specific *Ir* knockout models have been examined in mice (Kitamura et al. 2003). Skeletal muscle is the primary site of insulin-dependent glucose clearance from blood, and insulin resistance in skeletal muscle is an essential part of the disease progression in type 2 diabetes (Cline et al. 1999). Notably, skeletal muscle-specific *Ir* knockout mice led to impaired insulin signaling without systemic insulin resistance, indicating the presence of compensatory mechanisms through the IGF1R and increased uptake of glucose by other tissues (Shefi-Friedman et al. 2001). Similarly, adipose-specific *Ir* knockout produced selective insulin resistance in adipose tissue that did not affect whole body glucose metabolism (Guerra et al. 2001, Blueher et al. 2002). The liver plays a vital role in physiological glucose homeostasis as it is subjected to intricate regulation by insulin, glucagon, and many other hormones. Consequently, liver-

specific *Ir* knockout mice exhibited hyperinsulinemia, severe insulin resistance, and glucose intolerance, suggesting the importance of liver IR on glucose homeostasis and facilitation of insulin clearance (Michael et al. 2000).

### 1.11 Insulin receptor and $\beta$ -cells

Type 2 diabetes disease progression is closely associated with  $\beta$ -cell failure, particularly the impairment of glucose-stimulated insulin secretion. To elucidate the role of insulin signalling in mature  $\beta$ -cells, several  $\beta$ -cell-specific *Ir* knockout studies using the *rat insulin promoter* have been conducted in mice. These mice displayed progressive age-dependent glucose impairment starting as early as 5 weeks of age concomitant with islet mass reduction, suggesting its importance in maintaining  $\beta$ -cell survival and function (Kulkarni et al. 1999, Ueki et al. 2006, Okada et al. 2007). Alternatively, mice with  $\beta$ -cell-specific deletion of the *Igf1r* exhibited glucose intolerance likely due to the defective glucose stimulated insulin secretion but their  $\beta$ -cell mass, islet size, and pancreatic insulin content was unaltered (Xuan et al. 2002, Kulkarni et al. 2002). Taken together, it seems like  $\beta$ -cell IR, but not IGF1R, is required for postnatal islet survival. Importantly, both  $\beta$ -cell-specific *Ir* and *Igf1r* knockout mice are phenotypically normal at birth and show no alterations to prenatal pancreatic development (Kulkarni et al. 1999, Kulkarni et al. 2002, Okada et al. 2007). Therefore, it appears that  $\beta$ -cell IR and IGF1R play a minor role in pancreatic organogenesis, but are necessary for adaptive islet function in response to increasing metabolic stress during postnatal life (Smith et al. 1991). Due to the importance of IR in  $\beta$ -cell health and functionality along with the possibility of compensatory response from IGF1R, IGF1 and IGF2, an in-depth analysis of  $\beta$ -cell IR functionality during islet development at the molecular morphological level needs to be implemented.

### 1.12 High-fat diet, $\beta$ -cell insulin resistance and dysfunction

Genetic factors and obesity are often associated with the progression of type 2 diabetes. In various strains of diabetic mouse models, an increase in dietary fat content has been shown to generate obese mice that develop diabetes. The C57BL/6J mouse (also

known as B6) is a widely used type 2 diabetes model as it spontaneously develops obesity, peripheral insulin resistance, hyperinsulinemia, and hyperglycemia when restricted to high-fat diet, and often remain physically lean and maintain normal phenotypes under low-fat chow. Generally, B6 mice develop diabetic symptoms as early as 1 month after the introduction of high-fat diet (Surwit et al. 1988, Collins et al. 2004, Okada et al. 2007). At the morphological level, increased  $\beta$ -cell proliferation causes islet compensatory growth after 14 weeks on high-fat diet. However, these mice exhibited impaired *in vivo* glucose tolerance and glucose-stimulated insulin secretion, indicating that islets are replicating in an attempt to compensate for increased metabolic demand and insulin resistance, but are insufficient or functionally defective and unable to maintain normal glucose tolerance (Roat et al. 2014).

Few studies have investigated the role of  $\beta$ -cell insulin signalling in high-fat diet fed pre-diabetic B6 mice. After 20 weeks of high-fat diet (with 55% fat content), wild-type,  $\beta$ -cell-specific *Ir* knockout, and  $\beta$ -cell-specific *Igf1r* knockout mice all displayed obesity, hyperinsulinemia, and hyperglycemia. Out of all the experimental groups,  $\beta$ -cell-specific *Ir* knockout mice demonstrated the most severe hyperglycemia and glucose intolerance, and 30% died after 16 weeks on high-fat diet (Okada et al. 2007). In terms of pancreatic morphology, these mice failed to develop the islet compensatory growth response normally seen in wild-type and  $\beta$ -cell-specific *Igf1r* knockout groups on high-fat diet, indicating the importance of IR signalling in  $\beta$ -cell growth and survival in response to metabolic stress during postnatal life. In addition, nuclear Pdx-1 levels were reduced in these mice, suggesting impaired  $\beta$ -cell growth and function as well as defects in insulin production (Okada et al. 2007). Consistent with these findings, heterozygous insulin knockout B6 mice did not develop islet compensatory growth, hyperinsulinemia, or obesity under high-fat diet (with 58% fat content)(Mehran et al. 2012). Taken together, these studies highlight the necessity of insulin signalling in modulating islet proliferation responses in B6 mice on a high-fat diet, and suggest that differing degrees of insulin signalling affect the progression of diabetes.

### 1.13 Rationale, objectives, and hypothesis

Appropriate pancreatic embryogenesis and remodeling is crucial for the development of dynamic  $\beta$ -cells that can adapt to changing metabolic demands. Despite its importance in  $\beta$ -cell function and survival, the molecular mechanisms involved in the IR signalling pathway, which affects transcription factor expression and proliferation, during different developmental periods have yet to be studied. We propose investigate the temporal role of the  $\beta$ -cell IR autocrine/paracrine signalling in fetal and postnatal islet maturation and function, as well as postnatal mice under high-fat diet conditions, by utilizing tamoxifen-inducible Cre recombinase under control of the *mouse insulin promoter (MIP)* to drive  $\beta$ -cell-specific *Ir* knockout (Wicksteed et al. 2010, Hayashi et al. 2002, Liu et al. 2010, Tamarina et al. 2014). In contrast to previous studies, we chose to use *MIP* instead of *RIP* because *MIP* mice appear to lack the ectopic expression seen in the hypothalamus of *RIP* mice (Wicksteed et al. 2010, Tamarina et al. 2014). Previous studies suggested normal pancreatic development at birth despite a lack of  $\beta$ -cell IR from conception, indicating the presence of network adaptation from other signalling pathways (Kulkarni et al. 1999, Okada et al. 2007, Ueki et al. 2006). This project investigates the in-depth characterization of islet morphology during fetal pancreatic development after a temporal  $\beta$ -cell *Ir* knockout induced at the secondary transition of pancreas development (endocrine differentiation and proliferation), and explores the consequential adaptive signalling from the homologous receptor IGF1R and its ligands, IGF1 and IGF2, that may contribute to proper pancreatic embryogenesis. In addition, previous  $\beta$ -cell-specific *Ir* knockout studies utilized a mouse model with  $\beta$ -cell-specific *Ir* knockout at conception, and as a result, these mice lack  $\beta$ -cell IR throughout pancreas embryogenesis. In contrast, this thesis focuses on the role of  $\beta$ -cell IR in the postnatal life by inducing  $\beta$ -cell-specific *Ir* knockout 4 weeks after birth, allowing undisturbed pancreatic maturation and remodelling in third transition (**Figure 1.2**). Lastly, this thesis will utilize the postnally induced  $\beta$ -cell-specific *Ir* knockout mice subjected to high-fat diet to investigate the gene-dose dependent effect of *Ir* (wild-type, heterozygous, null) on islet proliferation and function during diabetes progression.

## Objective

To investigate the temporal role of the  $\beta$ -cell IR autocrine/paracrine signalling in fetal and postnatal islet formation and function, as well as during high-fat diet induced diabetes pathogenesis.

## Hypothesis

1. The  $\beta$ -cell IR is required for normal islet formation and remodelling in prenatal life
2.  $\beta$ -cell autocrine/paracrine insulin signalling is necessary for the maintenance of  $\beta$ -cell function and survival in postnatal life

## Specific Questions

1. Does  $\beta$ -cell-specific *Ir* knockout affect islet formation during secondary transition?
2. Could the  $\beta$ -cell-specific *Ir* knockout promote activity of homologous signalling pathways?
3. Is the level of islet vascularization associated with islet growth during prenatal life?
4. Do postnatally induced  $\beta$ -cell-specific knockout mice exhibit age-dependent glucose intolerance?
5. Do postnatally induced  $\beta$ -cell-specific knockout mice exhibit glucose intolerance after high-fat diet stress?

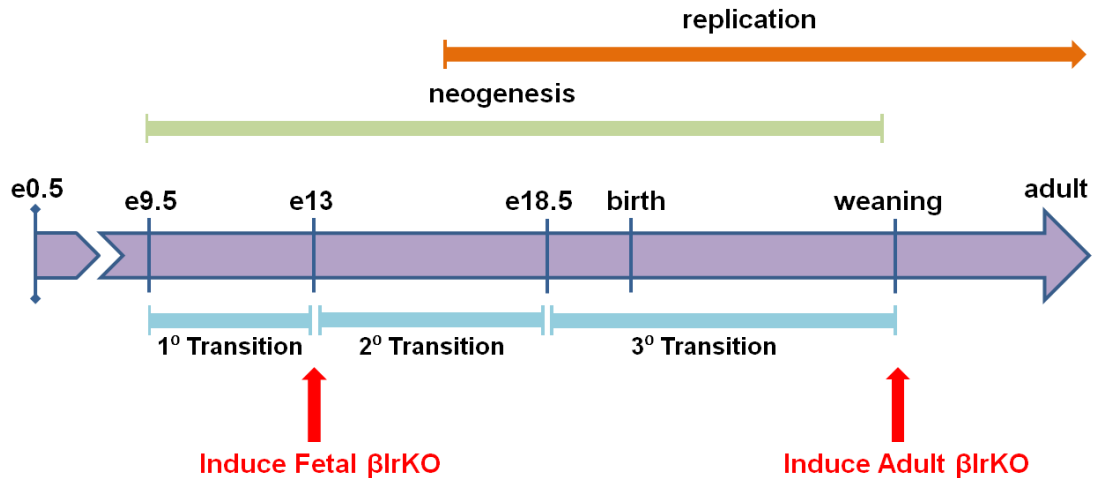


***Figure 1.2.* A schematic of experimental  $\beta$ -cell *Ir* knockout time points with reference to important islet development events in rodents.**

In rodents, pancreatic development can be separated into 3 transitional phases starting around embryonic day 9.5 (e9.5). Generally, prenatal  $\beta$ -cell neogenesis persists throughout prenatal pancreatic formation and maturation, but diminishes after birth and is replaced by  $\beta$ -cell replication, which becomes the primary mechanism contributing to postnatal  $\beta$ -cell growth. For our fetal  $\beta$ IrKO studies, tamoxifen was administered (via intraperitoneal) into pregnant females at e13, and pups were subsequently dissected for pancreata collection at e19. For our postnatal  $\beta$ IrKO studies,  $\beta$ -cell *Ir* was knocked out 3-4 weeks after birth.

## Chapter 2 - Materials and Methods

### 2.1 Generation of $\beta$ -cell-specific *Ir* knockout mice

*B6.129S4(FVB)-Insr<sup>tm1Khn</sup>/J* mice (*IR<sup>fl/fl</sup>*) with *loxP* sites flanking exon 4 of the *Ir* gene were obtained from The Jackson Laboratories (Bar Harbor, MA, USA; stock number: 006955). Transgenic *Tg(Ins1-Cre/ERT)<sup>1Lphi</sup>* (*MIPCreERT*) mice with tamoxifen inducible Cre-recombinase expression under the control of the *mouse insulin 1 promoter* were obtained from Dr. Louis Philipson's laboratory (University of Chicago, Chicago, IL, USA). To verify the *mouse insulin 1 promoter*-driven Cre recombinase expression in pancreatic islets, *MIPCreERT* mice were crossed with a *B6.Cg-Gt(ROSA)26Sor<sup>tm9(CAG-tdTomato)Hze</sup>/J* reporter strain (stock number: 007909; The Jackson Laboratories). The transgenic mouse lines *MIPCreERT* and *IR<sup>fl/fl</sup>* were crossed at our research facility (Victoria Research Laboratories, Victoria Hospital, London, ON, CA) to generate *MIPCreERT<sup>+/-</sup>;IR<sup>fl/+</sup>* mice, which were subsequently mated with each other to generate experimental groups consisting of *MIPCreERT<sup>+</sup>;IR<sup>+/+</sup>* (control), *MIPCreERT<sup>-</sup>;IR<sup>fl/fl</sup>* (control), *MIPCreERT<sup>+</sup>;IR<sup>fl/+</sup>* (heterozygous), and *MIPCreERT<sup>+</sup>;IR<sup>fl/fl</sup>* ( $\beta$ IrKO) groups (**Figure 2.1A**). These genotypes were identified through the polymerase chain reaction (PCR) procedure described below.

All mice were provided *ad libitum* access to both food and water. All animal use protocols were approved by the Animal Use Subcommittee at Western University in accordance with the Canadian Council of Animal Care.

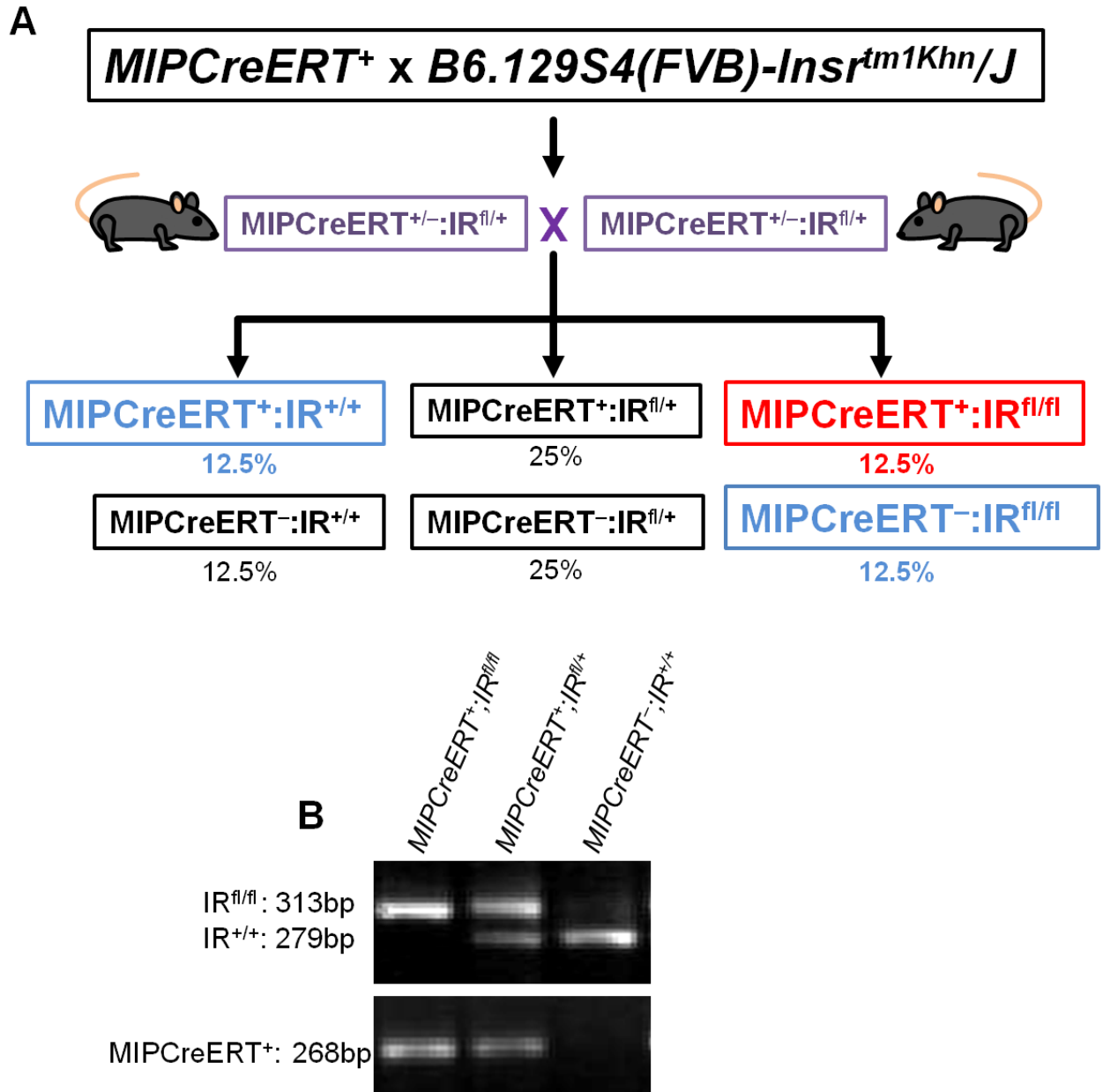


**Figure 2.1. Generation of experimental mouse groups**

(A) The breeding schematic to generate experimental groups. By intercrossing  $MIPCreERT^{+/-}; IR^{fl/+}$  mice, we produced experimental animals with the  $\beta$ IrKO genotype ( $MIPCreERT^+; IR^{fl/fl}$ , red) alongside control mice ( $MIPCreERT^+; IR^{+/+}$  and  $MIPCreERT^-; IR^{fl/fl}$ , blue). (B) Genotypes of fetal mice were determined PCR of the *Ir* and *MIPCreERT* genes, followed by gel electrophoresis. Representative images are shown.

## 2.2 Mouse genotyping

DNA was extracted from fetal (obtained at e19) or adult (obtained at p21) tail snips using 50  $\mu$ L of base solution (25 mM NaOH; 0.2 mM EDTA) and placed on a heat block set at 95  $^{\circ}$ C for 30 min followed by 1 hour cool down at room temperature. Subsequently, 50  $\mu$ L of 40 mM Tris HCl (pH 5.5) was added to each sample for neutralization and centrifuged at 15616 x g for 1 min. Samples were subjected to PCR to determine the genotype for each mouse. Primers used for PCR of the *IR<sup>fl/fl</sup>* mutation were *oIMR6765* (5'-GATGTGCACCCCATGTCTG-3') and *oIMR6766* (5'-CTGAATAGCTGAGACCACAG-3'). Alternatively, primers for *MIP* (5'-CCTGGCGATCCCTGAACATGTCCT-3') and *CreERT* (5'-TGGACTATAAAGCTGGTGGGCAT-3') detection were used. PCR products were separated by an ethidium bromide-containing 2% agarose gel for ~90 min at 80 V. Gels were imaged under UV light with Gene Genius Bio Imaging System (SynGene; Frederick, MD, USA) and GeneSnap 7.12 software (SynGene; Cambridge, England). For *Ir* PCR products, three genotype groups were determined based on the following fragment sizes: 313bp (*IR<sup>fl/fl</sup>*), 279bp (*IR<sup>+/+</sup>*), or 313bp and 279bp (*IR<sup>fl/+</sup>*). In addition, the presence of a 268bp fragment in *MIPCreERT* PCR products marked the presence of *MIPCreERT* in mice (**Figure 2.1B**).

## 2.3 Tamoxifen preparation and administration

Tamoxifen (Sigma-Aldrich, St. Louis, MO, USA) was prepared by dissolving in 100% ethanol at 300 mg/mL, and preparation of injectable tamoxifen was done by heating the 300 mg/mL solution to 60  $^{\circ}$ C and diluting to 30 mg/mL in corn oil (Sigma-Aldrich, St. Louis, MO, USA).

For fetal studies, a single dose of tamoxifen at 6 mg per 40g of body weight (Hayashi et al. 2002) was administered by intraperitoneal (i.p.) injection to pregnant female mice at e13 (**Figure 1.3**). On e19, pregnant mice were euthanized by CO<sub>2</sub> inhalation. Each fetus was immediately dissected to obtain tail tissue for genotyping, whereas pancreatic tissue was processed for protein extraction and morphological analyses.

For postnatal studies, the  $\beta$ -cell-specific *Ir* knockout was induced in 3-4 week old mice via 3 consecutive days of i.p. tamoxifen injection at 4 mg per 20g of body weight (**Figure 1.3**). The same dosage of tamoxifen was injected into age-matched control littermates. Post injection, mice were fed normal chow containing 10% kcal fat up to 24 weeks of age.

For the high-fat diet study,  $\beta$ IrKO, heterozygous, and control mice at 6 weeks of age (2 weeks after i.p. tamoxifen injection) were fed with high-fat diet containing 60% kcal fat (D12492, Research Diets, New Brunswick, NJ, USA) for 6 weeks.

## 2.4 Postnatal glucose metabolic studies

Since our preliminary results demonstrated that all postnatal female groups exhibited near identical phenotype and glucose metabolism, females were excluded from further adult studies. Body weight, fasting blood glucose, and intraperitoneal glucose tolerance tests (IPGTT) were performed at 4, 8, and 20 weeks post-tamoxifen injection (at 8, 12, 24 weeks of age, respectively) in  $\beta$ IrKO, heterozygous, and control mice on normal chow diet. In addition, glucose-stimulated insulin secretion (GSIS) was performed at 8 weeks post-tamoxifen injection, and intraperitoneal insulin tolerance test (IPITT) was performed at 20 weeks post-tamoxifen injection. All metabolic experiments were also completed in experimental groups treated with 6 weeks of high-fat diet at 8 weeks post-tamoxifen injection, a time-point matched to the normal chow diet groups.

For the IPGTT, following a 16 hour fast, glucose [D-(+)-glucose; dextrose; Sigma-Aldrich Canada Co., Oakville, ON, CA] was administered through i.p. at a dosage of 2 mg/g of body weight, and blood glucose levels were examined at 0, 15, 30, 60, 90 and 120 minutes after injection. Area under the curve (AUC) was used to quantify glucose responsiveness and data are expressed as units of ([mmol/l] x min) (Allison et al. 1995, Krishnamurthy et al. 2007).

For the IPITT, following a 4 hour fast, human insulin (Humalin, Eli Lilly, Toronto, Ontario, Canada) at 1 U/kg of body weight was injected intraperitoneally, and blood

glucose levels were measured at 0, 15, 30, 60 and 120 minutes (Krishnamurthy et al. 2007, Feng et al. 2013).

For the GSIS, following a 16 hour fast, blood samples (~50 $\mu$ l) were collected before (0 minutes) and after glucose loading at 5 and 35 minutes via the tail vein. Each sample was centrifuged and supernatant was stored in -20 °C. Insulin secretion levels were assessed by an ultrasensitive enzyme-linked immunosorbent assay (ELISA) (Krishnamurthy et al. 2007, Feng et al. 2013).

## 2.5 Pancreatic islet isolation

Islet isolation was performed at 20 weeks post-tamoxifen injection (24 weeks of age) under normal chow diet groups and at 8 weeks post-tamoxifen injection (12 weeks of age) under high-fat diet groups. In brief, the bile duct was sutured closed to prevent injecting into the duodenum, and the pancreas was infused with 3 mL of collagenase V (1 mg/mL, Sigma) through the common bile duct. The inflated pancreas was excised and placed into a 15 mL BD Falcon tube with 3 mL of cold dissociation buffer (Hank's balanced salt solution with HEPES, 0.6% g/mL), then incubated in a 37 °C water bath for 30 minutes. Dissociated pancreatic fragments were washed with HBSS washing buffer to stop enzyme activity. The islet purification was completed using a Ficoll gradient with purity at ~80%, as described previously (Wang et al. 2004), and processed for protein extraction.

## 2.6 Insulin enzyme-linked immunosorbent assay (ELISA)

Islet insulin content was measured using a mouse ultrasensitive insulin ELISA kit (ALPCO, Salem, NH, USA) with a sensitivity of 0.15 ng/mL, according to the manufacturer's instructions. Insulin release was expressed as ng/mL. Insulin content at each time point was measured using a Multiskan Spectrum microplate spectrophotometer (Thermo Electron Corp., Waltham, MA, USA).

## 2.7 Tissue processing, immunohistology, and TUNEL

Dissected fetal or adult pancreata were fixed in 4% paraformaldehyde (PFA) (Fisher Scientific Company; Ottawa, ON, Canada) at 4 °C overnight. Tissues were then washed with 1x PBS and processed through a series of increasing ethanol concentrations, toluene, and wax using an automatic tissue embedding machine (Shandon Citadel™ Tissue Processor, Citadel 1000, Thermo Electron Corporation; Waltham, MA, USA). Subsequently, embedded pancreatic tissue blocks were cut into 2-4 µm thick sections with microtome (Leica RM2245, Leica Biosystems).

After overnight incubation at 37 °C, tissue sections were rehydrated through a series of xylene washes followed by decreasing ethanol concentrations (100% to 70%). For the staining of nuclear transcription factors, sections were pretreated with citrate antigen retrieval solution (pH 6.0) and heated in microwave for 20 min. Blocking solution with 10% normal goat serum (Invitrogen; Frederick, MD, USA) was applied for 30 min at room temperature to block non-specific antibody binding. Immunofluorescence staining was performed with appropriately diluted primary antibodies (**Table 1**) incubated overnight at 4 °C. Afterwards, diluted (1:50) fluorescently-labelled secondary antibodies conjugated with either fluorescein isothiocyanate (FITC) or tetramethyl rhodamine isothiocyanate (TRITC) (Jackson ImmunoResearch Laboratories; West Grove, PA, USA) that was reactive to the selected primary antibody were applied (**Table 1**). Cell nuclei were briefly counterstained with diluted (1:1000) 4'-6'-diamidino-2-phenylindole (DAPI) (Sigma-Aldrich, St. Louis, MO, USA). Cover slips were secured to slides and stored at -20 °C in the dark. Either primary or secondary antibody was excluded from staining for negative controls.

To examine islet IGF1, IGF2, and MafA levels, immunohistochemical staining was used with the streptavidin-biotin horseradish peroxidase complex and developed with aminoethyl carbazole substrate kit (Invitrogen, Burlington, ON, Canada). Immunohistochemical sections were counterstained with hematoxylin.

Apoptotic  $\beta$ -cells were identified using the terminal deoxynucleotidyl transferase dUTP nick end-labeling (TUNEL) assay. Pancreatic sections were pretreated in 20  $\mu\text{g}/\text{mL}$  proteinase K for 10 min at room temperature. TUNEL staining was carried out with 1:10 dilution of enzyme solution in label solution of the In Situ Cell Death Detection Kit (Roche Applied Science, Quebec City, QC, Canada).

**Table 1: List of Antibodies used for Immunostaining and Western-Blot Analyses**

<b>Primary Antibodies</b>		<b>Dilution</b>	<b>Company</b>
Anti-Akt	Rabbit polyclonal	1:3000*	Cell Signaling (Temecula, CA, USA)
Anti-Calnexin	Mouse monoclonal	1:1500*	BD Biosciences (Missauga, ON, CA)
Anti-Caspase 3	Rabbit polyclonal	1:1000*	Cell Signaling (Temecula, CA, USA)
Anti-cleaved Caspase-3 (Asp175)	Rabbit polyclonal	1:200 / 1:1000*	Cell Signaling (Temecula, CA, USA)
Anti-GAPDH	Rabbit polyclonal	1:2000*	Santa Cruz Biotechnology (Santa Cruz, CA, USA)
Anti-Glucagon	Rabbit polyclonal	1:50	Santa Cruz Biotechnology (Santa Cruz, CA, USA)
Anti-Glut-2	Rabbit Polyclonal	1:100	Chemicon (Temecula, CA, USA)
Anti-IGF1	Rabbit polyclonal	1:200	Abcam (Cambridge, MA, USA)
Anti-IGF2	Rabbit polyclonal	1:200 / 1:1000*	Abcam (Cambridge, MA, USA)
Anti-Insulin	Guinea pig polyclonal	1:50 / 1:1000*	Zymed (San Francisco, CA, USA)
Anti-Insulin Receptor	Mouse monoclonal	1:200 / 1:1000*	Millipore (Temecula, CA, USA)
Anti-Islet-1	Mouse monoclonal	1:100	DSHB (University of Iowa, Iowa City, IA, USA)
Anti-Ki67	Rabbit polyclonal	1:100	Abcam (Cambridge, MA, USA)
Anti-MafA	Rabbit polyclonal	1:100	Bethyl Laboratory (Montgomery, TX, USA)
Anti-Nkx6.1	Mouse monoclonal	1:100	DSHB (University of Iowa, Iowa City, IA, USA)
Anti-p53	Mouse monoclonal	1:2000*	Cell Signaling (Temecula, CA, USA)
Anti-pan-Cytokeratin	Mouse monoclonal	1:50	Santa Cruz Biotechnology (Santa Cruz, CA, USA)

Anti-Pdx-1	Rabbit polyclonal	1:800	Dr. Wright (University of Vanderbilt, Nashville, TN, USA)
Anti-PECAM-1	Rabbit polyclonal	1:50	Santa Cruz Biotechnology (Santa Cruz, CA, USA)
Anti-phospho-Akt (Ser473)	Mouse monoclonal	1:2000*	Cell Signaling (Temecula, CA, USA)
Anti-phospho-p53 (Ser15)	Rabbit polyclonal	1:1000*	Cell Signaling (Temecula, CA, USA)
Anti-Vegf-a	Rabbit polyclonal	1:100 / 1:1000*	Abcam (Cambridge, MA, USA)
Anti-β-actin	Mouse monoclonal	1:5000*	Sigma-Aldrich (St. Louis, MO, USA)
<b>Secondary Antibodies</b>			
Horseradish peroxidase-linked secondary antibodies	Broad Spectrum	1:1 (no dilution)	Invitrogen (Burlington, ON, CA)
Anti-mouse secondary antibody	Goat Polyclonal	1:50	JRL (West Grove, PA, USA)
Anti-rabbit secondary antibody	Goat Polyclonal	1:50	JRL (West Grove, PA, USA)

---

\* dilution factor applied to western blot analysis. DSHB, Developmental Studies Hybridoma Bank; JRL, Jaskcon Immunoresearch Laboratories.

## 2.8 Morphometric analysis

Images of stained tissue sections were obtained and islet morphologies were blindly analyzed with Image-Pro Plus software (MediaCybernetics; Rockville, MD, USA). An islet was defined as a dense cell cluster containing at least 3 insulin<sup>+</sup> cells. Islet number (density) was calculated by total number of islets divided by the total area of the pancreas section. For islet size distribution, every individual islet size was measured and grouped into different size classes, and expressed as a percentage of the total number of islet per section. To quantify total islet,  $\alpha$ - (glucagon<sup>+</sup>) and  $\beta$ -cell (insulin<sup>+</sup>) area, every islet in sections from all groups were all manually traced and measured with a minimum of four pancreata per age group per experimental group, then  $\alpha$ - and  $\beta$ -cell masses were calculated using previously described methods (Wang et al. 1994). In brief,  $\beta$ -cell mass (mg) = ( $\beta$ -cell area \* pancreas mass)/pancreas area.

The levels of transcription factors (Pdx-1, Nkx6.1, Islet-1, MafA) localized in  $\beta$ -cells were determined by double immunofluorescence staining and quantified using the manual cell counter function in the Image-Pro Plus software. Insulin<sup>+</sup> cells positively stained for transcription factors are normalized to the total number of insulin<sup>+</sup> cells per islet and expressed as a percentage. The percentage of Ki67 localized in  $\beta$ -cell nuclei was determined from at least 12 random islets per pancreatic section, where a minimum of five pancreata per experimental group was analysed.

Islet capillary area was imaged with anti-mouse platelet endothelial cell adhesion molecule (PECAM-1) staining, then manually traced for every islet per section. Islet capillary density, capillary area per islet, and average islet capillary size was measured to determine the proportion of vessels present in the islet area. Islet capillary density was calculated by total number of capillary divided by total islet area. Capillary area per islet is expressed as a ratio of the total islet capillary area to the islet area. Average islet capillary size was determined by dividing the sum of individual islet capillary area by the total number of islet capillaries present in each section. A minimum of five pancreata per experimental group was analysed.

Pan-cytokeratin (pan-CK) staining was performed to demonstrate the presence of epithelial ducts cells within or adjacent to pancreatic islet clusters. The number of pan-CK<sup>+</sup> cells co-localized with Pdx-1 were expressed as a percentage of total number of pan-CK<sup>+</sup> cells per section area. A minimum of five pancreata per experimental group was analysed.

## 2.9 Protein extraction and western blot analyses

Fetal pancreata and isolated islets from postnatal groups were sonicated in Nonidet-P40 lysis buffer (Sigma-Aldrich; St Louis, MO, USA) and placed on ice for 30 min. Samples were centrifuged at 15871 x g for 20 min at 4 °C, and supernatant was subsequently collected and stored in -80 °C freezer for protein assay and western blot analysis. Protein concentrations were measured with the Bradford dye protein assay (Bio-Rad Laboratories; Mississauga, ON, Canada). The protein assay standards were prepared from bovine serum albumin (BSA) at increasing concentrations of 0, 0.05, 0.1, 0.2, 0.3, 0.4, and 0.5 mg/mL. 10 µL of each standard and 1 µL of sample protein solution was loaded into micro titer plate in duplicate and mixed with colorimetric dye. Following 20 min incubation in room temperature on a shaker, assay reading was performed at 595 nm with Multiskan spectrum spectrophotometer (Thermo Scientific).

Equal amounts of protein lysate were prepared (10-20 µg) for each western blot, and separated by either 5, 7.5, or 10% sodium dodecyl sulphate–polyacrylamide gel electrophoresis (SDS-PAGE). A constant voltage of 40V initially separated samples until migration through the stacking gel was complete, then was increased to 80V until the dye flowed through the bottom. Protein samples were then wet transferred to a nitrocellulose membrane (Bio-Rad Laboratories; Mississauga, ON, Canada) with transfer buffer containing glycine (192 mM), Tris (25 mM), and methanol (20 % v/v), and transferred at a constant current of 250 mA for 2 hours in an ice bucket. Membranes were briefly stained with Ponceau S stain to confirm proper protein transfer. After washing in Tris buffered-saline containing 0.1 % Tween-20 (TBST), membranes were incubated in 5% non-fat dry milk with TBST at room temperature for 1-2 hours. Membranes were then incubated with appropriately diluted primary antibodies overnight at 4 °C or 1 hour at

room temperature (**Table 1**), washed with TBST, and incubated in secondary antibody at room temperature for 1 hour. Membranes were washed in TBST after secondary antibody and proteins were visualized with ECL<sup>TM</sup>-Plus Western Blot detecting reagents (PerkinElmer; Waltham, MA, USA), and imaged with a Versadoc Imaging System (Bio-Rad Laboratories; Mississauga, ON, Canada) using Quantity One software (Bio-Rad Laboratories; Mississauga, ON, Canada). Densitometric analyses of images were completed with Image Lab 3.0 software (Bio-Rad Laboratories; Mississauga, ON, Canada) and data were normalized to appropriate loading controls.

## 2.10 Statistical analysis

Data is presented as means  $\pm$  SEM. Statistical analyses were performed using either one-way ANOVA and Bonferroni's multiple comparison post hoc tests or Student's unpaired t-test with GraphPad Prism 6 (GraphPad Software; La Jolla, CA, USA). Differences in results were considered statistically significant when  $p < 0.05$ .

## Chapter 3 - Results

### 3.1 Verification of $\beta$ -cell-specific *Ir* knockout in fetal $\beta$ IrKO mice

We first tested the  $\beta$ -cell tissue specificity of the *MIP* expression by crossing *MIPCre* mice with the *B6.Cg-Gt(ROSA)26Sor<sup>tm9(CAG-dTomato)Hze/J</sup>* reporter strain, which expresses the red fluorescence protein (dTomato) after breeding with *MIPCre* mice. The Cre recombinase expression in tissue-specific *MIPCre* mice will excise the LoxP-stop-LoxP signal, which is present 5' to the dTomato, leading to activation and expression of the dTomato reporter as red fluorescence observed under a fluorescence microscope. In contrast to *MIPCre<sup>-</sup>* control mice, *MIPCre<sup>+</sup>* mouse pancreatic islets expressed red fluorescence in freshly isolated islets (**Figure 3.1A**).

To verify the  $\beta$ -cell *Ir* knockout in the fetal pancreas, western blot analysis was performed on fetal pancreata collected at e19. A significant knockdown of IR protein levels in  $\beta$ IrKO pancreata was observed in comparison to control groups (**Figure 3.1B**).

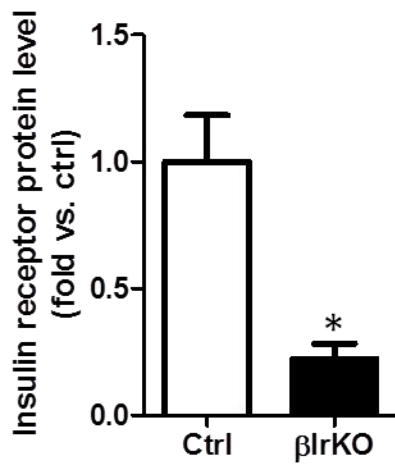
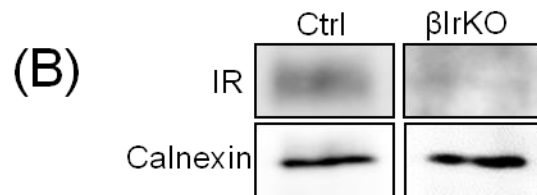
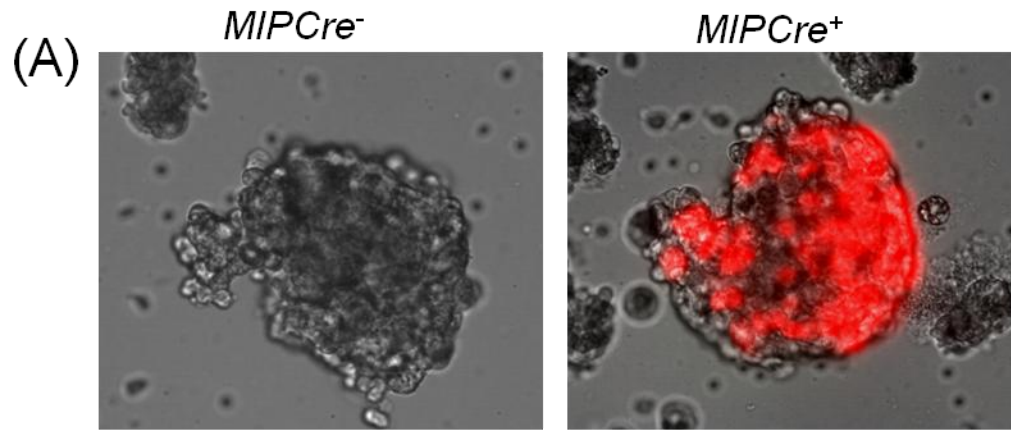


**Figure 3.1. Confirmation of  $\beta$ -cell specific *Ir* knockout**

(A) dTomato (red) reporter gene is expressed only when Cre recombinase (*MIPCre*<sup>+</sup>) excises the stop codon upstream of the reporter gene. While no fluorescence was detected in brain or other tissues, the presence of red fluorescence in  $\beta$ -cells confirms the specificity of *MIP*-driven Cre recombinase expression in pancreatic  $\beta$ -cells. (B) Western blot analysis demonstrated a significant reduction of IR protein levels in fetal  $\beta$ IrKO pancreata relative to controls ( $n = 3-4$ ). Representative blotting image is shown. White bar, control group; black bar,  $\beta$ IrKO group. Data are expressed as means  $\pm$  SEM. \* $p < 0.05$ .

## 3.2 Fetal $\beta$ IrKO mice exhibit a hyperplastic islet growth response

When fetal pups were dissected at e19, no significant differences in body weight and blood glucose levels were observed between  $\beta$ IrKO and control groups. In order to unravel the role of  $\beta$ -cell IR activity during fetal pancreatic development, we performed immunofluorescence staining to characterize  $\beta$ -cells and overall islet morphology (**Figure 3.2A**). Although not statistically significant, morphometric analyses suggest an increased islet density (islet number/mm<sup>2</sup>) in fetal  $\beta$ IrKO pancreata (**Figure 3.2B**). In  $\beta$ IrKO mice, the percent of islet area (percentage of total islet/ total pancreas area; **Figure 3.2C**), mean islet area ( $\mu\text{m}^2$ ) (**Figure 3.2D**), and percent  $\beta$ -cell area (percentage of total insulin<sup>+</sup>/ total pancreas area; **Figure 3.2E**) were significantly increased. Alternatively,  $\alpha$ -cell area (percentage of total glucagon<sup>+</sup>/ total pancreas area) showed no change in  $\beta$ IrKO compared to control pancreata (**Figure 3.2F**).

To further characterize fetal islet morphology, we evaluated various size distributions of islets in control and  $\beta$ IrKO pancreata. We observed that  $\beta$ IrKO pancreata had a significantly decreased number of small islets (< 1000  $\mu\text{m}^2$ ) and a significantly increased number of large islets (> 10000  $\mu\text{m}^2$ ) compared to controls (**Figure 3.2G**), indicating relative hyperplastic growth of the islets in  $\beta$ IrKO pancreata. Thus, it appears that reduction of  $\beta$ -cell-specific IR promotes islet growth through expansion of the  $\beta$ -cells.

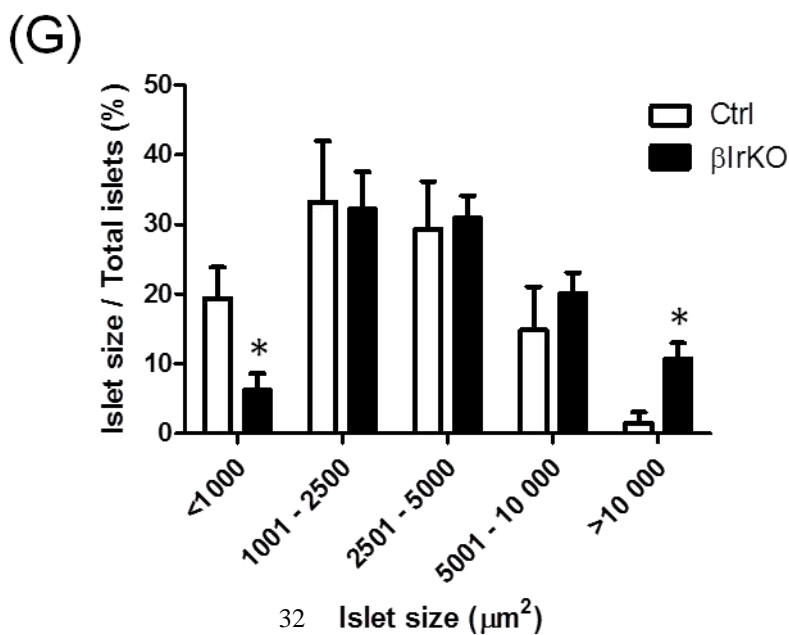
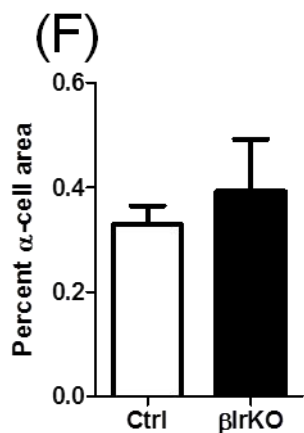
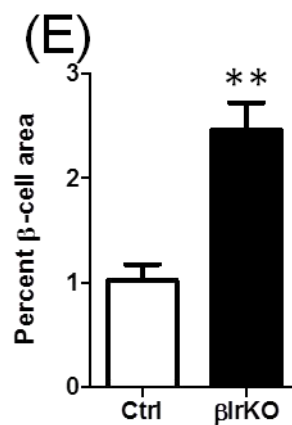
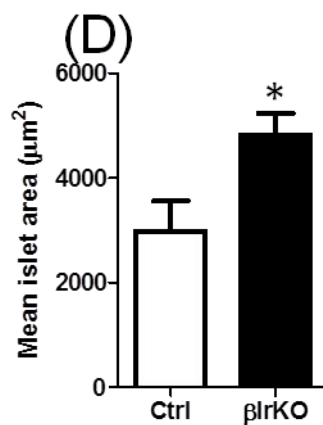
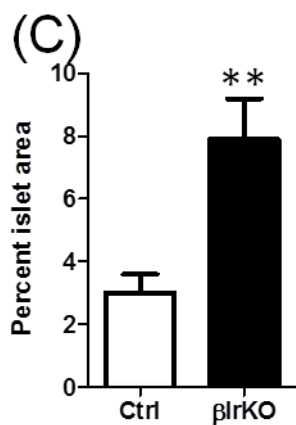
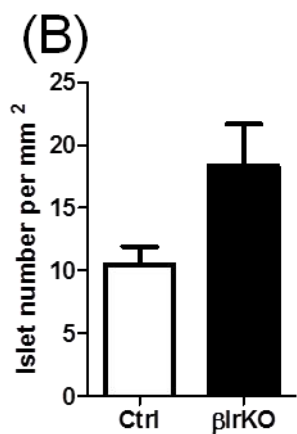
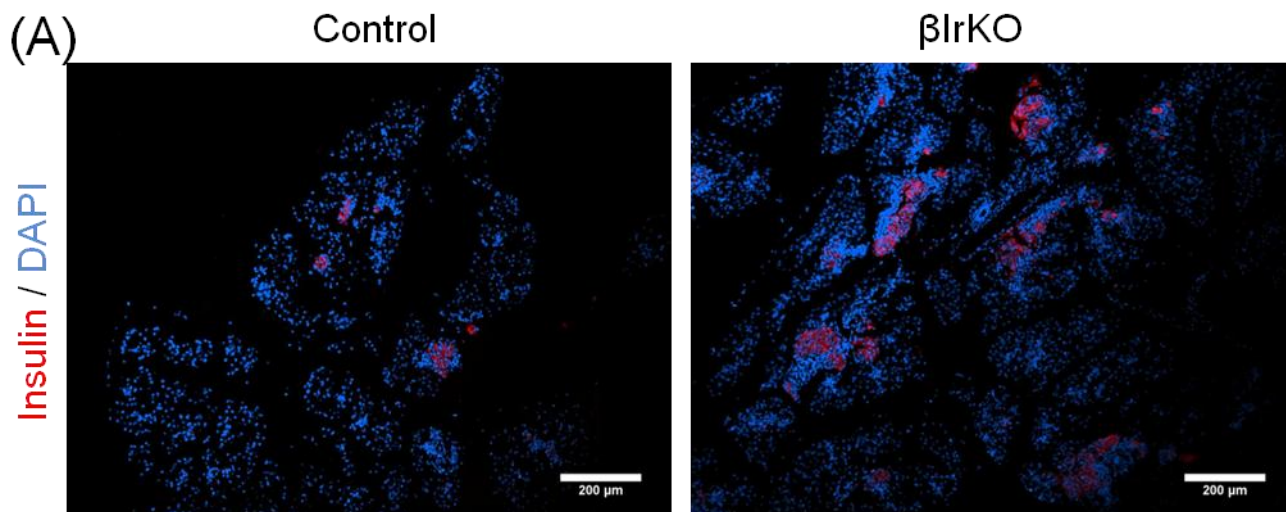


**Figure 3.2. Islet growth in fetal  $\beta$ IrKO pancreata**

(A) Representative immunofluorescence image depicting the expansion of  $\beta$ -cells within fetal  $\beta$ IrKO pancreata compared to controls. Scale bar: 200  $\mu$ m. Morphometric analysis of (B) number of islets per  $\text{mm}^2$ , (C) percent islet area, (D) mean islet area, (E) percent  $\beta$ -cell area, and (F) percent  $\alpha$ -cell area relative to whole pancreas area. (G) Quantification of different islet sizes shows that  $\beta$ IrKO pancreata had a significantly greater percentage of large islets (islets  $> 10\,000\ \mu\text{m}^2$ ) and significantly reduced percentage of small islets (islets  $< 1\,000\ \mu\text{m}^2$ ). White bars, control group; black bars,  $\beta$ IrKO group. Data are expressed as means  $\pm$  SEM ( $n = 5-6$ ). \* $p < 0.05$ , \*\* $p < 0.01$ .

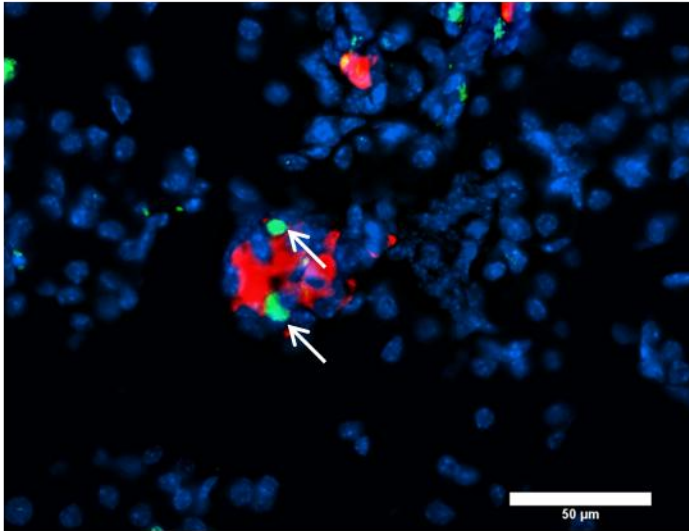
### 3.3 Increased $\beta$ -cell proliferation in $\beta$ IrKO mice

To investigate the molecular mechanisms contributing to islet growth response in  $\beta$ IrKO mice, we first assessed  $\beta$ -cell proliferation using double immunofluorescence staining for insulin and Ki67 proliferation marker (**Figure 3.3A**). We quantified the percentage of insulin<sup>+</sup> cells with nuclear localization of Ki67.  $\beta$ IrKO pancreata had significantly greater number of proliferating insulin<sup>+</sup> cells compared to controls ( $p < 0.001$ ; **Figure 3.3B**). In addition, we sought to determine if the increased  $\beta$ -cell proliferation in  $\beta$ IrKO pancreata was due to increased islet neogenesis. During islet development, islet neogenesis initiates from the pancreatic ductal epithelium and are always Pdx-1 positive, which is a marker for early  $\beta$ -cell differentiation. Therefore, we assessed the percentage of pan-CK<sup>+</sup> epithelial ducts cells (within or adjacent to pancreatic islet clusters) positively stained for the Pdx-1 transcription factor, as an indicator for islet neogenesis. There was no significant difference in the percentage of pan-CK<sup>+</sup>/Pdx-1<sup>+</sup> cells between  $\beta$ IrKO (~6.5%) and control (~8.3%) pancreata (**Figure 3.4**). Taken together, these results suggest that the islet hyperplastic growth seen in  $\beta$ IrKO mice is likely attributed to the increased replication of pre-existing  $\beta$ -cells, rather than ductal-to-islet neogenesis.

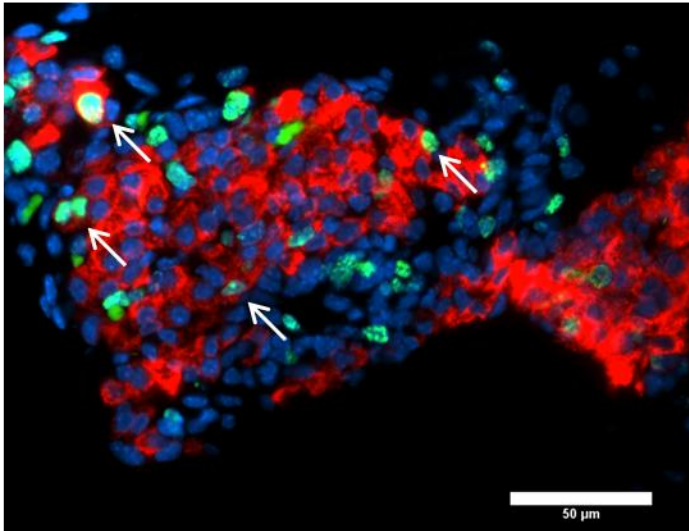
Next, we determined if decreased apoptosis of developing islet cells also contributes to the islet growth response seen in  $\beta$ IrKO mice. TUNEL staining did not show a difference in the percentage of insulin<sup>+</sup> cells with nuclear TUNEL positivity in  $\beta$ IrKO pancreata relative to control mice (**Figure 3.5**). Similarly, western blot analyses were unable to detect a difference in cleaved caspase-3 levels between  $\beta$ IrKO and control pancreata (**Figure 3.6C**). Therefore, apoptosis does not appear to play an important role in islet hyperplasia observed in fetal  $\beta$ IrKO pancreata.

(A) Ki67 / Insulin / DAPI

Control



$\beta$ IrKO



(B)

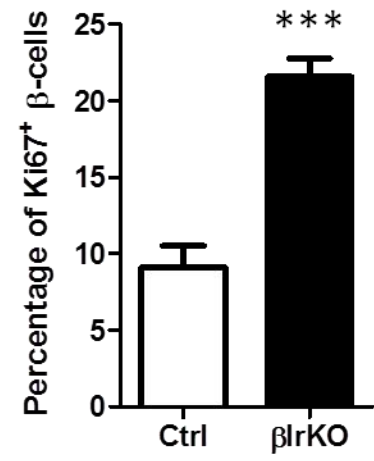
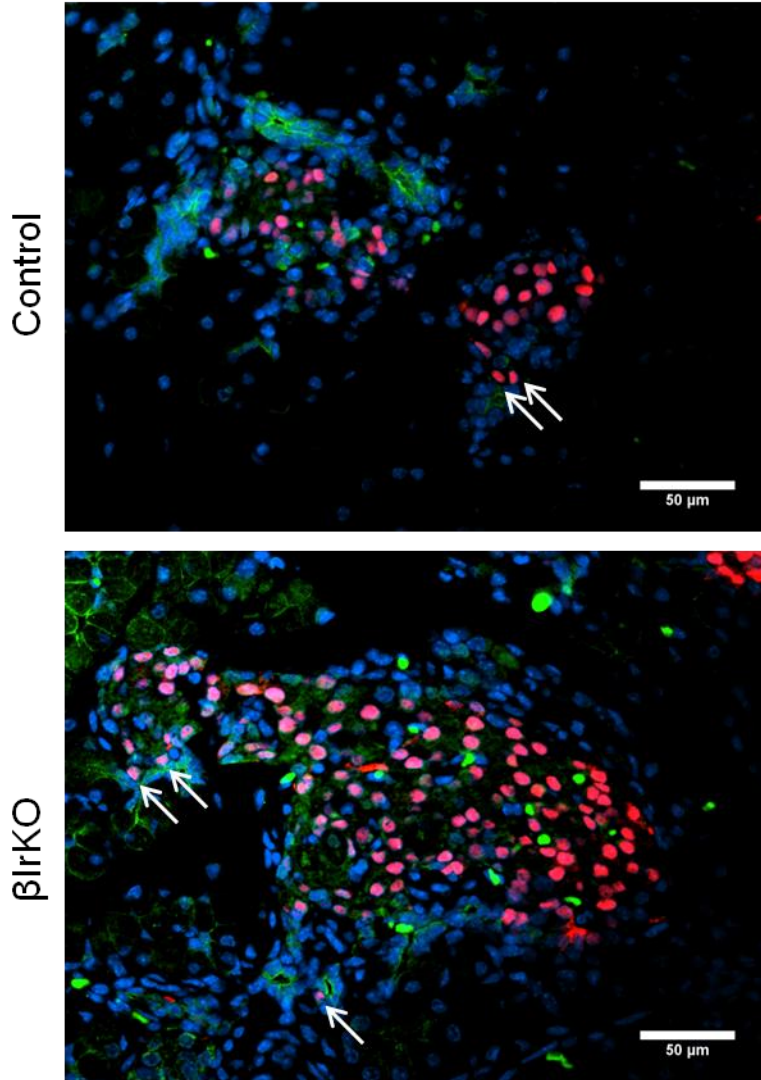


**Figure 3.3. Enhanced  $\beta$ -cell proliferation in fetal  $\beta$ IrKO pancreata**

(A) Representative double immunofluorescence images demonstrating a significantly increased percentage of insulin<sup>+</sup> cells with nuclear Ki67 staining in  $\beta$ IrKO islets compared to control. White arrows indicate cells positive for Ki67. Scale bar: 50  $\mu$ m. (B) Quantification of immunofluorescence images by cell counting show a significant increase of Ki67 positive  $\beta$ -cells in  $\beta$ IrKO islets relative to controls. White bar, control group; black bar,  $\beta$ IrKO group. Data are expressed as means  $\pm$  SEM ( $n = 5$ ). \*\*\* $p < 0.001$ .

(A) pan-CK / Pdx-1 / DAPI



(B)

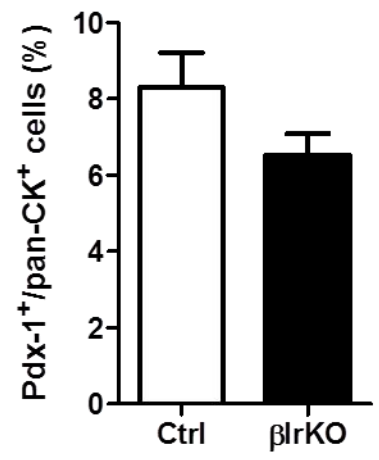
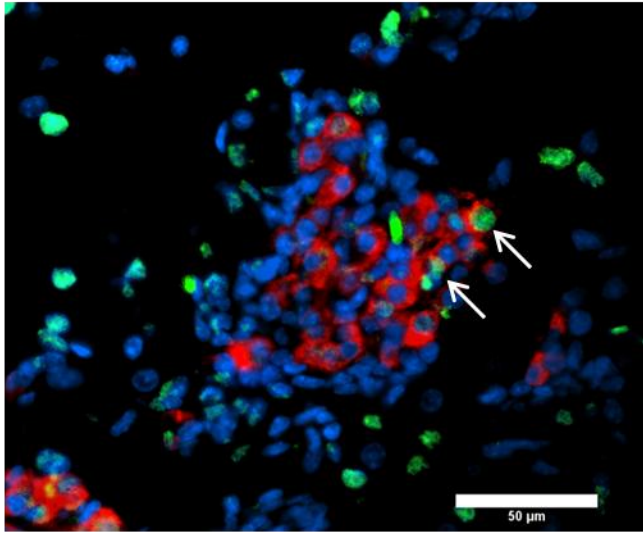


***Figure 3.4.* Similar levels of islet neogenesis from epithelial ducts in fetal  $\beta$ IrKO and control pancreata**

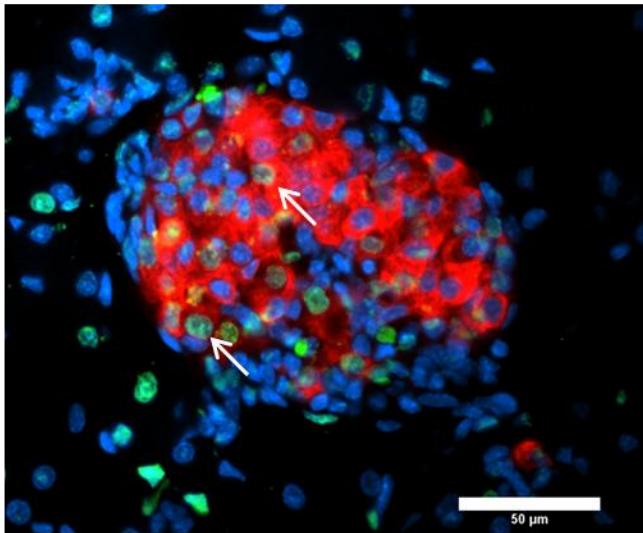
(A) Representative double immunofluorescence images of fetal islets with adjacent epithelial duct cells, marked by pan-CK staining (green), and Pdx-1 (red). Pdx-1<sup>+</sup> duct cells indicate potential islet neogenesis. White arrows indicate Pdx-1 nuclear localization in duct cells. Scale bar: 50  $\mu$ m. (B) Quantification of the percentage of epithelial duct cells (adjacent to islets) positive for Pdx-1. White bar, control group; black bar,  $\beta$ IrKO group. Data are expressed as means  $\pm$  SEM ( $n = 5$ ).

(A) TUNEL / Insulin / DAPI

Control



$\beta$ IrKO



(B)

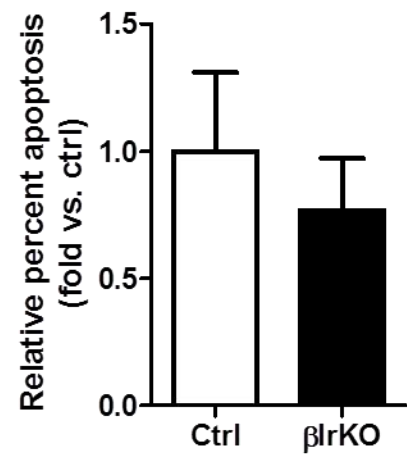


***Figure 3.5. No change in cell apoptosis in fetal  $\beta$ IrKO pancreata***

(A) Double immunofluorescence images demonstrating similar levels of insulin<sup>+</sup> cells with nuclear TUNEL staining in  $\beta$ IrKO islets compared to control. White arrows indicate nuclear localization. Scale bar: 50  $\mu$ m. (B) Quantification of the percentage of insulin<sup>+</sup> cells with nuclear TUNEL staining. Data are normalized to control and expressed as means  $\pm$  SEM ( $n = 4-5$ ).

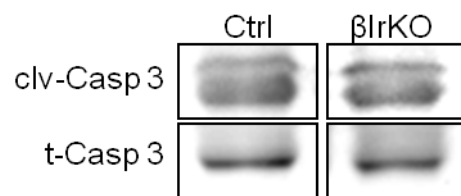
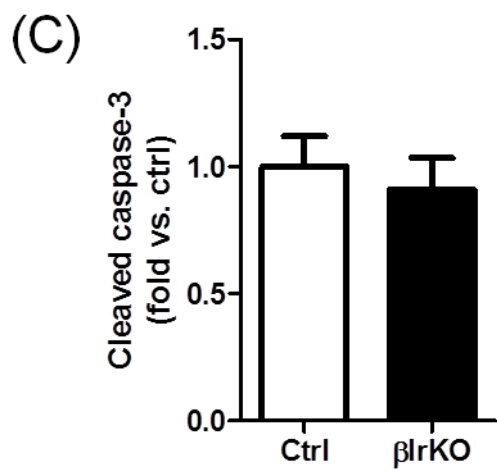
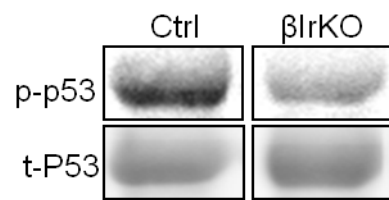
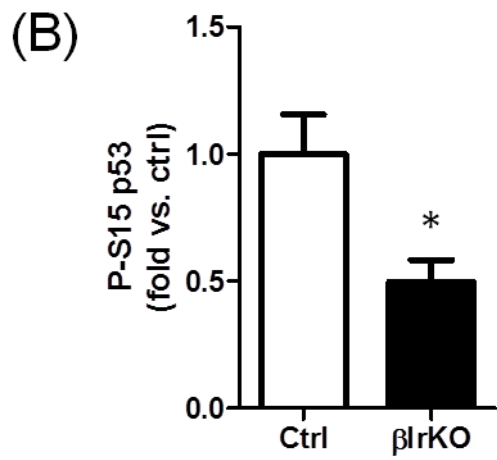
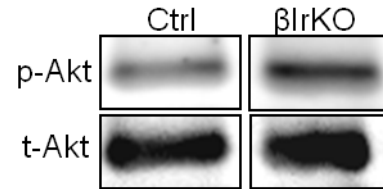
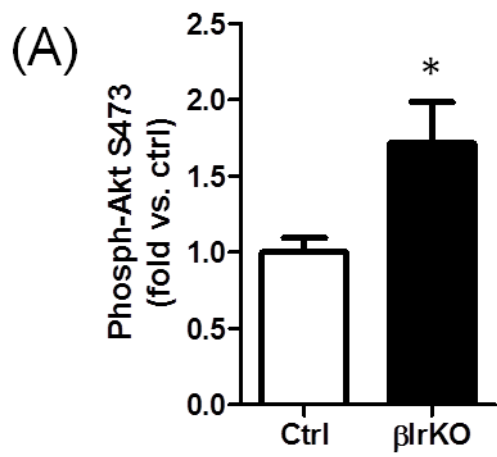


**Figure 3.6. Downstream IR signalling pathway analysis**

Western blot analyses demonstrated that  $\beta$ IrKO had significantly upregulated levels of (A) phospho-S473 Akt ( $n = 4$ ), and significantly downregulated levels of (B) phospho-S15 p53 ( $n = 3-4$ ). (C) However, the apoptotic activity, marked by cleaved caspase-3, was not different between fetal  $\beta$ IrKO and controls. Representative blotting images are shown. White bars, control group; black bars,  $\beta$ IrKO group. Data are normalized to control and expressed as means  $\pm$  SEM.  $*p < 0.05$ .

### 3.4 Fetal $\beta$ IrKO islet cells present enhanced replication and pro-survival signalling pathway activity

To account for increased islet replication and growth, we investigated signalling pathways involved in cell survival. Akt is part of the IR downstream signalling cascade and has an influential role in the regulation of  $\beta$ -cell replication. Fetal  $\beta$ IrKO exhibited a robust increase in phospho-Akt (S473) levels compared to control pancreata ( $p < 0.05$ ; **Figure 3.6A**). Previous studies have shown that activated Akt can prevent apoptosis by indirectly inhibiting downstream p53 activity (Mayo et al. 2001, Wrede et al. 2002). In agreement with increased phosphorylation of Akt in  $\beta$ IrKO mice, phospho-p53 (S15), a marker for apoptosis, was significantly reduced in  $\beta$ IrKO pancreata relative to control ( $p < 0.05$ ; **Figure 3.6B**). These results suggest that reduced  $\beta$ -cell IR levels may elicit an adaptive signalling mechanism through the homologous IGF1R signalling pathway. To explore this further, we investigated the levels of the IGF1 and IGF2 ligands. In particular, IGF2 has been demonstrated to be highly localized to islets during fetal development, and it has a relatively high affinity for both IGF1R and IR. Furthermore, studies suggest a close relationship between IGF2 levels and  $\beta$ -cell expansion. Immunohistochemical staining showed localization of IGF2 in fetal pancreatic islets with a relatively high density of staining observed in the  $\beta$ IrKO islets (**Figure 3.7A**). On the other hand, IGF1 levels were low in fetal islets (**Figure 3.7B**). Further western blot analyses revealed a significantly increased IGF2 levels in fetal  $\beta$ IrKO pancreata compared to fetal control pancreata ( $p < 0.005$ ; **Figure 3.7C**). These data imply that fetal  $\beta$ IrKO elicits a signalling pathway network adaptation that involves enhanced IGF2 production and activity through homologous receptors, with corresponding increases and decreases in Akt and p53 activity, respectively. Overall, this signalling cascade likely promotes  $\beta$ -cell proliferation.

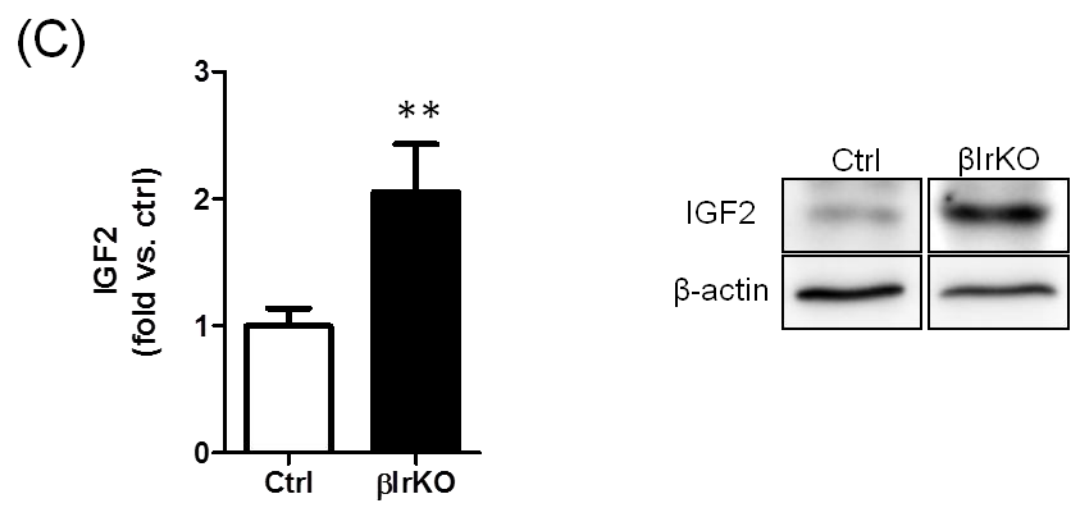
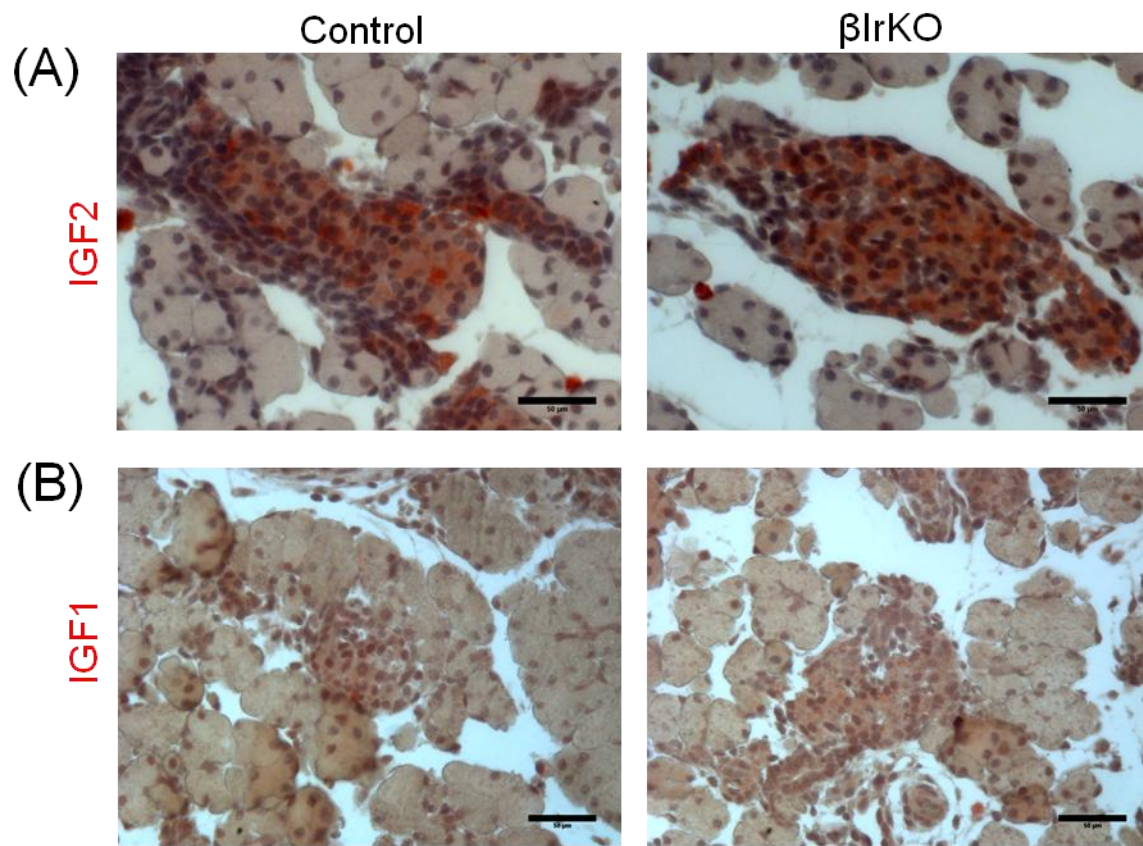


***Figure 3.7. Strong localization and increased levels of IGF2 in fetal  $\beta$ IrKO pancreata***

(A) Representative immunohistochemical staining showing strong IGF2 localization (brown) in pancreatic islets. (B) IGF1 levels were very low in fetal pancreata. Nuclei were counterstained with hematoxylin. Scale bar: 50  $\mu$ m. (C) Western blot analyses showed that fetal  $\beta$ IrKO pancreata had significantly upregulated IGF2 protein levels relative to control (n=5-13). Representative blotting image is shown. White bar, control group; black bar,  $\beta$ IrKO group. Data are normalized to control and expressed as means  $\pm$  SEM. \* $p < 0.01$ .

### 3.5 Increased vascularization in fetal $\beta$ IrKO pancreatic islets

A previous study has demonstrated a correlation between fetal islet compensatory growth response and increased islet vascularization in insulin-null mice (Duvillie et al. 2002). We also assessed the possibility that increased vascularization could be another contributing factor to the hyperplastic islets observed in fetal  $\beta$ IrKO mice. Islet vasculature was assessed by quantifying the percentage of islet PECAM-1 area over total islet area, mean vessel area, and mean islet vessel density in pancreatic sections (**Figure 3.8A**). Immunofluorescence staining demonstrated a significant increase in the percent of PECAM-1 area/total islet area (**Figure 3.8B**) and islet vessel density in  $\beta$ IrKO mice relative to controls (**Figure 3.8C**). However, the average islet capillary size was similar amongst all experimental groups, indicating increased islet angiogenesis, as opposed to enlargement of pre-existing capillaries (**Figure 3.8D**). In accordance with these findings, fetal  $\beta$ IrKO pancreata had significantly elevated Vegf-a levels, as demonstrated by immunofluorescence (**Figure 3.9A**) and western blot (**Figure 3.9B**). These results supported our finding of enhanced IGF2 levels in  $\beta$ IrKO pancreata since IGF2 could promote islet vascularization via upregulation of Vegf-a levels.

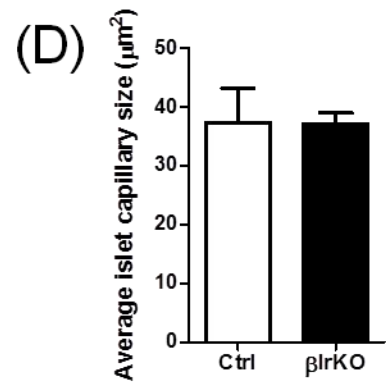
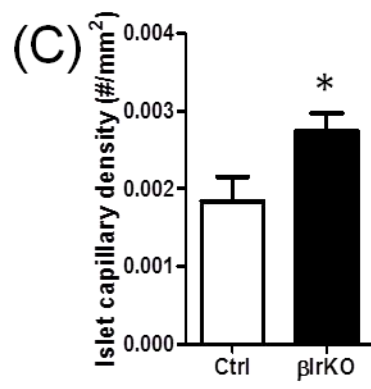
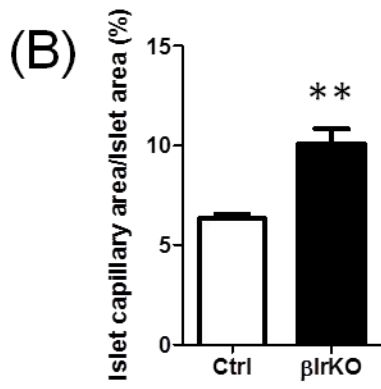
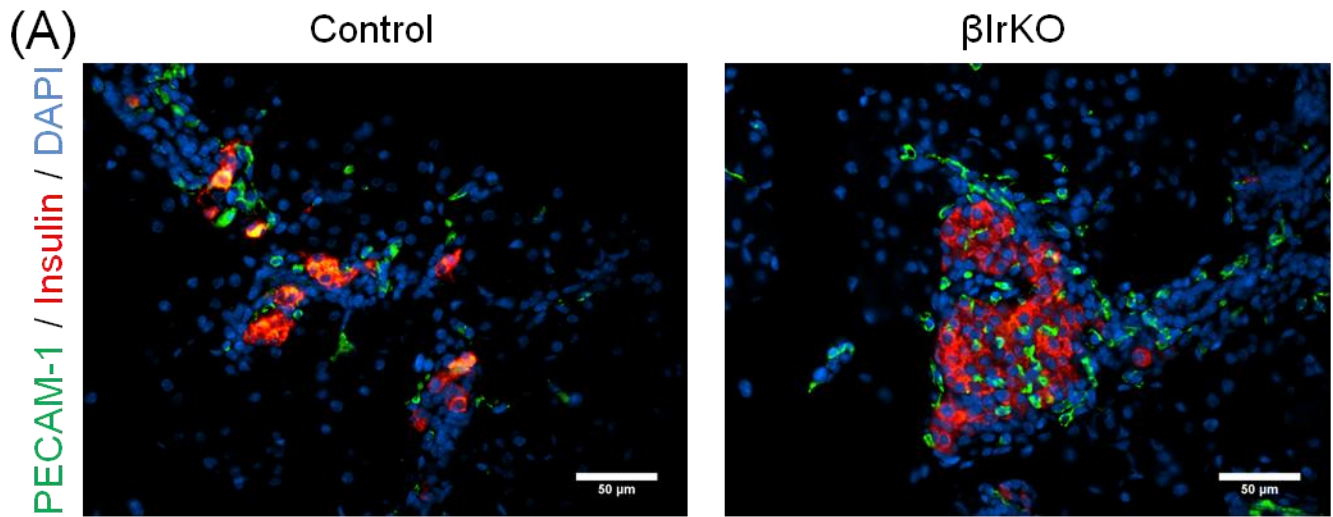


**Figure 3.8. Fetal  $\beta$ IrKO display increased vascularization**

(A) Representative double immunofluorescence images show increased vascularization (green) in pancreatic islets in  $\beta$ IrKO mice. Scale bar: 50  $\mu$ m. Quantification of immunofluorescence images demonstrates that (B) the percent of PECAM-1 area/islet area ( $n = 4-5$ ) and (C) islet vessel density ( $n = 4-5$ ) were significantly increased in  $\beta$ IrKO pancreata compared to control. (D) Average islet capillary size was similar between the groups. White bars, control group; black bars,  $\beta$ IrKO group. Data are expressed as means  $\pm$  SEM. \* $p < 0.05$ , \*\* $p < 0.01$ .

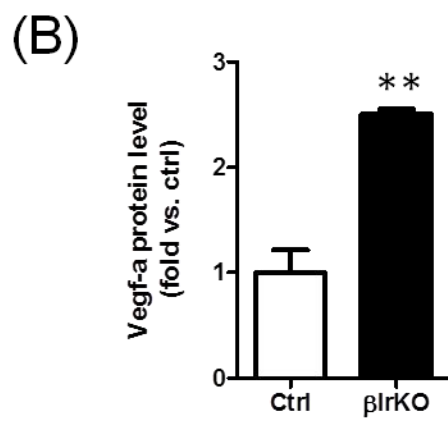
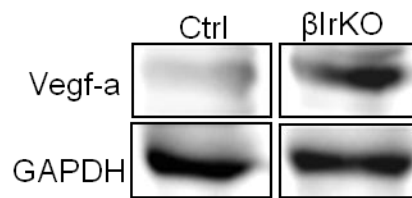
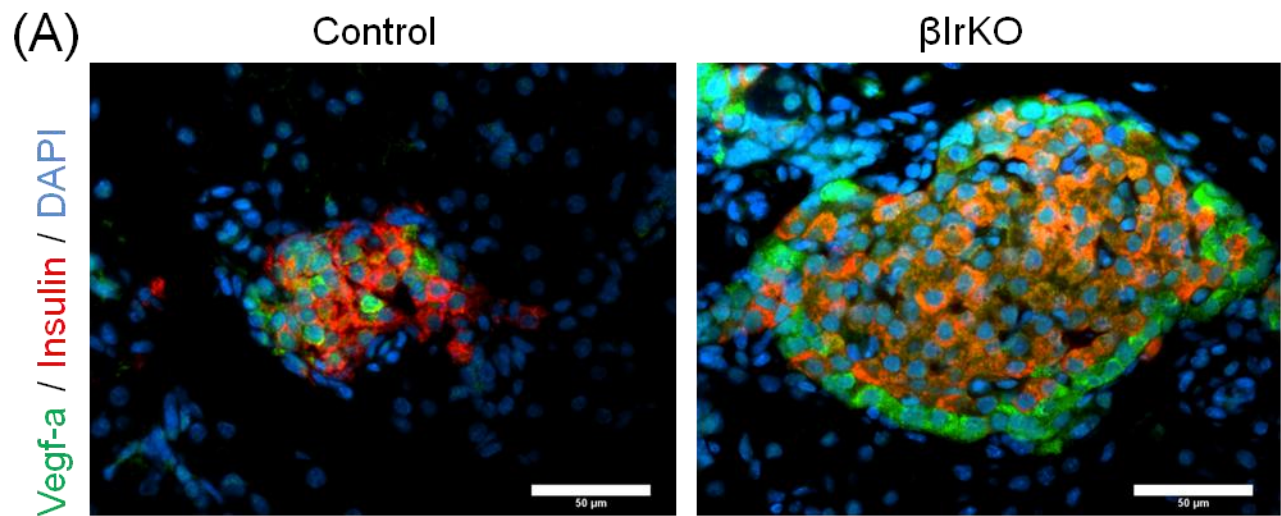


**Figure 3.9. Increased Vegf-a levels in fetal  $\beta$ IrKO pancreata**

(A) Representative double immunofluorescence images demonstrating increased Vegf-a (green) levels in insulin<sup>+</sup> cells (red) of pancreatic islets in  $\beta$ IrKO animals. Scale bar: 50  $\mu$ m. (B) Western blotting shows that corresponding protein levels of Vegf-a was significantly upregulated in  $\beta$ IrKO pancreata relative to controls ( $n = 3-5$ ). Representative blotting images are shown. White bar, control group; black bar,  $\beta$ IrKO group. Data are normalized to control and expressed as means  $\pm$  SEM. **\*\* $p < 0.01$ .**

### 3.6 $\beta$ -cell-specific *Ir* knockout at the second transition of pancreatic development does not affect $\beta$ -cell identity

To determine the role of  $\beta$ -cell IR activity in  $\beta$ -cell differentiation and identity during fetal pancreatic development, immunofluorescence and immunohistochemistry staining was performed on fetal pancreatic tissue sections. These morphological analyses characterize the potential for altered transcription factor levels, where normal expression is critical for the maintenance and development of  $\beta$ -cell differentiation and function. Qualitative observations revealed that approximately all  $\beta$ -cells (identified by insulin positivity) had nuclear Pdx-1 (**Figure 3.10A**), Nkx6.1 (**Figure 3.10B**), Islet-1 (**Figure 3.10C**), and MafA (**Figure 3.10D**) in both  $\beta$ IrKO and control mice. Previously, glucose transporter 2 (Glut-2) has been associated with glucose-dependent insulin secretion and  $\beta$ -cell development, and thus, we examined the levels of Glut-2 in the fetal islets of all groups. Although  $\beta$ IrKO islets were generally larger in size, they possessed similar intensity and membrane-localization of Glut-2 in the insulin<sup>+</sup> cells compared to control pancreata (**Figure 3.10E**). Therefore, it appears that  $\beta$ -cell-specific *Ir* knockout during fetal pancreatic development does not alter  $\beta$ -cell identity or function.

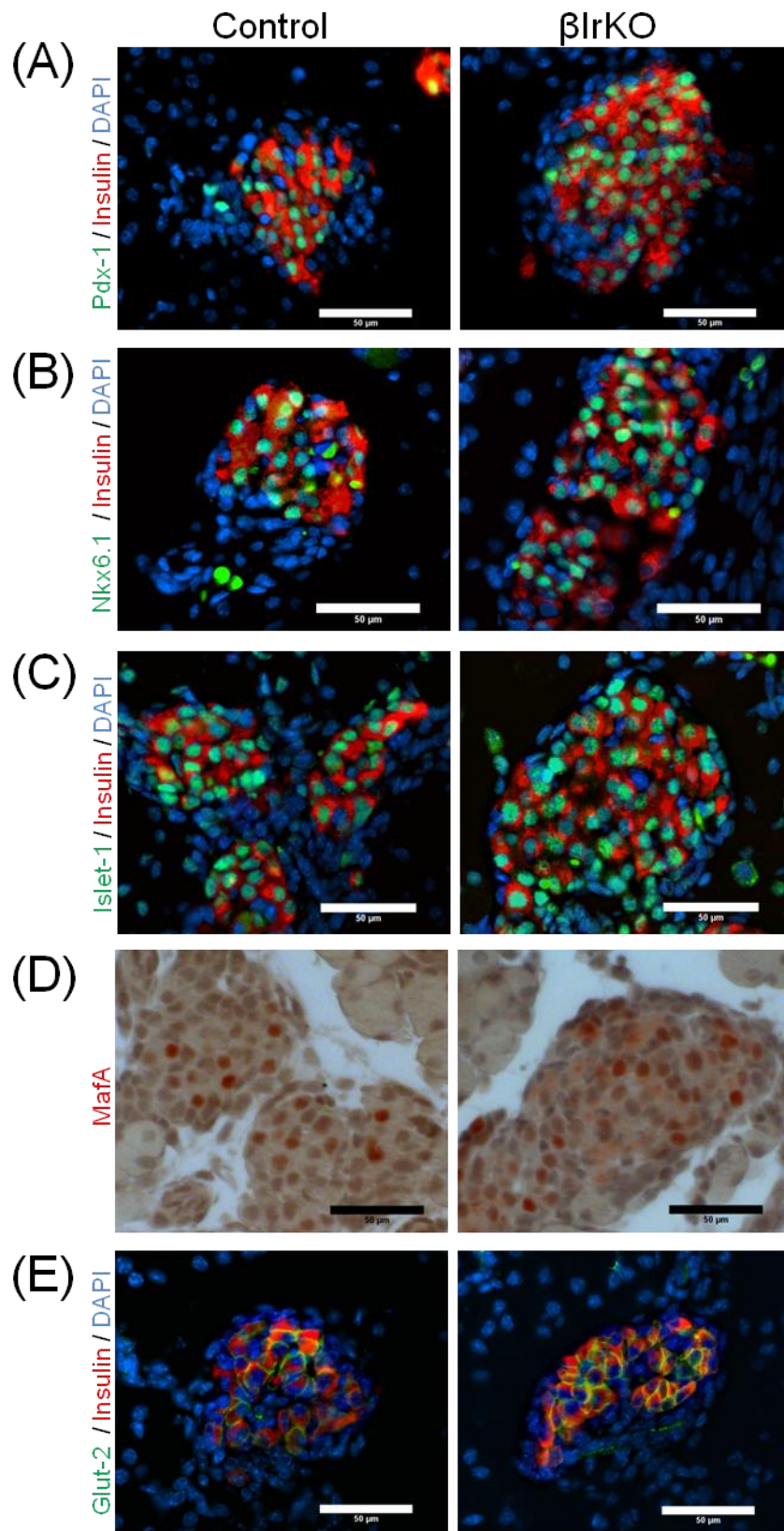


***Figure 3.10. Fetal  $\beta$ IrKO islets expressed TFs necessary for  $\beta$ -cell identity and function***

Representative double immunofluorescence images showing that insulin<sup>+</sup> cells (red) of both  $\beta$ IrKO and control pancreata display nuclear localization of transcription markers (all represented as green) critical for  $\beta$ -cell identity and function (A) Pdx-1, (B) Nkx6.1, (C) Islet-1. (D) Immunohistochemical staining demonstrates similar levels of MafA in both experimental groups. (E) Glut-2 immunofluorescence staining demonstrating similar levels in both  $\beta$ IrKO and control pancreata. Scale bar: 50  $\mu$ m.

### 3.7 Postnatal $\beta$ IrKO confirmation

Since the exocrine compartment of the pancreas also expresses insulin receptors on acinar cell membranes, we carefully isolated the pancreatic islets from the whole pancreas to verify the  $\beta$ -cell-specific *Ir* knockout in the adult mice experimental groups. Using western blot analysis, we observed a ~50% knockdown of IR protein levels in  $\beta$ IrKO pancreata in comparison to control groups (**Figure 3.11**). However, the heterozygous group displayed highly varying levels of IR protein.

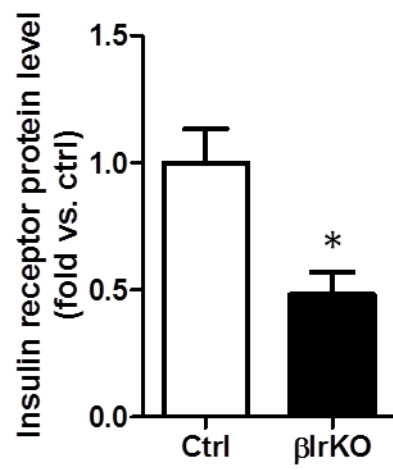
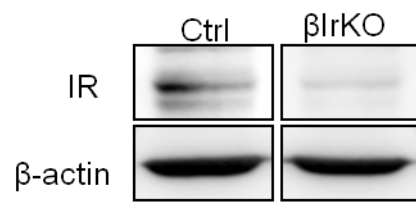


**Figure 3.11. Western blot analysis of  $\beta$ -cell *Ir* knockout efficiency**

Western blot analysis of isolated islets from postnatally induced  $\beta$ IrKO male mice demonstrated a significant reduction in IR protein levels in  $\beta$ IrKO pancreata relative to controls ( $n = 6$ ). Representative blotting image is shown. White bar, control group; black bar,  $\beta$ IrKO group. Data are normalized to control and expressed as means  $\pm$  SEM. \* $p < 0.05$ .

### 3.8 Phenotypical analysis of postnatally induced $\beta$ -cell specific *Ir* knockout mice

Postnatal breeding produced experimental  $\beta$ IrKO mice with *MIPCreERT<sup>+</sup>;IR<sup>fl/fl</sup>*, heterozygous  $\beta$ IrKO mice with *MIPCreERT<sup>+</sup>;IR<sup>fl/+</sup>*, and control mice that consisted of genotypes *MIPCreERT<sup>-</sup>;IR<sup>fl/fl</sup>* and *MIPCreERT<sup>+</sup>;IR<sup>+/+</sup>*. Based on previous reports, and due to lack of differences in our preliminary *in vivo* metabolic studies between heterozygous  $\beta$ IrKO and control groups, the heterozygous  $\beta$ IrKO group was omitted at 8 and 20 weeks post-tamoxifen time points. The body weights of male  $\beta$ IrKO mice did not significantly differ at 4, 8, and 20 weeks post-tamoxifen when compared to the control and heterozygous groups, indicating that  $\beta$ -cell IR does not affect the gross phenotypes of these mice (**Figure 3.12A**). Similarly, 16 hour overnight fasting blood glucose levels were not different between the experimental groups at all ages analyzed (**Figure 3.12B**).

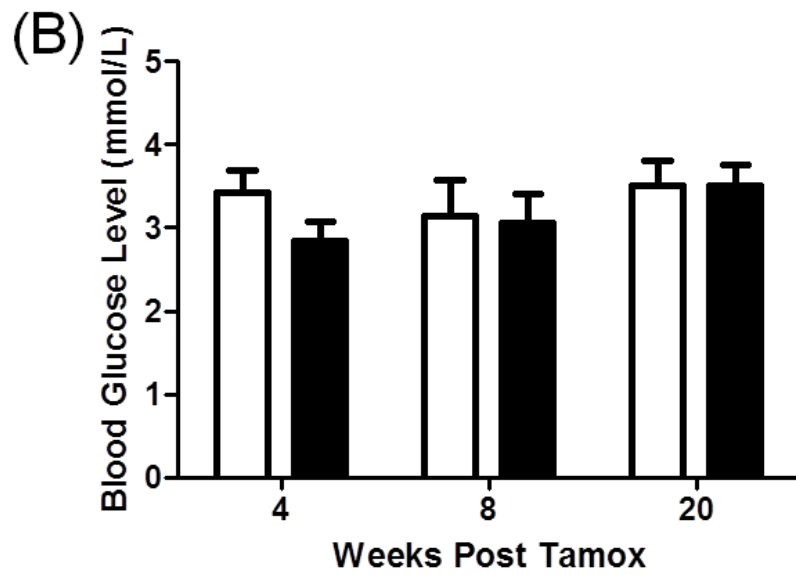
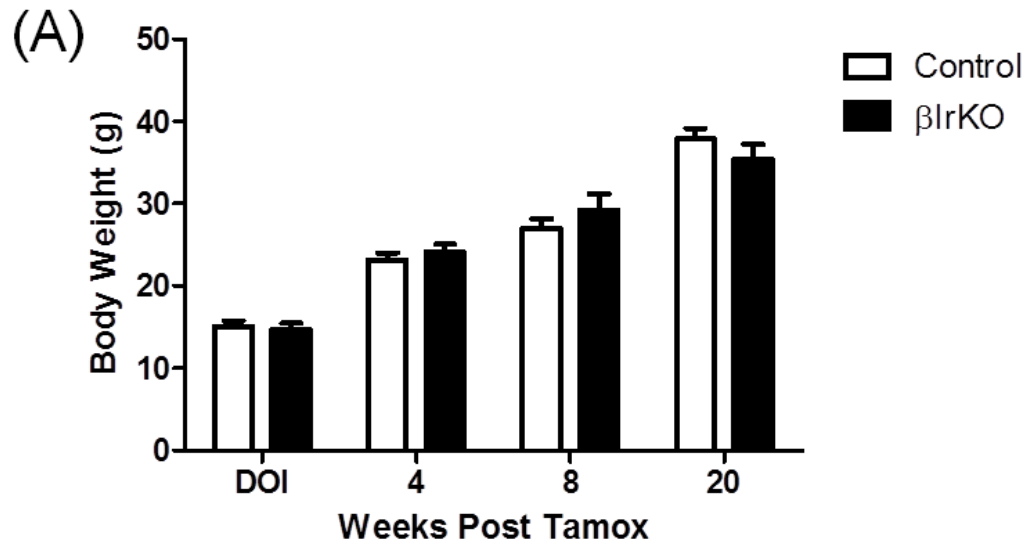


**Figure 3.12. Phenotypic analysis of postnatal tamoxifen-induced  $\beta$ IrKO mice**

(A) Fasting body weights at 0, 4, 8, and 20 weeks post-tamoxifen injection in male mice ( $n = 5-10$ ). (B) Overnight (16hrs) fasted blood glucose levels at 4, 8, 20 weeks post-tamoxifen injection in male mice ( $n = 5-10$ ). DOI stands for “date of tamoxifen injection”. White bar, control group; black bar,  $\beta$ IrKO group. Data are expressed as means  $\pm$  SEM.

### 3.9 Metabolic studies of postnatally induced $\beta$ IrKO mice

Glucose tolerance (GTT), insulin tolerance (ITT), and glucose-stimulated insulin secretion (GSIS) tests were performed at various ages to determine the effects of  $\beta$ -cell-specific *Ir* knockout on glucose metabolism. No significant changes in IPGTT were observed in male  $\beta$ IrKO when compared to control and heterozygous groups at 4 weeks post-tamoxifen (**Figure 3.13A**). At 8 weeks post-tamoxifen,  $\beta$ IrKO mice showed no statistically significant differences in AUC in comparison with experimental groups, despite the relatively higher peak at 60 and 90 minutes after i.p. injection of glucose (**Figure 3.13B**). In addition, *in vivo* GSIS at 8 weeks post-tamoxifen injection demonstrated similar insulin secretion responses between  $\beta$ IrKO and control groups (**Figure 3.13C**). When these mice were aged to 20 weeks post-tamoxifen, both  $\beta$ IrKO and control mice exhibited higher glucose levels at 60, 90, and 120 minutes following glucose injection when compared to experimental mice at 4 and 8 weeks post-tamoxifen injection. However, IPGTT of  $\beta$ IrKO did not significantly differ from the control mice (**Figure 3.14A**), suggesting that these  $\beta$ -cells are still functional when *Ir* knockout is induced after birth. This age-dependent increase in glucose intolerance is most likely due to the increased body weight and genetic composition of the B6 mice (Almind et al. 2004).

To determine whether insulin resistance plays a role in these mice, IPITT was performed at 20 weeks post-tamoxifen injection. Both  $\beta$ IrKO and control mice exhibited normal metabolic response to a dose of insulin, demonstrating that these mice did not develop insulin resistance (**Figure 3.14B**).

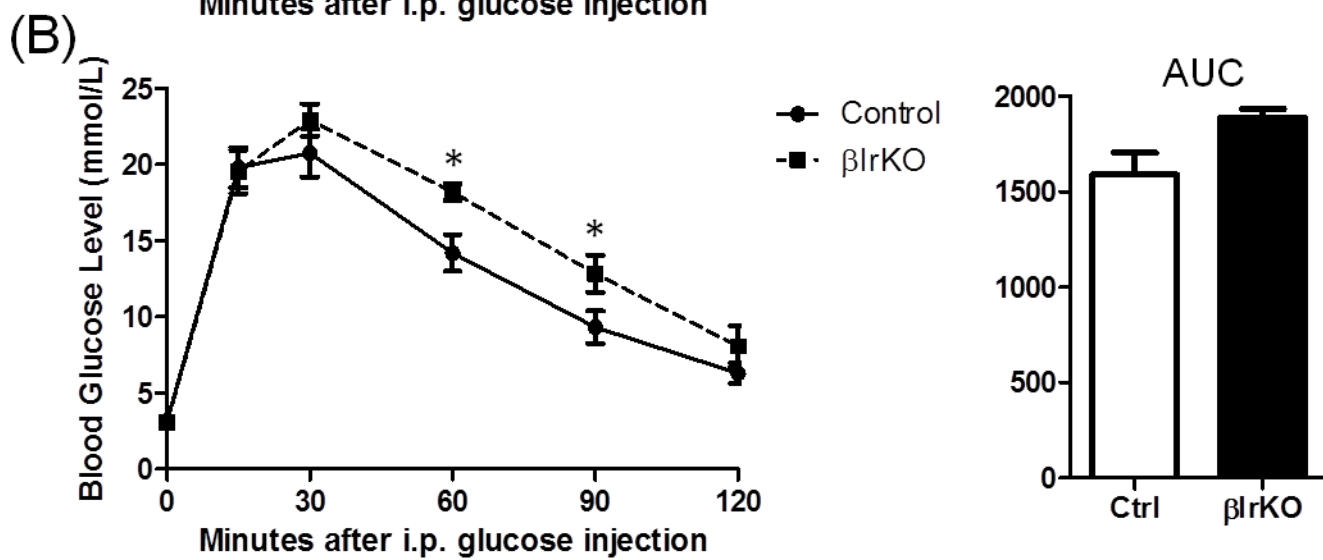
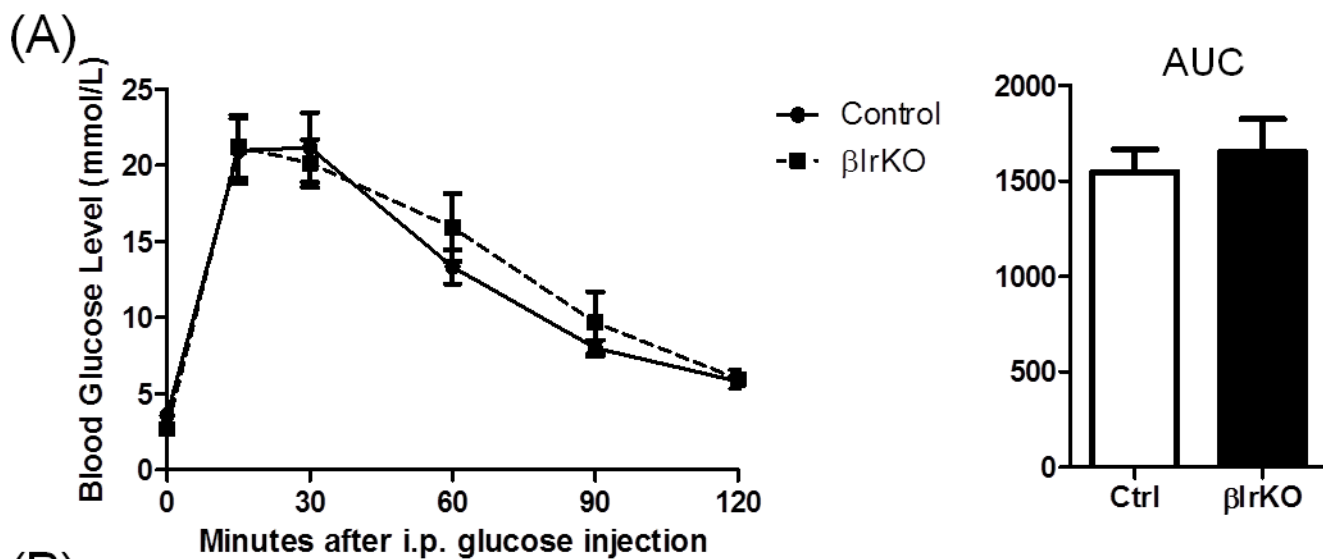


***Figure 3.13. Adult  $\beta$ IrKO mice demonstrate normal glucose metabolism at 4 and 8 weeks after *Ir* knockout***

Overnight (16hrs) fasted IPGTT at (A) 4 weeks and (B) 8 weeks post-tamoxifen in  $\beta$ IrKO and control groups. Glucose responsiveness of the corresponding experimental groups is shown as a measurement of AUC of the IPGTT graphs ( $n = 6-7$ ). (C) Overnight fasted (16hrs) *in vivo* glucose-stimulated insulin secretion at 8 weeks post-tamoxifen injection shows a lack of difference between the experimental groups ( $n = 6-7$ ). White bars, control group; black bars,  $\beta$ IrKO group. Data are expressed as means  $\pm$  SEM. \* $p < 0.05$ .

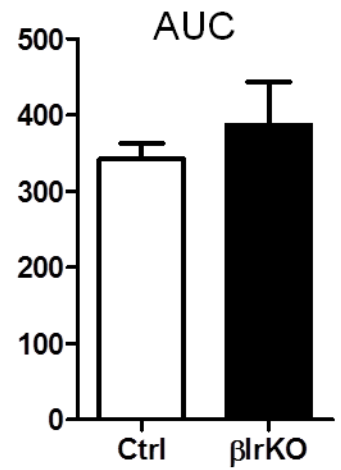
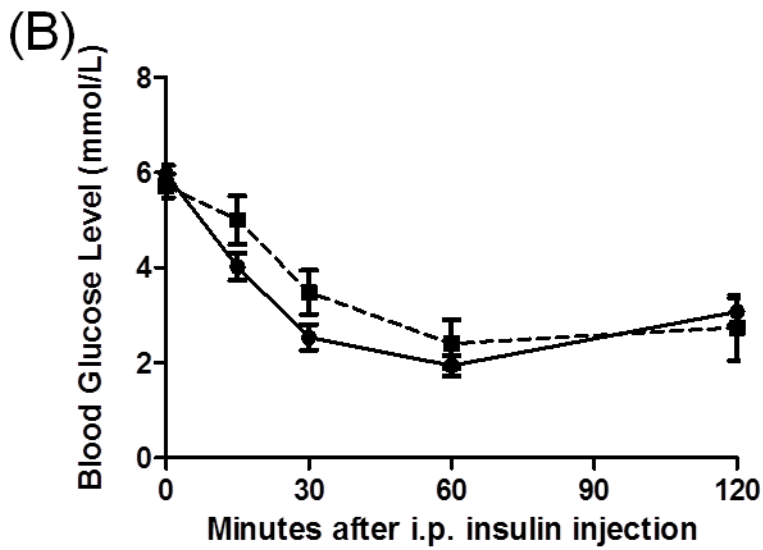
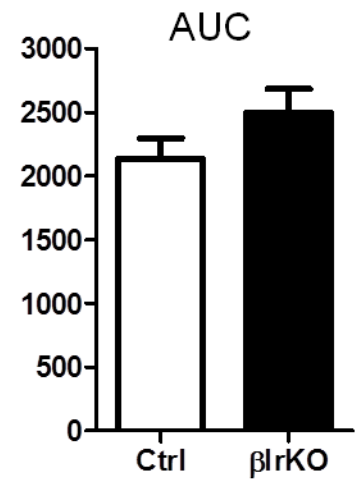
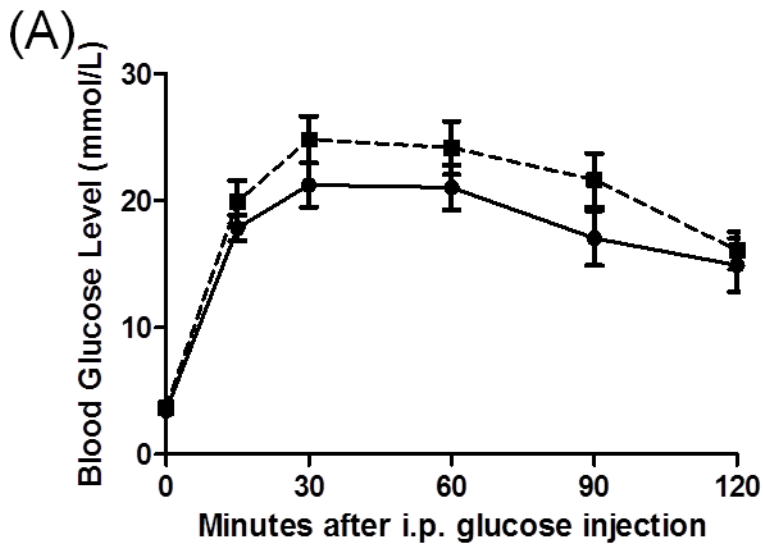


***Figure 3.14. Aged experimental groups appear to exhibit similar levels of glucose intolerance***

At 20 weeks post-tamoxifen injection, (A) overnight (16hrs) fasted IPGTT and (B) 4 hours fasted IPITT were completed ( $n = 6-7$ ). Glucose or insulin responsiveness of the corresponding experimental groups is shown as a measurement of AUC of the IPGTT and IPITT graphs. White bars, control group; black bars,  $\beta$ IrKO group. Data are expressed as means  $\pm$  SEM.

### 3.10 Pancreas morphology at 20 weeks post-tamoxifen injection

Since  $\beta$ IrKO and control groups both exhibited glucose intolerance compared to earlier age groups, morphometric analyses of the pancreas were performed after 20 weeks post-tamoxifen to further examine the effects of  $\beta$ -cell-specific IR deficiency under metabolic stress. At 20 weeks post-tamoxifen injection, mice were euthanized and pancreas weights were measured, but no significant difference was observed between  $\beta$ IrKO and control groups (**Figure 3.15A**). There was no difference in islet number per  $\text{mm}^2$  (**Figure 3.15E**) and islet size distribution (**Figure 3.15B**) between  $\beta$ IrKO and control groups. Quantitative analysis of  $\beta$ -cell mass (**Figure 3.15C**) and  $\alpha$ -cell mass (**Figure 3.15D**) further showed no changes between the experimental groups.

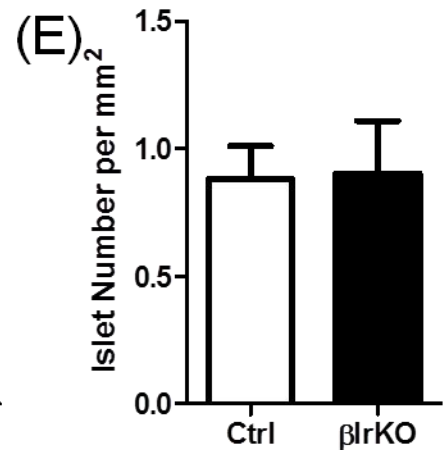
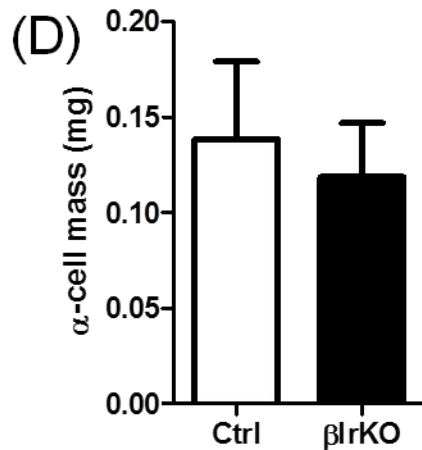
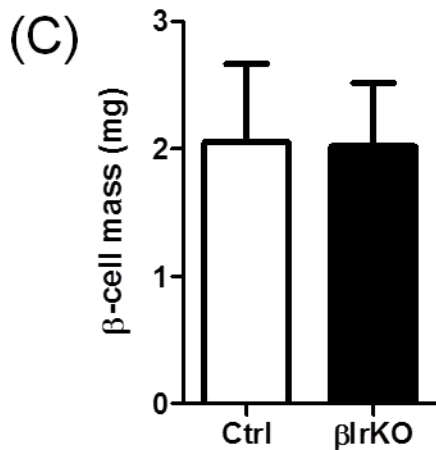
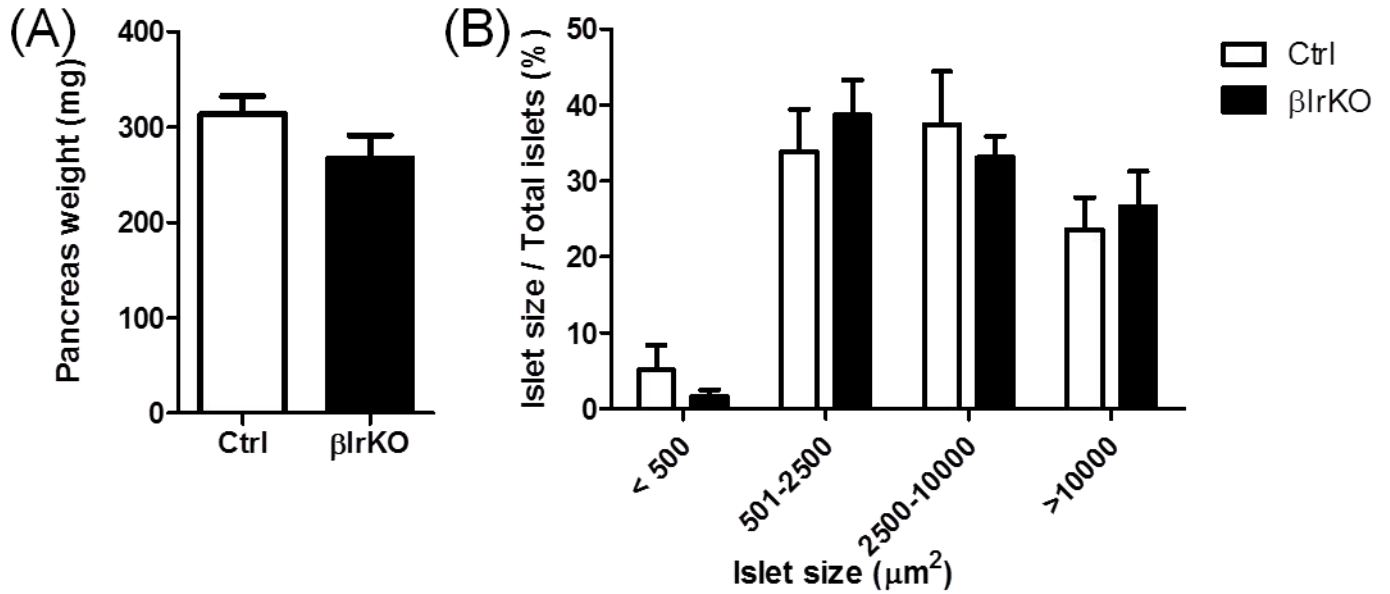
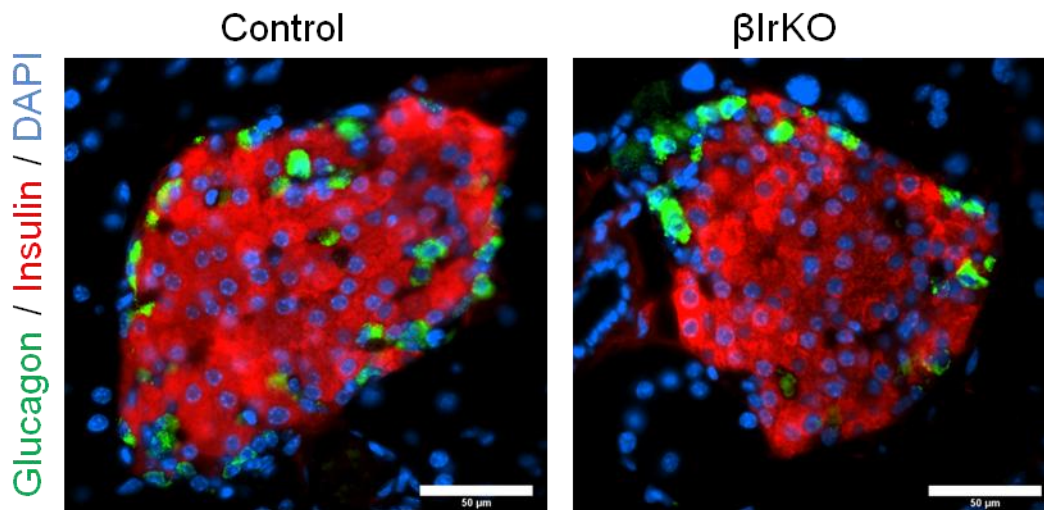


***Figure 3.15.* No differences in pancreatic morphology were observed between  $\beta$ IrKO and control mice**

Representative pancreatic islets are shown, with glucagon<sup>+</sup>  $\alpha$ -cells (green) and insulin<sup>+</sup>  $\beta$ -cells (red). Male mice were dissected at 20 weeks post-tamoxifen injection. Pancreatic morphological analysis of (A) pancreas weight, (B) islet size distribution, (C)  $\beta$ -cell mass, (D)  $\alpha$ -cell mass, and (E) islet number/mm<sup>2</sup> show similar islet morphology between experimental groups ( $n = 4$ ). White bars, control group; black bars,  $\beta$ IrKO group. Data are expressed as means  $\pm$  SEM.

### 3.11 Under high-fat diet, postnatally induced $\beta$ IrKO mice display comparable glucose metabolism to control mice

Previous studies have suggested the importance of  $\beta$ -cell IR on postnatal islet compensatory growth in response to high-fat diet (Okada et al. 2007). We further investigated the effect of high-fat stress on postnatally induced  $\beta$ -cell-specific *Ir* knockout mice. Interestingly, after 6 weeks on high-fat diet, all study groups ( $\beta$ IrKO, heterozygous, and control) were similar in terms of body weight and fasting blood glucose, and they were not significantly different from mice on normal chow (**Figure 3.16**). Next, we sought to determine whether high-fat diet stress could accelerate  $\beta$ -cell dysfunction in  $\beta$ IrKO mice. When compared to same aged mice under chow diet (**Figure 3.13B**), all experimental groups demonstrated higher IPGTT levels, indicating an early onset of high-fat diet induced diabetes (**Figure 3.17A**). However, IPGTT results for  $\beta$ IrKO, heterozygous, and control mice were not significantly different from each other, further questioning the necessity of postnatal IR in  $\beta$ -cell maintenance and function. In addition, IPITT revealed normal insulin sensitivity in all study groups under high-fat diet (**Figure 3.17B**).

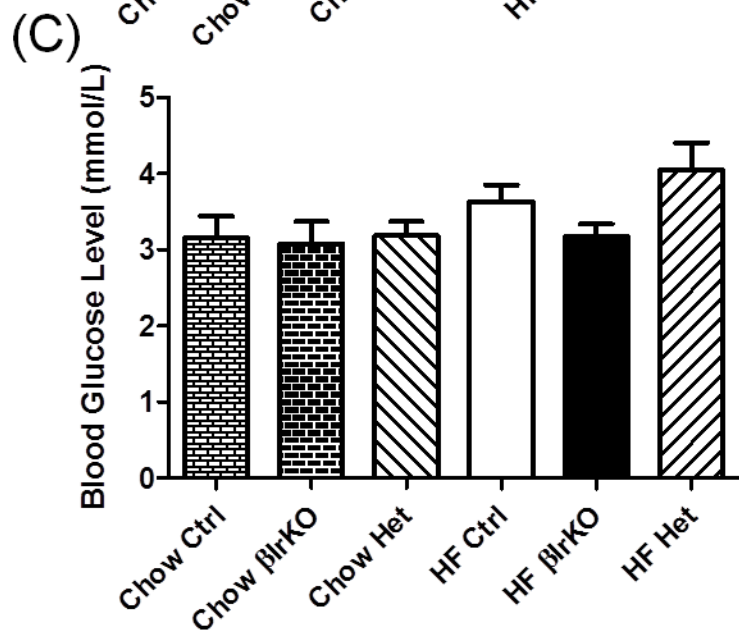
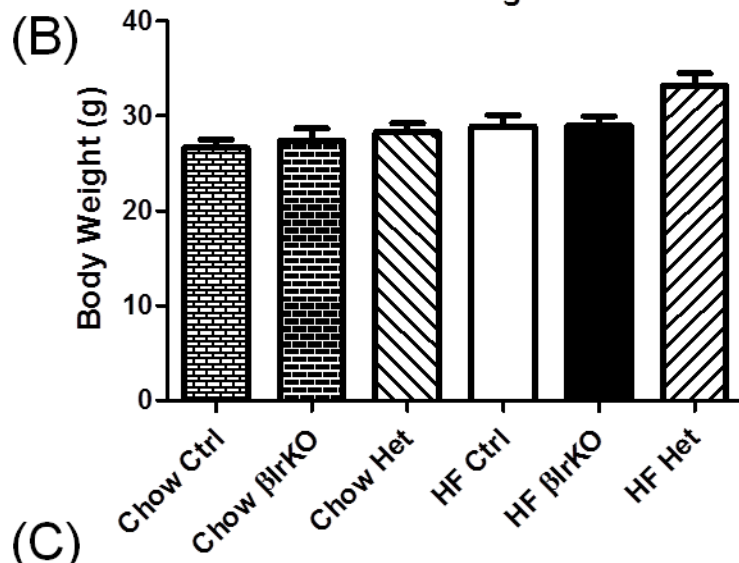
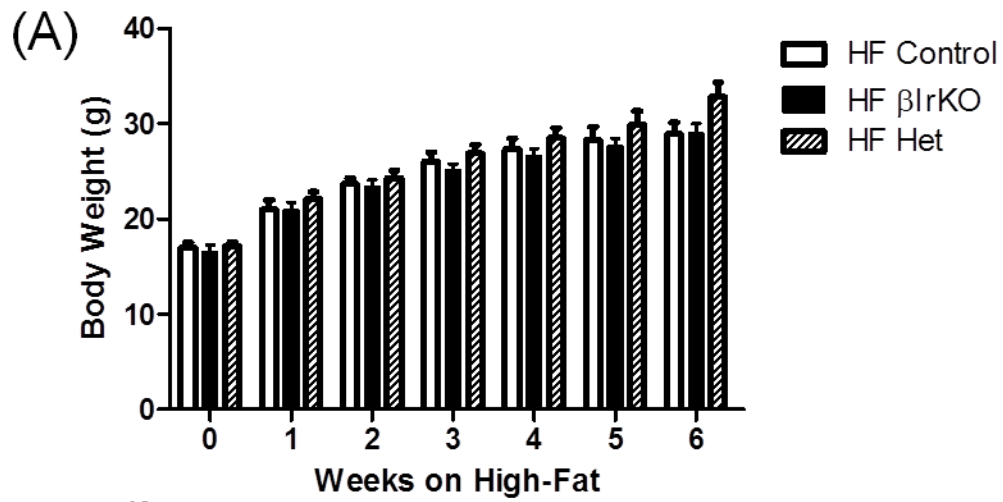


***Figure 3.16. Phenotypes of experimental male mice after 6 weeks of high-fat diet***

(A) Weekly body weights monitored for 6 weeks on high-fat diet. (B) Body weight and (C) overnight (16hrs) fasted blood glucose levels at the end of high-fat diet in  $\beta$ IrKO, heterozygous, and control groups ( $n = 6-9$ ). Data are expressed as means  $\pm$  SEM.

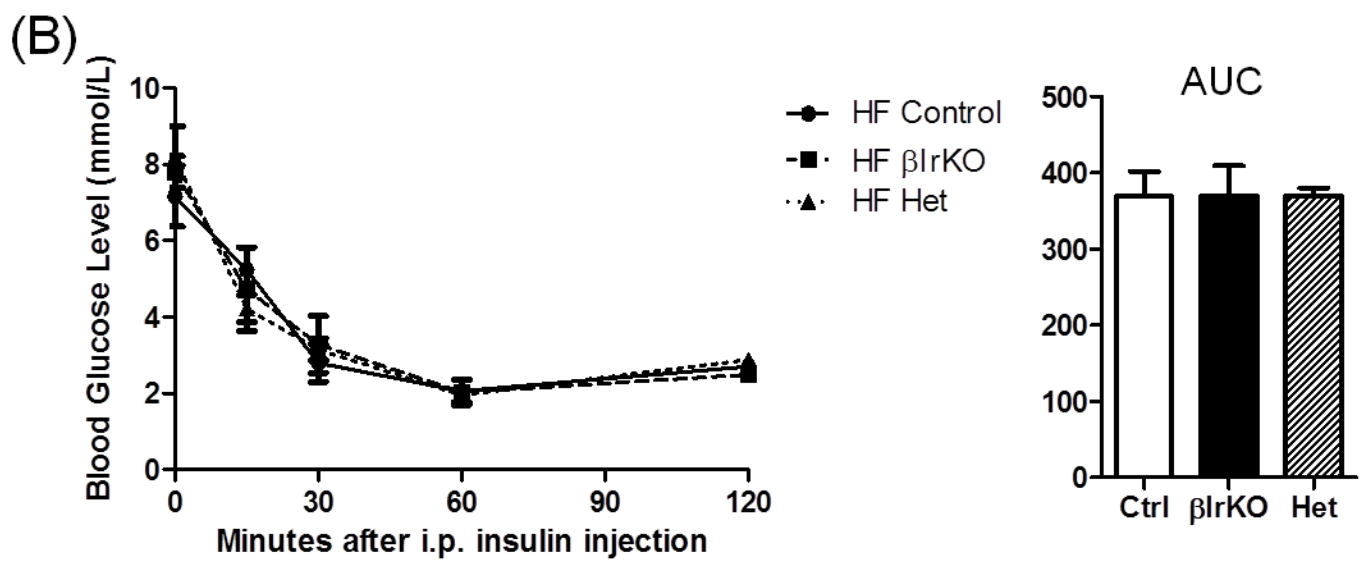
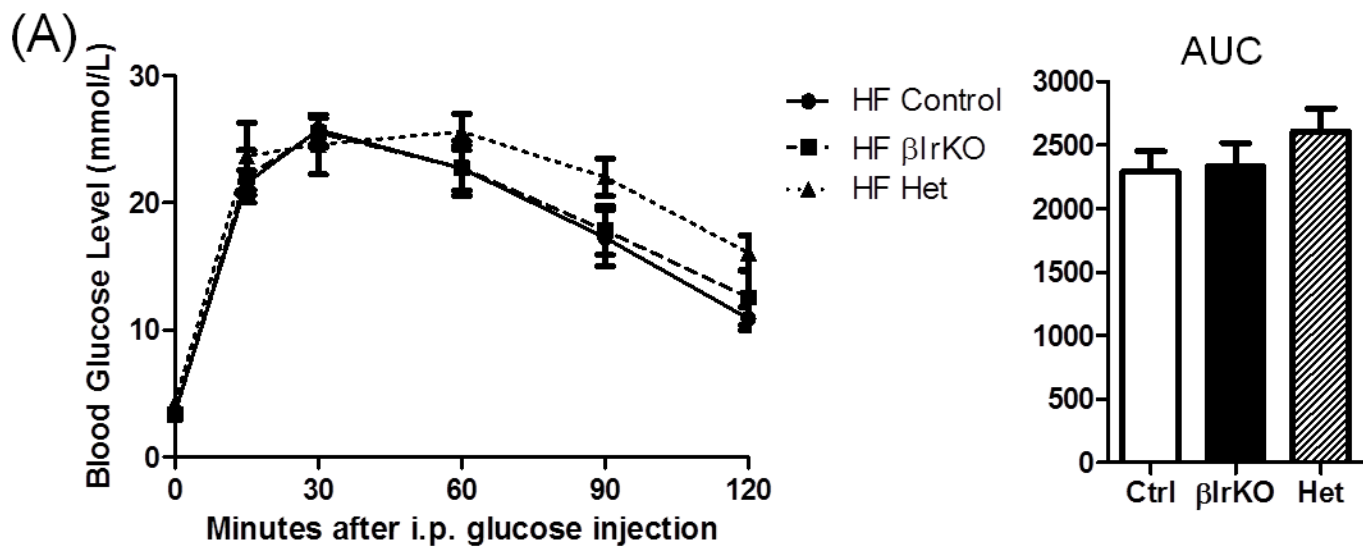


***Figure 3.17. Metabolic studies at 8 weeks post-tamoxifen in male mice after 6 weeks on a high-fat diet***

(A) Overnight (16hrs) fasted IPGTT (n = 6-8), and (B) 4 hours fasted IPITT (n = 3-6) were performed on all experimental groups. Glucose or insulin responsiveness of the corresponding experimental groups is shown as a measurement of AUC of the IPGTT and IPITT graphs. Data are expressed as means  $\pm$  SEM.

## Chapter 4 - Discussion

This project examined the *in vivo* role of  $\beta$ -cell-specific insulin receptor during different developmental stages using a novel conditional and temporal *Ir* knockout model. In contrast to many previous  $\beta$ IrKO that utilized the Cre/loxP system to facilitate congenital  $\beta$ -cell *Ir* knockout, our tamoxifen-inducible  $\beta$ IrKO mouse model allowed *Ir* knockout at various developmental ages. We demonstrated that  $\beta$ -cell-specific *Ir* knockout during the secondary transition of pancreatic development leads to an adaptive islet growth. The robust increase of  $\beta$ -cell proliferation was associated with significantly increased IGF2 levels, phospho-Akt activity, and enhanced islet vascularization. Interestingly,  $\beta$ IrKO after postnatal pancreatic remodelling in 3 week old adult mice failed to develop age-dependent glucose intolerance phenotype seen in previous studies. In addition, adult  $\beta$ IrKO, control, and heterozygous groups after 6 weeks of high-fat-diet stress developed impaired glucose tolerance, but they were indistinguishable from each other. Taken together, the results from this thesis suggest that the loss of  $\beta$ -cell-specific IR promotes  $\beta$ -cell replication during embryonic islet development, but IR may not be required for postnatal  $\beta$ -cell mass maintenance and function.

### 4.1 Does $\beta$ -cell-specific *Ir* knockout affect islet formation during secondary transition?

We first confirmed the specificity of the *MIPCreERT* expression to pancreatic  $\beta$ -cells by crossing the *MIPCreERT* mice with B6.Cg-*Gt(ROSA)26Sor<sup>tm9(CAG-tdTomato)Hze</sup>/J* reporter mice. In addition, western blot analysis of fetal pancreata demonstrated that  $\beta$ -cell IR levels were significantly reduced (~75%) in fetal  $\beta$ IrKO mice. Our recombination efficiency supports previous research demonstrating that 50 to 70% of Cre-recombination is achieved depending on the tamoxifen dosage (Hayashi et al. 2002).

Similar to previous  $\beta$ IrKO studies, the body weight of newborn pups did not differ between littermates, indicating overall normal embryonic development (Kulkarni et al. 1999, Okada et al. 2007). Although these studies did not conduct in-depth quantitative analyses of islet morphology during prenatal stages, they suggested that  $\beta$ -cell IR does

not play an essential role in fetal islet development and maturation (Kulkarni et al. 1999, Okada et al. 2007). Contrary to this statement, our results demonstrated a significant increase in  $\beta$ -cell area, mean and overall islet area when  $\beta$ -cell *Ir* was knocked out during the secondary transition. An explanation for this is that we are the first group to induce  $\beta$ -cell-specific *Ir* knockout at embryonic day 13 (e13) instead of congenital  $\beta$ -cell *Ir* knockouts seen in previous studies. Since the secondary transition is a period of rapid  $\beta$ -cell differentiation, expansion, and maturation, the loss of existing  $\beta$ -cell IR could lead to an immediate cell adaptation response seen in our  $\beta$ IrKO mice (Habener et al. 2005, Gunasekaran et al. 2012), implicating that *in vivo*  $\beta$ -cell-specific *Ir* knockout phenotypes are time-dependent. The current study demonstrated that the abrupt loss of IR signalling in  $\beta$ -cells during islet development, specifically during secondary transition, led to an islet hyperplastic growth response. Islet hyperplasia seen in fetal  $\beta$ IrKO is consistent with the congenital insulin knockout mouse model, where the loss of insulin led to increased islet size, proliferation, and vascularization at e19 (Duvillie et al. 2002). Together, these findings indicate that the loss of IR signalling has an adaptive stimulatory effect on prenatal  $\beta$ -cell growth.

To characterize whether islet hyperplasia in fetal  $\beta$ IrKO pancreas is due to either  $\beta$ -cell proliferation from pre-existing  $\beta$ -cell or neogenesis from progenitors, we examined  $\beta$ -cell proliferation using immunofluorescent Ki67 staining versus  $\beta$ -cell apoptosis by TUNEL staining. While TUNEL staining showed relatively similar levels of apoptosis, the proliferation of  $\beta$ -cells in fetal  $\beta$ IrKO mouse islets were significantly higher than that of littermate controls. This result indicates that  $\beta$ -cell replication from pre-existing  $\beta$ -cells likely contributed to islet hyperplasia in fetal  $\beta$ IrKO mice. This data is in agreement with previous studies that demonstrated  $\beta$ -cell replication starting around e16.5 is responsible for maintaining  $\beta$ -cell survival throughout postnatal development (Montanya et al. 2000, Dor et al. 2004). Generally, murine  $\beta$ -cell neogenesis from ductal cells begins at e9 and remains active for the first few weeks after birth until weaning. In order to determine whether  $\beta$ -cell neogenesis also contributed to islet hyperplasia, Pdx-1 localization in ductal cells in both fetal  $\beta$ IrKO and control pancreata were examined. We observed similar levels of Pdx-1<sup>+</sup> ductal cells between the groups, suggesting that fetal  $\beta$ -cell *Ir*

knockout may not have affected islet neogenesis. Consistent with our results, Du villie et al. (2002) showed enlarged fetal islets in insulin knockout mice without an increase in islet neogenesis. Therefore, we believe that the islet growth response in fetal  $\beta$ IrKO mice is likely due to the enhanced  $\beta$ -cell replication, rather than increased levels of islet neogenesis.

To examine whether fetal  $\beta$ IrKO altered proper  $\beta$ -cell maturation, we investigated transcription factors that are required for  $\beta$ -cell maturation. It is well documented that Pdx-1 in  $\beta$ -cells is necessary for insulin synthesis, glucose metabolism, and  $\beta$ -cell survival (Brissova et al. 2002, Gittes 2008). Similarly, Nkx6.1, MafA, and Islet-1 are necessary for  $\beta$ -cell differentiation and postnatal function. (Sander et al. 2000, Aguayo-Mazzucato et al. 2011, Ediger et al. 2014). There were similar levels of  $\beta$ -cell nuclear localization for both fetal  $\beta$ IrKO and control pancreata with Pdx-1, Nkx6.1, MafA, and Islet-1. In addition, we showed that the levels of Glut-2, a marker for  $\beta$ -cell glucose sensitivity, did not differ between  $\beta$ IrKO and control pancreas, further suggesting that these  $\beta$ -cells properly developed and are functional despite the early loss of  $\beta$ -cell IR.

## 4.2 Could the $\beta$ -cell-specific *Ir* knockout promote activity of homologous signalling pathways?

We sought to determine the signalling pathways that may contribute to increased replication of functional  $\beta$ -cells observed in fetal  $\beta$ -cell-specific *Ir* knockout mice. Western blot analysis revealed increased phosphorylation of Akt, an important regulator of  $\beta$ -cell proliferation and anti-apoptotic signalling, in fetal  $\beta$ IrKO pancreata. Similar to our results, overexpression of *Akt* in pancreatic  $\beta$ -cells has been associated with increased  $\beta$ -cell size and total islet mass (Tuttle et al. 2001). In addition, we detected decreased phosphorylation of the tumor suppressor p53 in  $\beta$ IrKO pancreata relative to control mice. Congruent with our findings of increased Akt and reduced p53 activity, numerous studies have suggested that active Akt downregulates p53 in the INS-1 rat insulinoma cell line and isolated pancreatic islets (Wrede et al. 2002, Feng et al. 2013, Ogawara et al. 2002). Since p53 plays a key role in the induction of apoptosis and cell cycle arrest, we

speculate that impaired regulation of cell cycle arrest could also contribute to the increased  $\beta$ -cell proliferation seen in  $\beta$ IrKO pancreata.

To account for the enhanced Akt activity seen in fetal  $\beta$ IrKO pancreata, we investigated IGF1 and IGF2 because they have the ability to stimulate both IR and IGF1R (Louvi et al. 1997, Nakae et al. 2001). During fetal development, IGF2 is strongly localized to pancreatic islets and is more abundant than IGF1 (Hill et al, 1999). Consistent with this finding, we showed that IGF1 levels were very low in the fetal pancreas and we conclude that Akt activity is likely induced by the elevated IGF2 protein levels localized to fetal  $\beta$ IrKO islets. In agreement with our results, IGF2 overexpressing transgenic mice exhibited robust islet cell hyperplasia and apoptotic inhibition (Petrik et al. 1999). Similarly, another group utilized the Goto-Kakizaki diabetic rat model to examine defective fetal IGF2 production, which led to a reduction in  $\beta$ -cell mass (Calderari et al. 2007). Our results suggest that the loss of fetal  $\beta$ -cell IR leads to an upregulation of IGF2 protein levels in the islets, which signals through the IGF1R to promote Akt-mediated  $\beta$ -cell proliferation during fetal development (**Figure 4.1**). Since our western blot analysis showed that  $\beta$ -cell-specific *Ir* was not entirely knocked out, it is also possible that IGF2 exerted its proliferative effects through remaining IR on the  $\beta$ -cells. However, IGF2 levels rapidly diminishes from birth to postnatal day 28 in rats (Hill et al, 1999), so it is of interest for further experiments to examine whether the increased islet growth seen in fetal  $\beta$ IrKO pancreas can be sustained neonatally. Interestingly, a recent study demonstrated that  $\beta$ -cell-specific *Igf2* overexpressing adult mice have disrupted islet structure, islet hyperplasia, and develop glucose intolerance, indicating  $\beta$ -cell dysfunction (Casellas et al, 2015). Therefore, further experiments are necessary to determine the consequences of increased prenatal IGF2 levels on neonatal  $\beta$ -cell function.

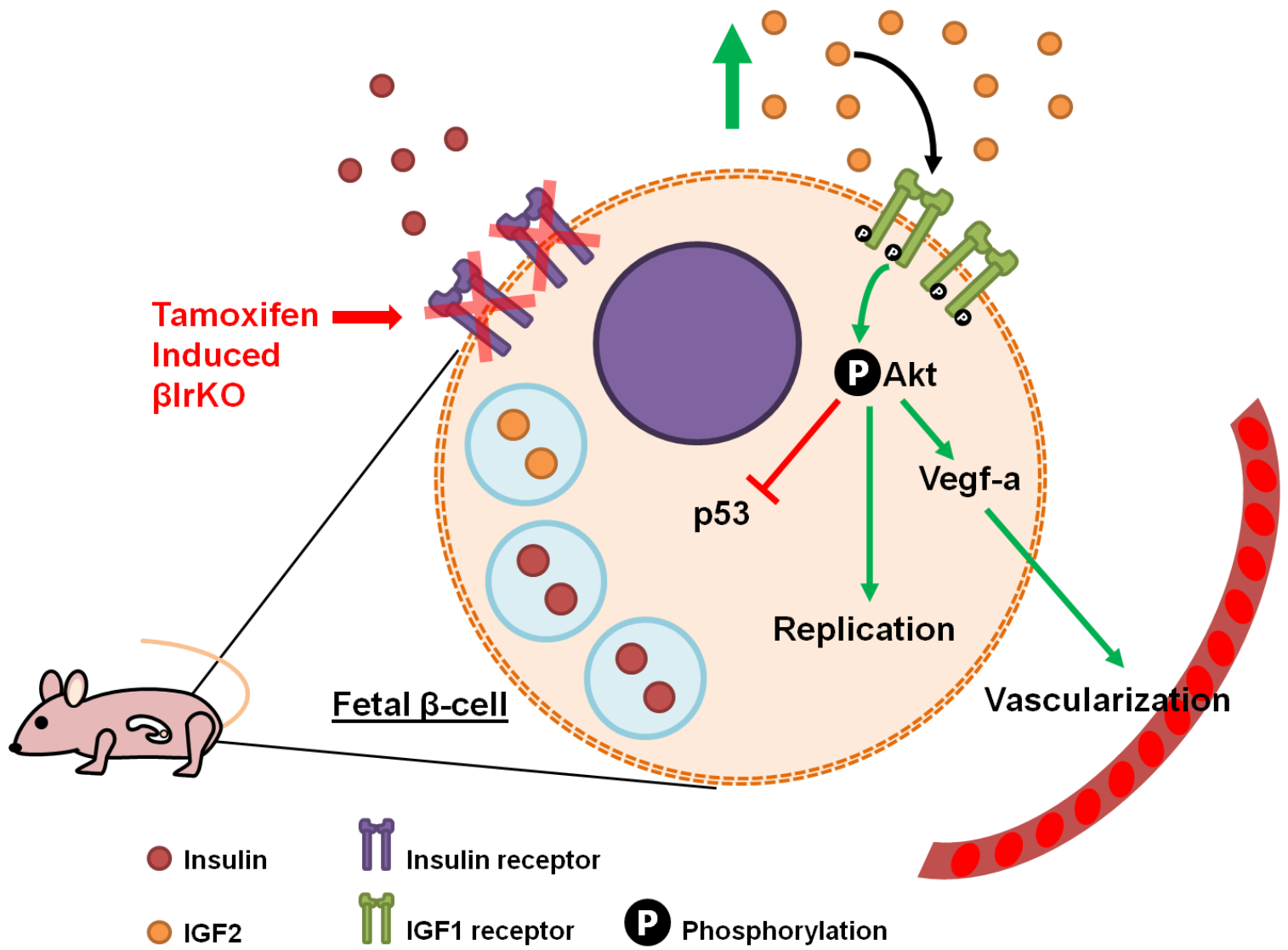


*Figure 4.1. Proposed adaptive signalling mechanisms in fetal  $\beta$ IrKO mice*

We demonstrated that the tamoxifen-induced loss of  $\beta$ -cell IR during fetal pancreatic development results in enhanced levels of IGF2. We propose that the IGF2 released from  $\beta$ IrKO  $\beta$ -cells exerts autocrine/paracrine activation of IGF1 receptors, causing an increase in Akt phosphorylation/activation and stimulation of downstream signalling pathways. Resulting upregulated Vegf-a production and secretion contribute to increased

vascularization. Consequently, enhanced Akt activity combined with increased islet vascularization promotes  $\beta$ -cell replication, inducing the islet growth response seen in  $\beta$ IrKO mice.

### 4.3 Is the level of islet vascularization associated with islet growth during prenatal life?

Previous studies have proposed that increased vascularization can promote  $\beta$ -cell differentiation and replication because the endothelium and its associated blood supply are essential for the  $\beta$ -cell differentiation and maintenance of  $\beta$ -cell function (Lammert et al. 2001, Nikolova et al. 2006, Brissova et al. 2006). In our study,  $\beta$ IrKO pancreata exhibited significantly increased islet capillary area (percent of PECAM-1<sup>+</sup> area/islet area), islet vessel density, and Vegf-a protein levels. Pancreatic  $\beta$ -cells produce Vegf-a to attract endothelial cells, which form capillaries throughout the islets. Similar to our results, insulin knockout mice also resulted in a simultaneous increase of  $\beta$ -cell mass and islet vascularization during fetal development (Duvillie et al. 2002). Therefore, our results further support the notion that increased islet vascularization promotes islet growth seen in fetal  $\beta$ IrKO mice. In addition, Duvillie et al. (2002) speculated the contribution of IGF2 to the islet hyperplasia but did not observe an increase in *Igf2* mRNA levels. In contrast, we demonstrated that IGF2 protein levels is increased, implying that there may be an altered posttranscriptional regulation that stimulates IGF2 protein production. IGF2 can further promote embryonic vasculogenesis by upregulating Vegf levels (Pieciewicz et al. 2012). In many tumours, tumour-derived IGF2 has been shown to bind to IGF1R, leading to increased Vegf production and subsequent angiogenesis (Bid et al. 2012, Bid et al. 2013). Taken together, our fetal  $\beta$ IrKO study suggests that  $\beta$ IrKO knockout in the developing mouse pancreas causes an adaptive upregulation of IGF2 levels in the islets, which contributes to the observed Akt elevation, increased Vegf-a protein levels, and subsequent islet vascularization. Together, Akt and increased islet vascularization stimulate  $\beta$ -cell replication (**Figure 4.1**).

## 4.4 Do postnatally induced $\beta$ -cell-specific knockout mice exhibit age-dependent glucose intolerance?

### 4.4.1 Recombination efficiency of inducible postnatal $\beta$ -cell-specific *Ir* knockout?

To better understand the role of  $\beta$ -cell IR exclusively during postnatal life, we induced  $\beta$ -cell-specific *Ir* knockout after postnatal pancreatic islet remodelling at 3-4 weeks of age in adult mice. Western blot analysis confirmed a significant reduction of the  $\beta$ -cell IR protein levels in isolated islets of  $\beta$ IrKO mice compared to controls, but was only found to be only ~50% reduced. The observed recombination efficiency is mainly attributed to the tamoxifen dosage that we utilized. The efficiency of the inducible Cre-loxP recombination in adult mice has been extensively evaluated with various reporter strains. Previous studies have used various dosages of tamoxifen injection, ranging from 3 consecutive days of 1 mg up to 5 days of 9 mg tamoxifen injection, resulting in a varying recombination efficiency of up to ~90% (Hayashi et al. 2002, Wicksteed et al. 2010, Reinert et al. 2012, Tamarina et al. 2014). These findings suggest that the recombination efficiency is tamoxifen dose-dependent, and multiple injections of even the highest dosage did not lead to any major changes in animal behaviour or physiological side effects (Hayashi et al. 2002). However, Reinert et al. (2012) observed incomplete absorption of corn oil vehicle as well as scrotal enlargement in tamoxifen treated mice, and the consequences of these side effects are unknown. Therefore, we utilized a lower dosage of 3 consecutive days of 4 mg / 20g of body weight tamoxifen injection for the postnatally induced  $\beta$ IrKO mice in an attempt to achieve an optimal level of recombination while avoiding potential side effects. Thus, the insufficient  $\beta$ -cell *Ir* knockout could have contributed to the insignificant changes for the phenotypes of  $\beta$ IrKO mice.

### 4.4.2 Does postnatal $\beta$ -cell-specific *Ir* knockout affect glucose metabolism?

The overnight fasting blood glucose levels and body weight measured at 4, 8, and 20 weeks post-tamoxifen injection showed no difference between control and  $\beta$ IrKO

mice. Previous studies utilizing congenital  $\beta$ IrKO mouse models have found similar fasting blood glucose results at 2 and 6 months of age (Kulkarni et al. 1991, Ueki et al. 2006). However, unlike our adult  $\beta$ IrKO mice, studies have observed glucose intolerance in congenital  $\beta$ IrKO mice, suggesting the importance of  $\beta$ -cell IR for glucose metabolism in adult life. Similar other reports have demonstrated impaired glucose homeostasis in  $\beta$ IrKO mice as early as 4-5 weeks of age (Ueki et al. 2006, Okada et al. 2007), or progressive age-dependent glucose intolerance from 2-6 months of age (Kulkarni et al. 1991). Furthermore, previous studies also demonstrated a loss of acute first-phase but normal second-phase insulin secretion in  $\beta$ IrKO mice at 1 month (Okada et al. 2007) and 3 months of age (Kulkarni et al. 1991). This functional change in insulin secretion was not observed in our postnatally induced  $\beta$ IrKO mice, which displayed similar glucose-stimulated insulin secretion during both 1<sup>st</sup> and 2<sup>nd</sup> phases.

The discrepancy between previous studies and our results may be attributed to the utilization of different promoters to drive  $\beta$ -cell-specific *Ir* knockout. Former *in vivo*  $\beta$ IrKO studies utilized the *RIP*, which is also actively expressed in the hypothalamus, leading to ectopic expression of Cre recombinase (Wicksteed et al. 2010). Subsequently, altered levels of IR in the brain could adversely affect glucose homeostasis. Another reason for this conflicting finding is the insufficient deletion of  $\beta$ -cell *Ir*. As we mentioned above, we only achieved an *Ir* knockout of ~50% in pancreatic islets, suggesting that the remaining  $\beta$ -cell IR are able to maintain normal glucose homeostasis. This is supported by one study that found that global heterozygous *Ir* knockout mice retained normal phenotypes and displayed similar levels of glucose tolerance as controls, whereas null *Ir* mice quickly died after birth due to severe ketoacidosis (Joshi et al. 1996, Acili et al. 1996). Taken together, we suggest that  $\beta$ -cells have a plethora of IR, and that a reduced amount of  $\beta$ -cell IR (~50%) is sufficient for proper  $\beta$ -cell maintenance and function in postnatal life. Additionally, previous studies have shown that double  $\beta$ -cell *Ir* and *Igf1r* knockout mice exhibit the most severe glucose intolerance and die from severe ketoacidosis starting at 6 weeks, suggesting that these receptors are able to compensate for each other to a certain extent (Ueki et al. 2006, Xuan et al. 2010).

All the previous studies utilized the same congenital *RIP*-driven  $\beta$ -cell-specific *Ir* knockout model, while we used an inducible *MIP*-driven  $\beta$ -cell-specific *Ir* knockout model where  $\beta$ -cell *Ir* was knocked out 4 weeks after birth (Ueki et al. 2006, Okada et al. 2007, Kulkarni et al. 1991). By inducing the  $\beta$ -cell *Ir* knockout around 4 weeks of age, we allowed proper fetal pancreatic formation, including the undisturbed completion of the third transition in pancreatic development, which spans from embryonic day 18 to postnatal day 21. The third transition, also defined as the pancreatic remodelling period, is an important stage of  $\beta$ -cell proliferation, apoptosis, and maturation (Kaung 1994, Scaglia et al. 1997). Previous congenital  $\beta$ IrKO mice lacked  $\beta$ -cell IR throughout essential prenatal pancreatic development and postnatal remodelling, causing these mice to exhibit early age-dependent  $\beta$ -cell dysfunction. In contrast, we induced  $\beta$ -cell *Ir* knockout in adult mice after postnatal remodelling, and demonstrated that these  $\beta$ IrKO mice were able to maintain euglycemic levels similar to control mice. This could be because our  $\beta$ IrKO mice underwent normal pancreatic formation and remodelling with the presence of  $\beta$ -cell IR, allowing proper  $\beta$ -cell maturation and prolonging  $\beta$ -cell function. These results suggest that  $\beta$ -cell IR could be crucial for  $\beta$ -cell remodelling during the first 21 days of postnatal life. The importance of fetal  $\beta$ -cell IR is further supported by our prenatal  $\beta$ IrKO results, where the loss of fetal  $\beta$ -cell IR elicited an islet growth response, indicating the importance of prenatal  $\beta$ -cell IR. Therefore, our postnatal inducible  $\beta$ IrKO study demonstrates that the protein levels of  $\beta$ -cell IR and  $\beta$ -cell IR loss at the examined age of interest could exert a key influence in  $\beta$ -cell function and  $\beta$ -cell mass maintenance.

Surprisingly, both control and  $\beta$ IrKO mice manifested impaired glucose tolerance at 20 weeks post-tamoxifen when compared to younger mice. This could be attributed to the genetic composition of the B6 mice. It has been reported that glucose tolerance tests performed on B6 mice after 18 weeks on either low- or high-fat diet revealed impaired glucose tolerance on both diets. Furthermore, the mixed genetic background of B6 and 129 manifested a larger degree of heterogeneity when it comes to dietary intake and spontaneous obesity (Almind et al. 2004). This may explain the observed variability in glucose tolerance tests at 20 weeks post-tamoxifen. Coinciding with these metabolic

studies, islet morphological analyses at 20 weeks post-tamoxifen did not show any differences in islet size or  $\beta$ -cell mass. Therefore, our statistically insignificant results are likely due to the genetic background and variable levels of *Ir* knock out in mice.

#### 4.5 Do postnatally induced $\beta$ -cell-specific knockout mice exhibit glucose intolerance after high-fat diet stress?

Previously, it has been shown that when congenital  $\beta$ IrKO mice were fed a high-fat diet for 20 weeks, a percentage of mice died prior to the end of the study while others manifested obesity and hyperglycemia (Okada et al. 2007). Morphologically, these  $\beta$ IrKO mice failed to develop the islet compensatory growth responses seen in control mice, suggesting the necessity of  $\beta$ -cell IR for growth response (Okada et al. 2007). In addition, Mehran et al. (2012) demonstrated that heterozygous insulin knockout B6 mice do not develop islet compensatory growth, hyperinsulinemia, or obesity under high-fat diet while control mice developed diabetic phenotypes, further suggesting that  $\beta$ -cell insulin signalling is required for  $\beta$ -cell compensatory response to high-fat diet. In an attempt to better understand the role of  $\beta$ -cell insulin signalling during metabolic stress, we fed postnatally induced  $\beta$ IrKO mice a 6-week of high-fat diet starting at 2 weeks after tamoxifen injection. We proposed to determine whether varying levels of  $\beta$ -cell IR could potentially prevent diet-induced obesity similar to the findings from the heterozygous insulin knockout mouse model (Mehran et al. 2012). Interestingly, all experimental groups (control, heterozygous, and  $\beta$ IrKO), displayed similar levels of impaired glucose tolerance compared to mice on chow-diet, but are equally sensitive to insulin after 6 weeks of high-fat diet. In addition, at the end of the high-fat diet period, the body weight and fasting blood glucose of these groups did not significantly differ from mice on chow-diet. This could be because these mice were subjected to high-fat diet for only 6 weeks, and  $\beta$ -cell compensatory proliferation may not be obvious until after 14 weeks on high-fat diet (Roat et al. 2014). Therefore, we need to implement a longer term high-fat diet study to determine the effect of postnatally induced  $\beta$ IrKO.

## 4.6 Limitations

The present study is performed on transgenic mouse models. Despite the similarity in genetic composition and conservation of the insulin receptor gene between humans and mice, significant differences exist. For instance, the organization of pancreatic islets is different, and IR appears to play different roles during embryonic development. Similar to mice, humans lacking *IR* expression during embryonic development are viable at birth. However, mutations of *IR* in humans lead to postnatal heterogeneous phenotypes ranging from mild insulin resistance to leprechaunism (Nakae et al. 2001). These similarities and differences should be considered when translating these studies to humans.

In addition, we utilized the *MIP* to drive Cre recombinase expression specifically limited to pancreatic  $\beta$ -cells (Tamarina et al. 2014). However, one study has demonstrated ectopic expression of *MIP* in neurons of the hypothalamus (Wang et al. 2014). Therefore, we may face similar limitations to previous studies that used the *RIP*, which also has ectopic expression in the hypothalamus. Ectopic activity of Cre recombinase, and the subsequent knockdown of *Ir*, in the hypothalamus during embryonic development could adversely affect energy homeostasis and metabolism in postnatal life (Wicksteed et al. 2010).

Another limitation is the incomplete knockout of  $\beta$ -cell IR protein levels in  $\beta$ IrKO mice. As mentioned above, we only observed around ~75% and ~50%  $\beta$ -cell *Ir* knockdown in fetal and adult  $\beta$ IrKO mice, respectively. Since remaining IR on  $\beta$ -cells are likely functional, we only investigated the effect of a partial  $\beta$ -cell *Ir* knockdown, but cannot determine the consequences of a complete  $\beta$ -cell *Ir* knockout. Furthermore, since we are unable to isolate islets from fetal pancreata due to technical difficulties, all fetal western blot data are representative of the whole pancreas, comprised of both the exocrine compartment and endocrine islets.

Lastly, because we observed an islet growth response in the fetal  $\beta$ IrKO study, we have attempted to generate neonatal mice in order to examine the consequences of diminishing

IGF2 levels after birth on the neonatal (p21) islet morphology. However, tamoxifen injected pregnant mothers have consistently killed newborn litters. Although it is not well documented, it is possible that the tamoxifen injection adversely affects the health of the pregnant mother or newborns and as a result, they are neglected by the mother. We are currently working to obtain neonatal samples by fostering with pregnant CD-1 mice.

## 4.7 Conclusion and Future directions

This thesis demonstrated that the  $\beta$ -cell IR plays an important role in fetal islet development, while the varying levels of  $\beta$ -cell IR did not affect postnatal glucose homeostasis. By understanding the temporal role of  $\beta$ -cell IR during different developmental stages, we can potentially promote the survival and function of clinically isolated islets by administering exogenous ligands, such as insulin and IGF2, to stimulate downstream insulin receptor signalling pathways in  $\beta$ -cells. This may improve the long-term success of current cell-based therapies for diabetes by altering the  $\beta$ -cell IR activity on donor islets prior to islet transplantation.

To further investigate the results from the fetal  $\beta$ IrKO study, we will continue to examine islet morphology during the neonatal period, up until p21. We concluded that the increased islet growth observed in fetal  $\beta$ IrKO mice is likely due to increased IGF2, but IGF2 levels rapidly diminishes after birth in rodents (Hill et al. 1999). Therefore, we should investigate the consequences of diminishing IGF2 on the pancreatic islet mass, and better understand the consequential adaptation between different signalling networks.

For the postnatally induced  $\beta$ IrKO studies, we should subject these experimental groups to high-fat diet for a longer period of time since we did not observe clear insulin resistance after 6 weeks of high-fat diet. Currently, we have *in vivo* metabolic data and islet morphology analyses at 24 weeks of age (20 weeks post-tamoxifen) for experimental mice on chow diet. Corresponding to this age group, we propose to subject animals on high-fat diet for 18 weeks starting at 6 weeks of age (2 weeks post-tamoxifen). We expect to observe decreased peripheral insulin sensitivity and diabetic phenotypes at the end of

the high-fat diet treatment, and will then examine the islet morphology and metabolic differences between  $\beta$ IrKO, heterozygous, and control mice.

## Chapter 5 - References

- Accili D, Drago J, Lee EJ, Johnson MD, Cool MH, Salvatore P, Asico LD, Jose PA, Taylor SI, Westphal H. 1996. Early neonatal death in mice homozygous for a null allele of the insulin receptor gene. *Nat Genet* 12(1):106-109.
- Aguayo-Mazzucato C, Koh A, El Khattabi I, Li WC, Toschi E, Jermendy A, Juhl K, Mao K, Weir GC, Sharma A, Bonner-Weir S. 2011. Mafa expression enhances glucose-responsive insulin secretion in neonatal rat beta cells. *Diabetologia* 54(3):583-93.
- Agudo J, Ayuso E, Jimenez V, Casellas A, Mallol C, Salavert A, Tafuro S, Obach M, Ruzo A, Moya M, et al. 2012. Vascular endothelial growth factor-mediated islet hypervascularization and inflammation contribute to progressive reduction of  $\beta$ -cell mass. *Diabetes* 61(11):2851-2861.
- Alejandro EU, Kalynyak TB, Taghizadeh F, Gwiazda KS, Rawstron EK, Jacob KJ, Johnson JD. 2010. Acute insulin signaling in pancreatic beta-cells is mediated by multiple Raf-1 dependent pathways. *Endocrinology* 151(2):502-512.
- Al-Hasani K, Pfeifer A, Courtney M, Ben-Othman N, Gjernes E, Vieira A, Druelle N, Avolio F, Ravassard P, Leuckx G, et al. 2013. Adult duct-lining cells can reprogram into  $\beta$ -like cells able to counter repeated cycles of toxin-induced diabetes. *Dev Cell* 26(1):86-100.
- Allison DB, Paultre F, Maggio C, Mezzitis N, Pi-Sunyer FX. 1995. The use of areas under curves in diabetes research. *Diabetes Care* 18(2):245-250.
- Almind K, Kahn CR. 2004. Genetic determinants of energy expenditure and insulin resistance in diet-induced obesity in mice. *Diabetes* 53(12):3274-3285.
- Aspinwall CA, Lakey JR, Kennedy RT. 1999. Insulin-stimulated insulin secretion in single pancreatic beta cells. *J Biol Chem*. 274(10):6360-6365.

Assmann A, Ueki K, Winnay JN, Kadowaki T, Kulkarni RN. 2009. Glucose effects on beta-cell growth and survival require activation of insulin receptors and insulin receptor substrate 2. *Mol Cell Biol* 29(11):3219-3228.

Bernal-Mizrachi E, Fatrai S, Johnson JD, Ohsugi M, Otani K, Han Z, Polonsky KS, Permutt MA. 2004. Defective insulin secretion and increased susceptibility to experimental diabetes are induced by reduced Akt activity in pancreatic islet beta cells. *J Clin Invest* 114(7):928-936.

Bernal-Mizrachi E, Wen W, Stahlhut S, Welling CM, Permutt MA. 2001. Islet beta cell expression of constitutively active Akt1/PKB alpha induces striking hypertrophy, hyperplasia, and hyperinsulinemia. *J Clin Invest* 108(11):1631-1638.

Bid HK, London CA, Gao J, Zhong H, Hollingsworth RE, Fernandez S, Mo X, Houghton PJ. 2013. Dual targeting of the insulin-like growth factor receptor and its ligands as an effective antiangiogenic strategy. *Clin Cancer Res* 19(11):2984-2994.

Bid HK, Zhan J, Phelps DA, Kurmasheva RT, Houghton PJ. 2012. Potent inhibition of angiogenesis by the IGF-1 receptor-targeting antibody SCH717454 is reversed by IGF-2. *Mol Cancer Ther* 11(3):649-59.

Blueher M, Michael MD, Peroni OD, Ueki K, Carter N, Kahn BB, Kahn CR. 2002. Adipose tissue selective insulin receptor knockout protects against obesity and obesity-related glucose intolerance. *Dev Cell* 3(1):35-48.

Brissova M, Shiota M, Nicholson WE, Gannon M, Knobel SM, Piston DW, Wright CV, Powers AC. 2002. Reduction in pancreatic transcription factor PDX-1 impairs glucose-stimulated insulin secretion. *J Biol Chem* 277(13):11225-11232.

Brissova M, Shostak A, Shiota M, Wiebe PO, Poffenberger G, Kantz J, Chen Z, Carr C, Jerome WG, Chen J. 2006. Pancreatic islet production of vascular endothelial growth factor-a is essential for islet vascularization, revascularization, and function. *Diabetes* 55(11):2974-2985.

Calderari S, Gangnerau MN, Thibault M, Meile MJ, Kassis N, Alvarez C, Portha B, Serradas P. 2007. Defective IGF2 and IGF1R protein production in embryonic pancreas precedes beta cell mass anomaly in the Goto-Kakizaki rat model of type 2 diabetes. *Diabetologia* 50(7):1463-1471.

Casellas A, Malloc C, Salavert A, Jimenez V, Garcia M, Agudo J, Obach M, Haurigot V, Vila L, Molas M, et al. 2015. Insulin-like growth factor 2 overexpression induces  $\beta$ -cell dysfunction and increases beta-cell susceptibility to damage. *J Biol Chem* 290(27):16772-16785.

Christofori G, Naik P, Hanahan D. 1995. Vascular endothelial growth factor and its receptors, flt-1 and flk-1, are expressed in normal pancreatic islets and throughout islet cell tumorigenesis. *Mol Endocrinol* 9(12):1760-1770.

Cline GW, Petersen KF, Krssak M, Shen J, Hundal RS, Trajanoski Z, Inzucchi S, Dresner A, Rothman DL, Shulman GI. 1999. Impaired glucose transport as a cause of decreased insulin-stimulated muscle glycogen synthesis in type 2 diabetes. *N Engl J Med* 341(4):240-246.

Collins S, Martin TL, Surwit RS, Robidoux J. 2004. Genetic vulnerability to diet-induced obesity in the C57BL/6J mouse: physiological and molecular characteristics. *Physiol Behav* 81(2):243-248.

De Leu N, Heremans Y, Coppens Y, Van Gassen N, Cai Y, D'Hoker J, Magenheim J, Salpeter S, Swisa A, Khalailah A, et al. 2014. Short-term overexpression of VEGF-A in mouse beta cells indirectly stimulates their proliferation and protects against diabetes. *Diabetologia* 57(1):140-147.

DeChiara TM, Efstratiadis A, Robertson EJ. 1990. A growth-deficiency phenotype in heterozygous mice carrying an insulin-like growth factor II gene disrupted by targeting. *Nature* 345(6270):78-80.

Dor Y, Brown J, Martinez OI, Melton DA. 2004. Adult pancreatic  $\beta$ -cells are formed by self-duplication rather than  $\beta$ -cell differentiation. *Nature* 429(6987):41-46.

Duvillie B, Cordonnier N, Deltour L, Dandoy-Dron F, Itier JM, Monthieux E, Jami J, Joshi R, Bucchini D. 1997. Phenotypic alterations in insulin-deficient mutant mice. *Proc Natl Acad Sci* 94(10):5137-5140.

Duvillie B, Currie C, Chrones T, Bucchini D, Jami J, Joshi RL, Hill DJ. 2002. Increased islet cell proliferation, decreased apoptosis, and greater vascularization leading to beta-cell hyperplasia in mutant mice lacking insulin. *Endocrinology* 143(4):1530-1537.

Ediger BN, Du A, Liu J, Hunter CS, Walp ER, Schug J, Kaestner KH, Stein R, Stoffers DA, May CL. 2014. Islet-1 is essential for pancreatic Islet-1  $\beta$ -cell function. *Diabetes* 63(12):4206-4217.

Feng ZC, Riopel M, Li J, Donnelly L, Wang R. 2013. Downregulation of Fas activity rescues early onset of diabetes in c-Kit(Wv/+) mice. *Am J Physiol Endocrinol Metab* 304(6):E557-565.

Folli F, Okada T, Perego C, Gunton J, Liew CW, Akiyama M, D'Amico A, La Rosa S, Placidi C, Lupi R, et al. 2011. Altered insulin receptor signalling and  $\beta$ -cell cycle dynamics in type 2 diabetes mellitus. *PLoS One* 6(11):e28050.

Frasca F, Pandini G, Scalia P, Sciacca L, Mineo R, Costantino A, Goldfine ID, Belfiore A, Vigneri R. 1999. Insulin receptor isoform A, a newly recognized, high-affinity insulin-like growth factor II receptor in fetal and cancer cells. *Mol Cell Biol* 19(5):3278-3288.

Gauthier BR, Wiederkehr A, Baquie M, Dai C, Powers AC, Kerr-Conte J, Pattou F, MacDonald RJ, Ferrer J, Wollheim CB. 2009. PDX1 deficiency causes mitochondrial dysfunction and defective insulin secretion through TFAM suppression. *Cell Metab* 10(2):110-118.

Gittes GK. 2008. Developmental biology of the pancreas: A comprehensive review. *Developmental biology* 326(2009):4-35.

Guerra C, Navarro P, Valverde AM, Arribas M, Bruning J, Kozak LP, Kahn CR, Benito M. 2001. Adipose tissue specific insulin receptor knockout shows diabetic phenotype without insulin resistance. *J Clin Invest* 108(8):1205-1213.

Gunasekaran U, Hudgens CW, Wright BT, Maulis MF, Gannon M. 2012. Differential regulation of embryonic and adult  $\beta$  cell replication. *Cell Cycle* 11(13):2431-2442.

Habener JF, Kemp DM, Thomas MK. 2005. Minireview: transcriptional regulation in pancreatic development. *Endocrinology* 146(3):1025-1034.

Hayashi S, McMahon AP. 2002. Efficient recombination in diverse tissues by a tamoxifen-inducible form of Cre: a tool for temporally regulated gene activation/inactivation in the mouse. *Dev Biol* 244(2):305-318.

Henderson JR, Moss MC. 1985. A morphometric study of the endocrine and exocrine capillaries of the pancreas. *Q J Exp Physiol* 70(3):347-356.

Hill DJ, Hogg J, Petrik J, Arany E, Han VK. 1999. Cellular distribution and ontogeny of insulin-like growth factors (IGFs) and IGF binding protein messenger RNAs and peptides in developing rat pancreas. *J Endocrinol* 160(2):305-317.

Jansson L, Carlsson PO. 2002. Graft vascular function after transplantation of pancreatic islets. *Diabetologia* 45(6):749-763.

Jansson L, Hellerstrom C. 1983. Stimulation by glucose of the blood flow the pancreatic islets of the rats. *Diabetologia* 25(1):45-50.

Johansson M, Mattsson G, Andersson A, Jansson L, Carlsson PO. 2006. Islet endothelial cells and pancreatic beta-cell proliferation: studies in vitro and during pregnancy in adult rats. *Endocrinology* 147(5):2315-2324.

Johnson JD, Alejandro EU. 2008. Control of pancreatic beta-cell fate by insulin signaling: the sweet spot hypothesis. *Cell Cycle* 7(10):1343-1347.

- Johnson JD, Bernal-Mizrachi E, Alejandro EU, Han Z, Kalynyak TB, Li H, Beith JL, Gross J, Warnock GL, Townsend RR. 2006. Insulin protects islets from apoptosis via Pdx1 and specific changes in the human islet proteome. *Proc Natl Acad S* 103(51):19575-19580.
- Joshi RL, Lamothe B, Cordonnier N, Mesbah K, Monthieux E, Jami J, Bucchini D. 1996. Targeted disruption of the insulin receptor gene in mouse results in neonatal lethality *EMBO J* 15(7):1542–1547.
- Kahn CR. 1994. Insulin action, diabetogenesis, and the cause of type II diabetes. *Diabetes* 43(8):1066-1084.
- Kaung HL. 1994. Growth dynamics of pancreatic islet cell populations during fetal and neonatal development of the rat. *Dev Dyn* 200(2):163-175.
- Kawaguchi Y, Cooper B, Gannon M, Ray M, MacDonald RJ, Wright CV. 2002. The role of the transcription factor Ptf1a in converting intestinal to pancreatic progenitors. *Nat Genet* 32(1):128-134.
- Kim MH, Hong SH, Lee MK. 2013. Insulin receptor-overexpressing  $\beta$ -cells ameliorate hyperglycemia in diabetic rats through Wnt signaling activation. *PLoS One* 8(7):e67802.
- Kitamura T, Kahn CR, Accili D. 2003. Insulin receptor knockout mice. *Annu Rev Physiol* 65:313-332.
- Krishnamurthy M, Ayazi F, Li J, Lyttle AW, Woods M, Wu Y, Yee SP, Wang R. 2007. c-Kit in early onset of diabetes: a morphological and functional analysis of pancreatic beta-cells in c-Kit<sup>W-v</sup> mutant mice. *Endocrinology* 148(11):5520-5530.
- Kulkarni RN, Bruning JC, Winnay JN, Postic C, Magnuson MA, Kahn CR. 1999. Tissue-specific knockout of the insulin receptor in pancreatic beta cells creates an insulin secretory defect similar to that in type 2 diabetes. *Cell* 96(3):329-339.

Kulkarni RN, Holzenberger M, Shih DQ, Ozcan U, Stoffel M, Magnuson MA, Kahn CR. 2002. Beta-cell-specific deletion of the Igf1 receptor leads to hyperinsulinemia and glucose intolerance but does not alter beta-cell mass. *Nat Genet* 31(1):111-115.

Lammert E, Cleaver O, Melton D. 2001. Induction of pancreatic differentiation by signals from blood vessels. *Science* 294(5542):564-567.

Lee J, Pilch PF. 1994. The insulin receptor: structure, function, and signaling. *Am J Physiol* 266(2):319-344.

Lee SR, Kim SH, Chae HD, Kim CH, Kang BM. 2012. Influence of vascular endothelial growth factor on the expression of insulin-like growth factor-II, insulin-like growth factor binding protein-2 and 5 in human luteinized granulosa cells. *Gynecol Endocrinol* 28(11):917-920.

Leibiger B, Leibiger IB, Moede T, Kemper S, Kulkarni RN, Kahn CR, de Vargas LM, Berggren PO. 2001. Selective insulin signaling through A and B insulin receptors regulates transcription of insulin and glucokinase genes in pancreatic beta cells. *Mol Cell* 7(3):559-570.

Leibiger IB, Leibiger B, Berggren PO. 2008. Insulin signaling in the pancreatic beta-cell. *Annu Rev Nutr* 28:233-251.

Leibiger IB, Leibiger B, Moede T, Berggren PO. 1998. Exocytosis of insulin promotes insulin gene transcription via the insulin receptor/PI-3 kinase/p70 s6 kinase and CaM kinase pathways. *Mol Cell* 1(6):933-938.

Liu JP, Baker J, Perkins AS, Robertson EJ, Efstratiadis A. 1993. Mice carrying null mutations of the genes encoding insulin-like growth factor 1 and type 1 IGF receptor. *Cell* 75(1): 59-72.

Liu Y, Suckale J, Masjkur J, Magro MG, Steffen A, Anastassiadis K, Solimena M. 2010. Tamoxifen-independent recombination in the RIP-CreER mouse. *PLoS One* 5(10):e13533.

- Louvi A, Accili D, Efstratiadis A. 1997. Growth-promoting interaction of IGF-II with the insulin receptor during mouse embryonic development. *Dev Biol* 189(1): 33-48.
- Mayo LD, Donner DB. 2001. A phosphatidylinositol 3-kinase/Akt pathway promotes translocation of Mdm2 from the cytoplasm to the nucleus. *Proc Natl Acad Sci* 98(20):11598-11603.
- Mehran AE, Templeman NM, Brigidi GS, Lim GE, Chu KY, Hu X, Botezelli JD, Asadi A, Hoffman BG, Kieffer TJ, et al. (2012). Hyperinsulinemia drives diet-induced obesity independently of brain insulin production. *Cell Metab* 16(6):723-737.
- Michael MD, Kulkarni RN, Postic C, Previs SF, Shulman GI, Magnuson MA, Kahn CR. 2000. Loss of insulin signaling in hepatocytes leads to severe insulin resistance and progressive hepatic dysfunction. *Mol Cell* 6(1):87-97.
- Montanya E, Nacher V, Biarnes M, Soler J. 2000. Linear correlation between beta cell mass and body weight throughout the lifespan in Lewis rats. *Diabetes* 49(8):1341-1346.
- Murphy LJ, Bell GI, Friesen HF. 1987. Tissue distribution of insulin-like growth factor I and II messenger ribonucleic acid in the adult rat. *Endocrinology* 120(4):1279-1282.
- Nakae J, Kido Y, Accili D. 2001. Distinct and overlapping functions of insulin and IGF-1 receptors. *Endocr Rev* 22(6):818-835.
- Nielsen JH, Svensson C, Galsgaard ED, Moldrup A, Billestrup N. 1999. Beta cell proliferation and growth factors. *J Mol Med* 77(1):62-66.
- Nikolova G, Jabs N, Konstantinova I, Domogatskaya A, Tryggvason K, Sorokin L, Fassler R, Gu G, Gerber HP, Ferrara N, et al. 2006. The vascular basement membrane: a niche for insulin gene expression and beta cell proliferation. *Dev Cell* 10(3):397-405.
- Offield MF, Jetton TL, Labosky PA, Ray M, Stein RW, Magnuson MA, Hogan BL, Wright CV. 1996. PDX-1 is required for pancreatic outgrowth and differentiation of the rostral duodenum. *Development* 122(3):983-995.

Ogawara Y, Kishishita S, Obata T, Isazawa Y, Suzuki T, Tanaka K, Masuyama N, Gotoh Y. 2002. Akt enhances Mdm2-mediated ubiquitination and degradation of p53. *J Biol Chem* 277(24):21843-21850.

Okada T, Liew CW, Hu J, Hinahult C, Michael MD, Krtzfeldt J, Yin C, Holzenberger M, Stoffel M, Kulkarni RN. 2007. Insulin receptors in beta-cells are critical for islet compensatory growth response to insulin resistance. *Proc Natl Acad Sci* 104(21):8977-8982.

Pan FC, Wright C. 2011. Pancreas organogenesis: from bud to plexus to gland. *Dev Dyn* 240(3):530-565.

Pessin JE, Saltiel AR. 2000. Signaling pathways in insulin action: molecular targets of insulin resistance. *J Clin Invest* 106(2):165–169.

Petrik J, Pell JM, Arany E, McDonald TJ, Dean WL, Reik W, Hill DJ. 1999. Overexpression of insulin-like growth factor-II in transgenic mice is associated with pancreatic islet cell hyperplasia. *Endocrinology* 140(5):2353-2363.

Piecewicz SM, Pandey A, Roy B, Xiang SH, Zetter BR, Sengupta S. 2012. Insulin-like growth factors promote vasculogenesis in embryonic stem cells. *PLoS One Science* 7(2):e32191.

Reinert RB, Brissova M, Shostak A, Pan FC, Poffenberger G, Cai Q, Hundemer GL, Kantz J, Thompson CS, Dai C, et al. 2013. Vascular endothelial growth factor-a and islet vasculature are necessary in developing, but not adult, pancreatic islets. *Diabetes* 62(12):4154-4164.

Reinert RB, Kantz J, Misfeldt AA, Poffenberger G, Gannon M, Brissova M, Powers AC. 2012. Tamoxifen-induced cre-loxp recombination is prolonged in pancreatic islets of adult mice. *PLoS One* 7(3):e33529.

Roat R, Rao V, Doliba NM, Matchinsky FM, Tobias JW, Garcia E, Ahima RS, Imai Y. 2014. Alterations of pancreatic islet structure, metabolism and gene expression in diet induced obese C57BL/6J mice. *PLoS One* 9(2): e86815.

Rorsman P, Eliasson L, Renstrom E, Gromada J, Barg S, Gopel S. 2000. The cell physiology of biphasic insulin secretion. *News Physiol Sci* 15:72-77.

Sander M, Sussel L, Connors J, Scheel D, Kalamaras J, Dela CF, Schwitzgebel V, Hayes-Jordan A, German M. 2000. Homeobox gene Nkx6.1 lies downstream of Nkx2.2 in the major pathway of beta-cell formation in the pancreas. *Development* 127(24):5533-5540.

Scaglia L, Cahill CJ, Finegood DT, Bonner-Weir S. 1997. Apoptosis participates in the remodeling of the endocrine pancreas in the neonatal rat. *Endocrinology* 138(4):1736-1741.

Shapiro AM. 2012. Islet transplantation in type 1 diabetes: ongoing challenges, refined procedures, and long-term outcome. *Rev Diabet Stud* 9(4):385-406.

Shefi-Friedman L, Wertheimer E, Shen S, Bak A, Accili D, Sampson SR. 2001. Increased IGFR activity and glucose transport in cultured skeletal muscle from insulin receptor null mice. *Am J Physiol Endocrinol Metab* 281(1):E16-E24.

Shymko RM, De Meyts P, Thomas R. 1997. Logical analysis of timing-dependent receptor signalling specificity: application to the insulin receptor metabolic and mitogenic signalling pathways. *Biochem J* 326(2):463-469.

Smith FE, Rosen KM, Villa-Komaroff L, Weir GC, Bonner-Weir S. 1991. Enhanced insulin-like growth factor 1 gene expression in regenerating rat pancreas. *Proc Natl Acad Sci* 88(14):6152-6156.

Surwit RS, Kuhn CM, Cochrane C, McCubbin JA, Feinglos MN. 1988. Diet-induced type II diabetes in C57BL/6J mice. *Diabetes* 37(9):1163-1167.

- Tamarina NA, Roe MW, Philipson L. 2014. Characterization of mice expression ins1 gene promoter driven creERT recombinase for conditional gene deletion in pancreatic  $\beta$ -cells. *Islets* 6(1):e27685.
- Taylor SI, Kadowaki T, Kadowaki H, Accili D, Cama A, McKeon C. 1990. Mutations in insulin-receptor gene in insulin-resistant patients. *Diabetes Care* 13(3):257–279.
- Ueki K, Okada T, Hu J, Liew CW, Assmann A, Dahlgren GM, Peters JL, Shackman JG, Zhang M, Artner I, et al. 2006. Total insulin and IGF-I resistance in pancreatic beta cells causes overt diabetes. *Nat Genet* 38(5):583-588.
- Van Schravendijk CF, Foriers A, Van den Brande JL, Pipeleers DG. 1987. Evidence for presence of type 1 insulin-like growth factor receptors on rat pancreatic A and B cells. *Endocrinology* 121(5):1784-1788.
- Wang M, Li J, Lim GE, Johnson JD. 2013. Is dynamic autocrine insulin signaling possible? a mathematical model predicts picomolar concentrations of extracellular monomeric insulin within human pancreatic islets. *PLoS One* 8(6):e64860.
- Wang R, Li J, Yashpal N. 2004. Phenotypic analysis of c-Kit expression in epithelial monolayers derived from postnatal rat pancreatic islets. *J Endocrinol* 182(1):113-122.
- Wang RN, Bouwens L, Kloppel G. 1994. Beta-cell proliferation in normal and streptozotocin-treated newborn rats: site, dynamics and capacity. *Diabetologia* 37(11):1088-1096.
- Wang ZC, Wheeler MB, Belsham DD. 2014. Isolation and immortalization of MIP-GFP neurons from the hypothalamus. *Endocrinology* 155(6):2314-2319.
- Wicksteed B, Brissova M, Yan W, Opland DM, Plank JL, Reinert RB, Dickson LM, Tamarina NA, Philipson LH, Shostak A. 2010. Conditional gene targeting in mouse pancreatic  $\beta$ -cells: analysis of ectopic Cre transgene expression in the brain. *Diabetes* 59(12):3090-3098.

Wrede CE, Dickson LM, Lingohr MK, Briaud I, Rhodes CJ. 2002. Protein kinase B/Akt prevents fatty acid-induced apoptosis in pancreatic beta cells (INS-1). *J Biol Chem* 277(51):49676-49684.

Xu GG, Rothenberg PL. 1998. Insulin receptor signaling in the beta-cell influences insulin gene expression and insulin content: evidence for autocrine beta-cell regulation. *Diabetes* 47(8): 1243-1252.

Xuan S, Kitamura T, Nakae J, Politi K, Kido Y, Fisher PE, Morroni M, Cinti S, White MF, Herrera PL, et al. 2002. Defective insulin secretion in pancreatic beta cells lacking type 1 IGF receptor. *J Clin Invest* 110(7):1011-1019.

Xuan S, Szabolcs M, Cinti F, Perincheri S, Accili D, Efstratiadis A. 2010. Genetic analysis of type-1 insulin like growth factor receptor signaling through insulin receptor substrate-1 and -2 in pancreatic beta cells. *J Biol Chem* 285(52) 41044-41050.

Zawalich WS, Zawalich KC. 2002. Effects of glucose, exogenous insulin, and carbachol on C-peptide and insulin secretion from isolated perfused rat islets. *J Biol Chem* 277(29):26233-26237.

## **Appendices**

## Appendix A: Classification II Laboratory Approval Form

### *University of Western Ontario* *Permit Summary*

**Permit Holder** Wang, Rennian  
**Permit #** BIO-LHRI-0046 **Classification** 2  
**Department** Physiology  
**Phone** \_\_\_\_\_ **Ext.** \_\_\_\_\_  
**Email** \_\_\_\_\_  
**Approval Date** Apr 25, 2014 **Expiration Date** Apr 24, 2017  
**BioSafety Officer's Signature** \_\_\_\_\_

**Organism**  
**Cell** Human (primary), fetal pancreas and duodenum, Rodent (primary), mouse pancreatic islets, human (established), PANC-1, HEK293, Rodent (established), INS-1, AR42J  
**Human** organs and tissues (unpreserved), organs and tissues (preserved)  
**Gene Therapy**  
**GMO**  
**Animals** B6 mice  
**Toxin** Streptozotocin, Tamoxifen  
**Plant/Insect**

Building	Room	Room Area	Lab Phone	Ext.	Level
Other	OFF CAMPUS				2

## *University of Western Ontario* *Permit Summary*

**Permit Holder** Wang, Rennian  
**Permit #** BIO-LHRI-0046 **Classification** 2  
**Department** Physiology  
**Phone** \_\_\_\_\_ **Ext.** \_\_\_\_\_  
**Email** \_\_\_\_\_  
**Approval Date** Apr 25, 2014 **Expiration Date** Apr 24, 2017  
**BioSafety Officer's Signature** \_\_\_\_\_

### Permit Conditions

- 1 INTERNAL PERMIT HOLDER RESPONSIBILITIES
 

Comply with UWO BioSafety Safety Policies and Standard Operating Procedures. Ensure that the Health Canada Biosafety Guidelines, relevant regulations and safe laboratory practices are followed.

  - 1.1 Receive adequate biosafety training from the institution. Permit Holders are responsible for the provision of specific training and instruction in biohazard agent handling that is necessary for the safe use of this material in their own laboratories. Supervisors must ensure that workers understand the health and safety hazards of the work or task (due diligence).
  - 1.2 Ensure that the UWO Biosafety Manual is available to all lab personnel under the permit.
  - 1.3 Report incidents of loss or theft of any biohazardous material immediately to the Biosafety Coordinator;
- 2 WORKER RESPONSIBILITIES
 

Be familiar with the UWO Biosafety Manual, attend all required safety training sessions and obey all safety regulations required by the UWO Biosafety Committee.

  - 2.1 Report to the Permit Holder any incident involving known or suspected exposure, personal contamination or a spill involving a biohazardous agent.

I accept the above responsibilities as a Internal Permit Holder and I am accountable for following UWO BioSafety Guidelines and Procedures Manual for Containment Level 1 and 2 Laboratories.

Permit Holder Name \_\_\_\_\_ Signed \_\_\_\_\_ Date \_\_\_\_\_

## Appendix B: Biosafety Approval Form



**Researcher: Dr. Rennian Wang**  
**Biosafety Approval Number: BIO-LHRI-0046**  
**Expiry Date: April 24, 2017**

April 28, 2014

Dear Dr. Wang:

Please note your biosafety approval number listed above. This number is very useful to you as a researcher working with biohazards. It is a requirement for your research grants, purchasing of biohazardous materials and Level 2 inspections.

Research Grants:

- This number is required information for any research grants involving biohazards. Please provide this number to Research Services when requested.

Purchasing Materials:

- This number must be included on purchase orders for Level 1 or Level 2 biohazards. When you order biohazardous material, use the on-line purchase ordering system ([www.uwo.ca/finance/people/](http://www.uwo.ca/finance/people/)). In the "Comments to Purchasing" tab, include your name as the Researcher and your biosafety approval number.

Annual Inspections:

- If you have a Level 2 laboratory on campus, you are inspected every year. This is your permit number to allow you to work with Level 2 biohazards.

To maintain your Biosafety Approval, you need to:

- Ensure that you update your Biohazardous Agents Registry Form at least every three years, or when there are changes to the biohazards you are working with.
- Ensure that the people working in your laboratory are trained in Biosafety.
- Ensure that your laboratory follows the University of Western Ontario Biosafety Guidelines and Procedures Manual for Containment Level 1 & 2 Laboratories.
- For more information, please see: [www.uwo.ca/hr/safety/biosafety/](http://www.uwo.ca/hr/safety/biosafety/).

Please let me know if you have questions or comments.

Regards,

Tony Hammoud  
Biosafety Coordinator for Western

## Appendix C: Animal Use Protocol



2008-038-04::6:

**AUP Number:** 2008-038-04

**AUP Title:** Pancreatic Beta Cell Development: The Role of the c-Kit and Integrin Receptors

**Yearly Renewal Date:** 11/01/2014

**The YEARLY RENEWAL to Animal Use Protocol (AUP) 2008-038-04 has been approved, and will be approved for one year following the above review date.**

This AUP number must be indicated when ordering animals for this project.

Animals for other projects may not be ordered under this AUP number.

Purchases of animals other than through this system must be cleared through the ACVS office.

Health certificates will be required.

### **REQUIREMENTS/COMMENTS**

Please ensure that individual(s) performing procedures on live animals, as described in this protocol, are familiar with the contents of this document.

The holder of this Animal Use Protocol is responsible to ensure that all associated safety components (biosafety, radiation safety, general laboratory safety) comply with institutional safety standards and have received all necessary approvals. Please consult directly with your institutional safety officers.

Submitted by: Kinchlea, Will D

on behalf of the Animal Use Subcommittee

# Curriculum Vitae

LIANGYI ZHOU (LARRY)

## UNIVERSITY EDUCATIONIONAL BACKGROUND:

<b>Master of Science</b> Department of Pathology, Western University	<b>2013 – present</b>
<b>Honours Bachelor of Medical Sciences</b> Honours Specialization in Pathology and Toxicology, Western University	<b>2009 – 2013</b>

## HONOURS, SCHOLARSHIPS AND AWARDS:

<b>Continuing Admission Scholarship</b> Western University	<b>2009 – 2013</b>
<b>Dean's Honor List</b> Western University	<b>2009 – 2013</b>
<b>Graduation with Distinction</b> Western University	<b>2013</b>
<b>Queen Elizabeth II Aiming for the Top Scholarship</b> Western University	<b>2009 – 2013</b>
<b>CIHR - Canada Graduate Scholarship (Masters)</b> Canadian Institutes of Health Research, Western University	<b>2014</b>
<b>Ontario Graduate Scholarship (OGS) - declined</b> Western University	<b>2014</b>
<b>Dutkevich Travel Award</b> Department of Pathology, Western University	<b>2014</b>

## RESEARCH EXPERIENCE:

<b>Research Assistant</b> (Undergraduate level) Department of Pathology, Western University Supervisor: Dr. Xiufen Zheng	<b>2012 – 2013</b>
--	--------------------

PUBLICATIONS:

**Zhou L.**, Zang G., Zhang G., et al. (2013). MicroRNA and mRNA signatures in Ischemia Reperfusion Injury in Heart Transplantation. *PLoSone* 8(11): e79805

Zang G., Thomas A., Liu Z., Chen D., Ling H., **Zhou L.**, Zhang F., Siu L., and Zheng X. (2013). Preventing Breast Cancer Growth by Cationic Cecropin B. *Biological Systems: Open Access* 2(112). doi: 10.4172/2329-6577.1000112

ABSTRACTS:

Published in a supplement issue of the *Canadian Journal of Diabetes*      **2014**  
Project Title: Temporally controlled knockout of the  $\beta$ -cell insulin receptor during in utero development induces an islet compensatory response

PRESENTATIONS:

**London Health Research Day**      **April 2015**  
Poster Presentation (Top 80) - London, Ontario  
Project Title: Determination of the mechanisms by which the pancreatic  $\beta$ -cell insulin receptor regulates  $\beta$ -cell growth, function, and survival via a temporal and conditional knockout

**Annual Pathology Research Day**      **March 2015**  
Poster Presentation - London, Ontario  
Project Title: Determination of the mechanisms by which the pancreatic  $\beta$ -cell insulin receptor regulates  $\beta$ -cell growth, function, and survival via a temporal and conditional knockout

**Diabetes Research Day**      **November 2014**  
Poster Presentation - London, Ontario  
Project Title: Temporally controlled knockout of the  $\beta$ -cell insulin receptor during in utero development induces an islet compensatory response

**17th Annual CDA/CSEM Professional Conference and Annual Meetings**      **October 2014**  
Oral Presentation - Winnipeg, Ontario  
Project Title: Temporally controlled knockout of the  $\beta$ -cell insulin receptor during in utero development induces an islet compensatory response

**5th Annual Developmental Biology Day**      **May 2014**  
Poster Presentation - Western University, London, Ontario  
Project Title: Temporal knockout of the  $\beta$ -cell insulin receptor during in utero development induces an islet compensatory response

**London Health Research Day**

**April 2014**

Poster Presentation - London, Ontario

Project Title: Fetal  $\beta$ -cell insulin receptor expression level influences murine islet development

**Annual Pathology Research Day**

**April 2014**

Poster Presentation - Western University, London, Ontario

Project Title: Determining the role of pancreatic  $\beta$ -cell insulin receptor on pancreatic islet maintenance and function

**Annual Pathology Research Day**

**April 2013**

Poster Presentation - Western University, London, Ontario

Project Title: MicroRNA and ischemia reperfusion injury in heart transplantation